Dissertations   Theses and Dissertations

1991

Behavioral Measures of Auditory Processing in the Chinchilla: A Comparison of Frequency Selectivity Derived from Critical Masking Ratios and Rippled Noise Masking

Andrew J. Niemiec
Loyola University Chicago

Follow this and additional works at: https://ecommons.luc.edu/luc_diss

Part of the Psychology Commons

Recommended Citation

BEHAVIORAL MEASURES OF AUDITORY PROCESSING IN THE

CHINCHILLA: A COMPARISON OF FREQUENCY SELECTIVITY DERIVED

FROM CRITICAL MASKING RATIOS AND RIPPLED NOISE MASKING

by

Andrew J. Niemiec

A Dissertation Submitted to the Faculty of the Graduate

School of Loyola University of Chicago in Partial

Fulfillment of the Requirements for the Degree of

Doctor of Philosophy

May

1991

Dedicated to the memory of my mother, Stella, and to the memory of my good friends MacDuff and T.J.

ACKNOWLEDGMENTS

I would like to express my gratitude and appreciation to Bill Yost, my advisor and dissertation director, for providing me with the privilege of studying at the Parmly Hearing Institute. He gave me invaluable assistance as a guide to the theory and methodology underlying this project, material support for its implementation, and inspiration and moral support throughout its duration. His help, determination, and faith in me are largely responsible for the completion of this dissertation.

I thank Toby Dye and Dick Fay, who were both friends and members of my dissertation committee, for their assistance with the logic and methodology of this project. I also acknowledge my gratitude to Bill Shofner for his friendship and many long and helpful discussions regarding this project.

This project would not have been possible without the help of Bill Clark and Cynthia Prosen who taught me to

train my chinchillas; Chuck Wheeles and Bill Madigan who provided the best technical support anyone could wish for; and Lisa Smith who cared for my subjects as if they were her own.

I would especially like to thank my father, my wife Lynne, and my aunt Josephine. This would not have been possible without their patience, understanding, and moral support.

Finally, I would like to thank my subjects. Their participation in this project has given us not only a better understanding of their world but a better understanding of ourselves as well.

VITA

The author, Andrew Joseph Niemiec, is the son of Andrew Niemiec and Stanislawa (Kuczak) Niemiec. He was born on March 17, 1962, in Chicago, Illinois.

His elementary education was obtained at St. Hyacinth's School, Chicago, Illinois. His secondary education was completed in 1980 at Gordon Technical High School, Chicago, Illinois.

In September, 1980, Mr. Niemiec entered Loyola University of Chicago, receiving the degree of Bachelor of Science in psychology in May, 1984.

In September, 1985, Mr. Niemiec was granted an assistantship in psychology at Loyola University of Chicago, enabling him to complete the Master of Arts in 1988. In 1989, Mr. Niemiec was granted a Loyola University Dissertation Fellowship which enabled him to complete the Doctor of Philosophy degree in 1991.

Mr. Niemiec is a member of the Acoustical Society of America, the American Psychological Society, the Association for Research in Otolaryngology, the Midwestern Psychological Association, and Sigma Xi.

TABLE OF CONTENTS

LIST OF TABLES

LIST OF FIGURES

CHAPTER I

INTRODUCTION

Under natural circumstances sounds do not usually occur in isolation. Instead, most sounds typically occur either simultaneously or close together in time. Therefore, a louder sound might obscure a softer sound which is occurring at the same time. The study of masking is concerned with these types of interactions of sounds. Specifically, masking is concerned with how one sound diminishes our ability to detect other sounds. By studying the physical parameters which affect masking, it is possible to determine how the auditory system analyzes and discriminates the various frequency components in a mixture of sounds. That is, it is possible to determine how the auditory system performs frequency analysis.

One very general conclusion of masking experiments is that a signal will be masked most easily by a sound which has spectral components close to or at the same frequency as the signal (Wegel and Lane, 1924; Fletcher, 1940; Hamilton, 1957; and Greenwood, 1961). This result

indicates that the ability to analyze and discriminate the various spectral components in complex sounds is at least partially determined by the frequency resolving ability of the auditory system.

Fletcher (1940) proposed the "critical band" to account for data obtained in masking experiments. This concept of the critical band is now fundamental to our comprehension of frequency selectivity. Fletcher suggested that the auditory system behaves as if it consisted of a bank of bandpass filters with continuously overlapping center frequencies that serve as discrete spectral information channels. When a listener attempts to detect a signal in a background of noise, a filter whose center frequency is close to that of the signal is monitored. Only those frequency components of the noise which pass through the filter will contribute to the masking of the signal. Thus the filter will pass the signal but remove a great deal of the noise and the signal threshold will be determined by the amount of noise passing through the filter.

To account for the masking of tonal signals by broadband noise, Fletcher made the simplifying assumption that the shape of the auditory filter could be approximated by a rectangle with a flat top and vertical edges. For this type of filter, all frequency components within the passband will be unattenuated and all frequency components

falling outside the passband will be removed. Fletcher called the width of the passband the critical bandwidth.

Thus the value of the critical band may be determined by measuring the threshold for a tonal signal masked by a broadband noise given the following two assumptions: 1) only a narrow band of frequency components surrounding the tone contribute to the masking of the tone; and 2) when the noise just masks the tonal signal, the power of the noise inside the critical band is equal to the power of the tone.

Noise power is specified in terms of the power of the noise in a 1 Hz band and is referred to as spectrum level (N_0). For a white noise, N_0 is not dependent on frequency. Therefore, for a frequency band W Hz wide the total noise power is N_0 X W. According to Fletcher, when the width of the frequency band equals the critical bandwidth, the total noise power in the band will equal the power of the tonal signal at masked threshold (P). Thus, according to Fletcher, $W = P/N_0$ and W can be estimated by measuring P and N_0. This type of experiment, which yields an indirect measure of the critical band, is referred to as a critical masking ratio experiment.

The assumption that only a narrow range of frequencies surrounding the tonal signal contribute to the masking of the tone has been confirmed by experiments in which the

threshold of a tone is measured in noise of various bandwidths (Hamilton, 1957 and Greenwood, 1961). Increasing the noise bandwidth beyond a certain critical bandwidth has little effect on the threshold for the tone. However, the second assumption (when the noise just masks the tone, the power of the noise inside the critical band is equal to the power of the tone) is not always true (Scharf, 1970). At most frequencies, this assumption leads to estimates of critical bandwidth which are 2.5 times smaller than measures obtained from more direct methods of estimating the critical band such as band-narrowing experiments.

The concept of the critical band and the critical ratio are widespread in psychoacoustics. However, the critical band and critical ratio measure only the "effective" bandwidth of the auditory filter. Furthermore, recent experiments (Patterson, Nimmo-Smith, Weber, and Milroy, 1982) have shown that the critical ratio estimate of critical bandwidth is more closely related to the efficiency with which subjects process complex sound than it is to auditory filter width. Efficiency, as used here, refers to the ratio of signal power to noise power required at the output of the auditory filter to achieve threshold. Experiments which focus on the shape of the auditory filter (Egan and Hake, 1950; Patterson, 1976; Houtgast, 1977; and

Moore, 1978) help to separate processing efficiency from frequency selectivity.

Although Fletcher approximated the shape of the auditory filter as a simple rectangle, it was known that the shape of the filter is not truly rectangular. Masked audiograms measured by Egan and Hake (1950) showed that the auditory filter has sloping edges. The width and shape of the auditory filter also changes with center frequency. When the frequency of the signal is changed, the listener will direct his attention to the auditory filter which gives the best signal-to-masker ratio. Therefore, a different auditory filter will be used for each signal frequency. The shape of the masked audiogram reflects this.

One method for measuring auditory filter shape is the psychophysical tuning curve (PTC). To measure a PTC, the signal is fixed in frequency and in level. The signal is usually presented at a relatively low level so that it presumably will activate only a few auditory filters. The masker is either a pure tone or a narrow band of noise. For several masker frequencies, the level of the masker needed to just mask the signal is measured. It is assumed that at threshold the masker produces a constant output from the filter in order to mask the signal. Consequently, the PTC measures the masker level needed to generate a

fixed output from the auditory filter as a function of frequency. If the auditory system is assumed to be linear, the shape of the auditory filter can be obtained by inverting the PTC.

One problem with using the PTC to measure auditory filter shape is "off-frequency listening." Since the listener will attend to the filter which gives the best signal-to-masker ratio, it may be the case that the listener does not attend to only one filter. When the masker frequency is below the signal frequency, the listener can improve performance by monitoring a filter centered just above the signal frequency. Conversely, when the masker frequency is above the signal frequency, the listener can improve performance by monitoring a filter centered just below the signal frequency. In these instances, the filters centered just above or below the signal frequency give the listener a better signal-to-masker ratio than the filter centered at the signal frequency. Studies involving off-frequency listening result in PTCs that have sharper tips than would be obtained if only one auditory filter were involved (O'Loughlin and Moore, 1981).

In an attempt to prevent listeners from using off-frequency listening, Patterson (1976) measured masked thresholds for tonal signals which were masked by noise

with a bandstop or notch centered at the signal frequency. Patterson varied the width of the notch and measured the signal threshold as a function of notch width. Patterson assumed that the auditory filter was symmetrical. For a signal placed symmetrically in a notched noise, the best signal-to-masker ratio is obtained with a filter centered at the signal frequency. Shifting the filter up in frequency will reduce the noise coming through the filter from the lower noise band, however, this will be offset by the increase in noise coming through the filter from the higher noise band.

As notch width is increased, the power of the noise passing through the filter decreases. Consequently, the threshold for the signal should decrease. Patterson assumed that the power in the signal at masked threshold is proportional to the power in the noise passed by the filter. If masked threshold corresponds to a constant signal-to-masker ratio at the output of the filter, then the change in masked threshold as a function of notch width shows how the area under the filter varies with notch width. By differentiating the function relating masked threshold to notch width, Patterson was able to estimate auditory filter shape. Patterson's experiment demonstrated that the auditory filter could be reasonably approximated

with a Gaussian which has a rounded top and fairly steep skirts.

Unlike Fletcher's rectangular filter, Patterson's filter cannot be completely specified with a single number such as the critical bandwidth. However, Patterson summarized the width of the auditory filters with two measures. One measure of bandwidth is the 3-dB bandwidth. The 3-dB bandwidth is the bandwidth at which the filter's response has fallen by a factor of two in power. Patterson's filter's had 3-dB bandwidths which were 10-15% of the center frequency. Another measure of bandwidth is the equivalent rectangular bandwidth (ERB). The ERB is the width a perfectly rectangular filter with a height equal to the measured auditory filter would need to be in order to cover the same area as the measured auditory filter. The ERBs of the auditory filters derived using Patterson's notched noise masking technique were 11-17% of the center frequency.

Houtgast (1974, 1977) measured auditory filter shape by using a rippled noise to mask a tonal signal. Rippled noise is a complex, non-periodic stimulus that has a cosinusoidal energy spectrum. There are two types of rippled noise: Cosine positive (Cos+) and Cosine negative (Cos-). Cos+ rippled noise is generated by delaying a source of white noise (which has a continuous, flat

spectrum) by some amount (τ sec) and adding the output of the delay back to the original noise source. This results in a continuous masking noise with a cosinusoidal energy spectrum in which the peaks occur at integer multiples of $1/\tau$. Cos- rippled noise is generated by subtracting the delayed version of the noise from the undelayed noise source. For cos- rippled noise the valleys occur at integer multiples of $1/\tau$. Rippled noise produces a pitch that is related to the delay (Yost, Hill, and Perez-Falcon, 1978; Yost and Hill, 1978; Yost and Hill, 1979; Yost, 1980; and Yost, 1982).

The spacing or density of the peaks and valleys in rippled noise is a function of the delay (τ). At very short delays, the peaks or valleys are at a low density. That is, they are spaced far apart in frequency. As the delay increases so does ripple density. (The peaks or valleys move closer together in frequency.) Houtgast used this attribute of rippled noise to measure frequency selectivity.

Houtgast measured masked thresholds for a pure tone signal masked by both cos+ and cos- rippled noise as the density of the ripple was varied. Houtgast measured a masking function by subtracting the masked thresholds for

cos- rippled noise from the masked thresholds for cos+ rippled noise as a function of ripple density. As the spacing of the peaks and valleys moved closer together in frequency, the difference between the cos+ and cos- masked thresholds decreased and the difference in masking approached zero. Houtgast assumed that the power in the signal at masked threshold is proportional to the power in the noise passed by the filter. If masked threshold corresponds to a constant signal-to-masker ratio at the output of the filter, then the change in masked threshold as a function of ripple density can be used to define an intensity weighting function which is the shape of the auditory filter. By an application of Fourier analysis to the rippled noise masking function and under the assumption of linearity, Houtgast was able to estimate auditory filter shape. Like Patterson (1976), Houtgast demonstrated that the auditory filter had a somewhat Gaussian shape with a rounded top and fairly steep skirts.

Although rippled noise had originally been used to derive estimates of frequency selectivity or psychophysical tuning in humans (Houtgast, 1974; Houtgast, 1977; Pick, 1980; and Yost, 1982), similar procedures have also been used by Pickles (1979) in the cat and by Fay, Yost, and Coombs (1983) in goldfish. Animal psychophysical studies are important in their own right as descriptions of

auditory function in non-human animals. Because the chinchilla audiogram is so similar to the human audiogram, the chinchilla often serves as a model of the human auditory system (Miller, 1970). Measuring the chinchilla's response to rippled noise allows for a comparison of frequency selectivity between the human and the chinchilla. By measuring the psychophysical tuning of the chinchilla using rippled noise, it also becomes possible to obtain information about the animal's perception of this stimulus and to place its response into a comparative and physiological context.

Measuring the psychophysical tuning of the chinchilla using rippled noise has gained additional importance following the work of Halpern and Dallos (1986). Halpern and Dallos used a forward masking paradigm to study auditory filter shape in the chinchilla. In the forward masking paradigm, the tonal signal is presented just after the masking noise. Halpern and Dallos showed that while their notched-noise masking technique yielded estimates of tuning that were similar to those obtained using other techniques, there was a major difference in the auditory filter shapes of humans and chinchillas. Specifically, the auditory filter shapes derived by Halpern and Dallos (1986) showed an unexpected dip in the region of the center frequency. By using a different technique, rippled noise

masking, additional light can be shed on these differences and similarities between human and chinchilla.

In order to determine the chinchilla's response to rippled noise, this study will examine how a continuous rippled noise masks pure tone signals. By varying the parameters of the rippled noise masker, the characteristics of the chinchilla's auditory filter can be derived. These characteristics of the chinchilla's auditory filters will be compared with measures of frequency selectivity obtained from humans as well as with other measures of frequency selectivity obtained from chinchillas.

CHAPTER II

EXPERIMENT 1 - CRITICAL MASKING RATIOS

As a first step in studying frequency selectivity in the chinchilla, this experiment measures the critical masking ratios of five adult chinchillas and compares these critical ratios with critical ratios measured using shock-avoidance paradigms. Measuring the critical masking ratios in chinchillas provides not only an estimate of the animals' frequency selectivity but also allows for a comparison of thresholds measured using a positive-reinforcement behavioral tracking task with thresholds measured using negative-reinforcement paradigms (Miller, 1964 and Seaton and Trahiotis, 1975).

THE PSYCHOPHYSICAL PROCEDURE

The animal psychophysical procedure used in this study was a behavioral adaptive tracking paradigm modeled after that used by Clark and Bohne (1978). In this paradigm, the animals were maintained at 80% of their normal ad libitum

body weight. The animals were trained to detect the presence of a tonal signal by reinforcing correct detections with food pellets. In order to perform this task the chinchilla was put into a testing cage housed inside a sound attenuating chamber. The cage inside the chamber contained a response lever and a reward chute which dispensed food pellets. The signal tone and the masking noise were presented via a loudspeaker housed inside the chamber, but outside the cage. Figure 1 shows the configuration of the testing cage.

The acoustics of the chamber were determined by placing a condenser microphone at the position the animal's head would normally occupy when it was in the testing cage. Wideband noise was presented to the microphone over the speaker and a Fast Fourier Transform (FFT) of the wideband noise was computed. This was repeated 100 times. The frequency response of the sound attenuating chamber was determined by averaging the 100 FFTs of the wideband noise. The chamber had a frequency response of ± 7 dB over the frequency range of 250-10000 Hz. The noise floor was determined by computing and averaging 100 FFTs of the ambient noise in the chamber. The frequency response and noise floor of the sound attenuating chamber are shown in Figure 2. The spikes seen in the chamber's noise floor spectrum are due to the chamber's ventilation fan. In

Figure 1.   A schematic diagram of the configuration of
              the testing cage housed inside the sound
              attenuating chamber.   The cage was
              constructed from hardware cloth and contained
              a response lever with a feeder chute mounted
              on it. A pellet dispenser issued food pellet
              rewards for correct responses.   A speaker
              placed outside the testing cage was used to
              present the signal tone and the masking
              noise.

SIDE VIEW OF TESTING CAGE

HARDWARE CLOTH

16"

12"

PELLET
DISPENSER

MICRO-
SWITCH

FEEDER CHUTE / RESPONSE LEVER

TOP VIEW OF TESTING CAGE

SPEAKER

PELLET
DISPENSER

FEEDER
CHUTE /

RESPONSE
LEVER

10"

16"
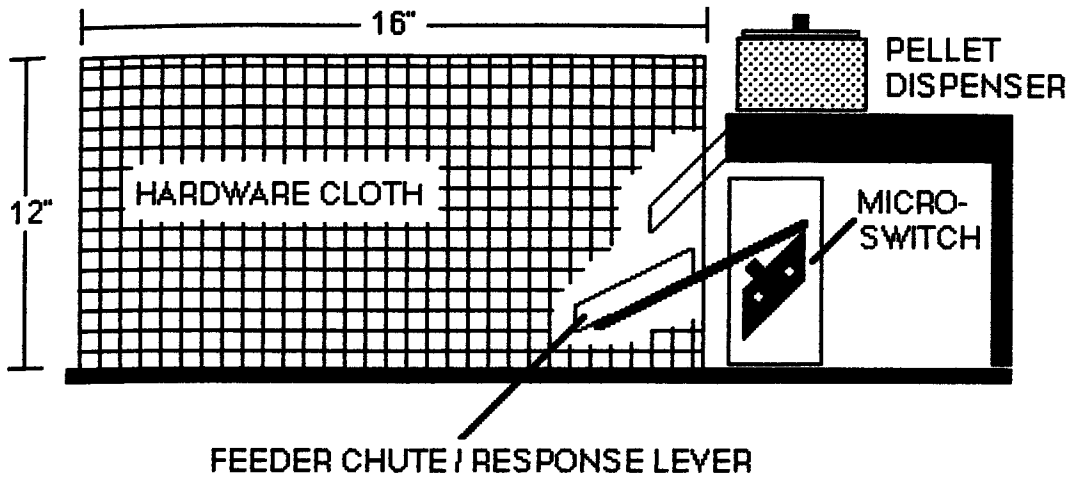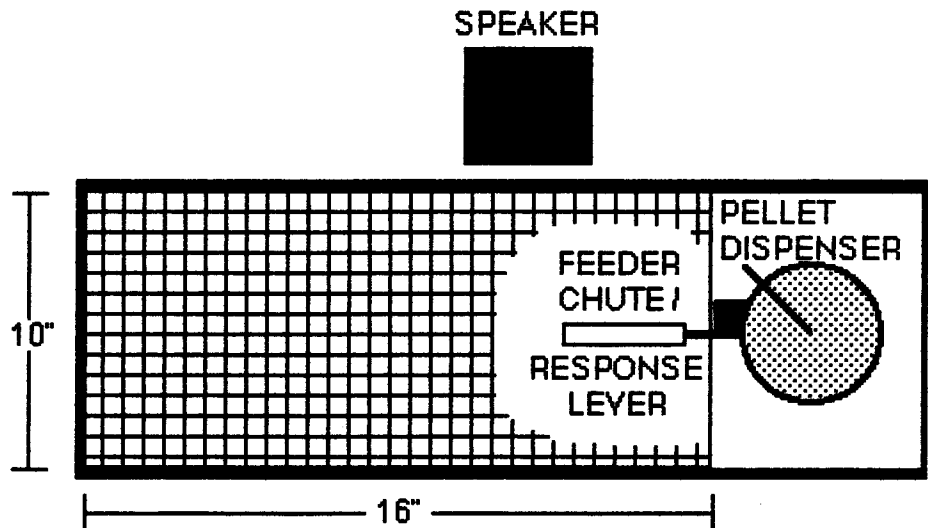
Figure 2.   The frequency response (top) and noise floor
(bottom) of the sound attenuating chamber.
The frequency response of the chamber was ± 7
dB from 250 to 10000 Hz. The spikes seen in
the noise floor spectrum are due to the
ventilation fan built into the chamber.
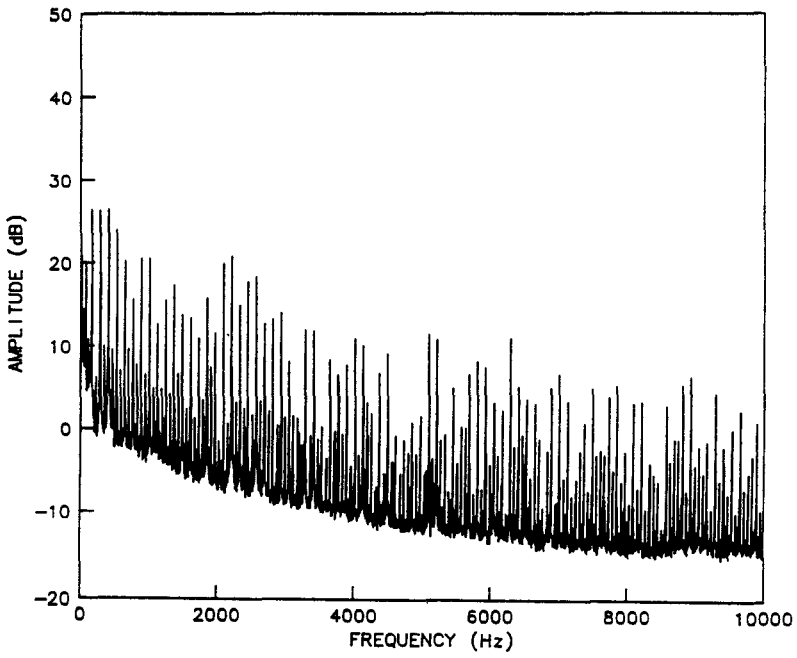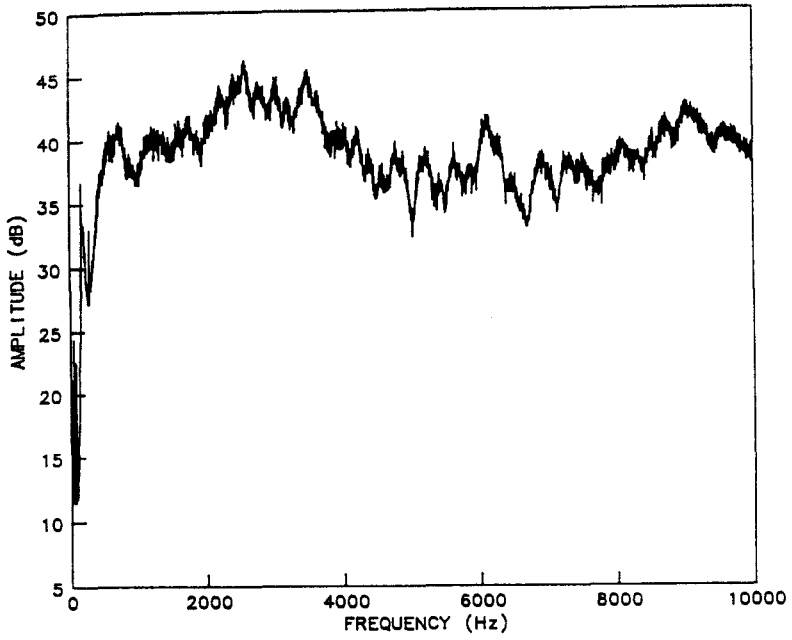
quiet, the overall noise level in the chamber was 43 dB SPL.

Figure 3 is a schematic representation of a typical trial in the adaptive tracking paradigm. To initiate a trial, the chinchilla pressed the response lever and held it down for a minimum of one-second. Following the one-second minimum hold time was a randomly determined variable hold time which lasted from 0-7 seconds. If the animal released the response lever during either the minimum or variable hold time, the entire process stopped and the computer waited for the animal to initiate a new trial. This procedure maintained the animal in a relatively fixed position so that the sound field at the animal's head did not differ greatly from trial to trial.

Once the animal held the lever past the minimum and variable hold times, a rectangular probability function determined whether a tone trial or a blank trial would be presented. During tone trials, which comprised 75% of the trials, a tonal signal was presented after the minimum and variable hold times elapsed. The chinchilla was to signal that it detected the tone by releasing the response lever. This type of correct response was classified as a hit. If a tone was presented and the animal failed to release the response lever, the incorrect response was classified as a miss. During blank trials, which comprised 25% of the

Figure 3.   Schematic representation of a typical trial
            in the positive-reinforcement adaptive
            tracking paradigm.   This figure shows the
            implementation of a two-down/one-up tracking
            rule which tracks the level that yields 70.7%
            correct detection for the tonal signal.
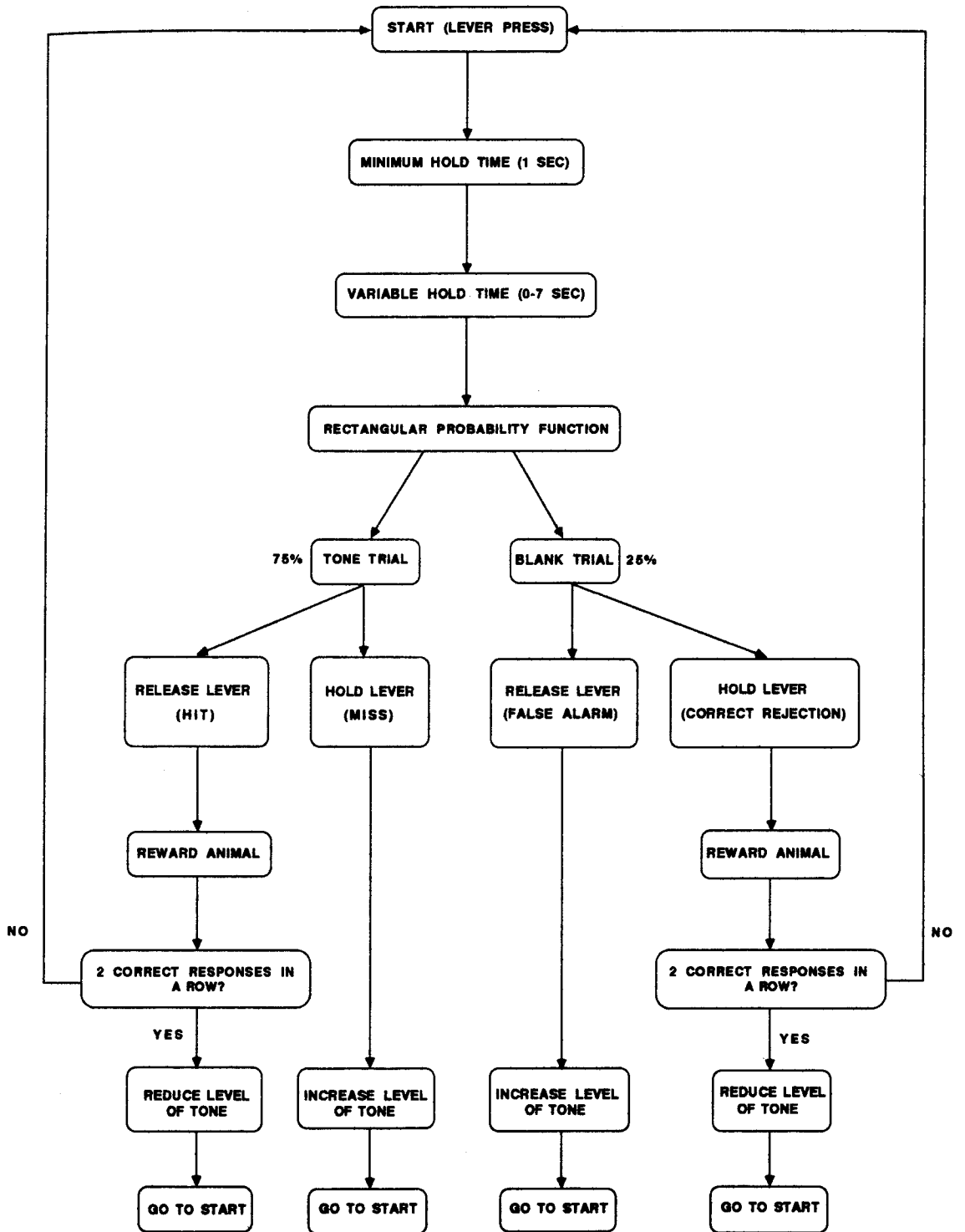
trials, a tone was not presented after the minimum and variable hold times elapsed. The chinchilla signaled that no tone was present by continuing to hold down the response lever for two seconds. This type of correct response was classified as a correct rejection. If a tone was not presented and the chinchilla released the response lever, the incorrect response was classified as a false alarm. After each correct response, either a hit or a correct rejection, the chinchilla was rewarded with a food pellet. Incorrect responses (misses and false alarms) were not rewarded.

The paradigm employed in this study used a two-down/one-up tracking rule. That is, the level of the tone was reduced after two correct responses in a row and increased after each incorrect response. The two-down/one-up rule tracks the level that gives 70.7% correct detection for the tonal signal (Levitt, 1971). After the chinchilla's response to a trial was classified, the stimulus parameters were altered according to the animal's performance and the computer waited for the animal to initiate a new trial.

Animals were run in this behavioral paradigm in fixed blocks of 30 trials. The initial step size for increasing or decreasing the level of the tone was 4 dB. After the first two reversals of the attenuator, the step size for incrementing or decrementing the level of the tone was

reduced to 2 dB. The large initial step size allowed the tracking rule to quickly increase or decrease the level of the tone to the vicinity of the animal's threshold. The change to a smaller step size allowed finer tracking of the animal's performance within the vicinity of the threshold. At the end of a 30-trial block, the first two reversals of the attenuator, which took place at the larger step size, were discarded. The remaining reversals were averaged in order to estimate the animal's threshold. Between 4 and 12 reversals were averaged to obtain a threshold estimate. Across all five animals, the average number of reversals used to estimate a threshold was 8.3. Threshold estimates were measured on at least three different days. Final thresholds were the average of at least three threshold estimates measured on three different days. Typically, a final threshold is the average of five threshold estimates measured on five different days.

METHODS

Figure 4 is a schematic description of the hardware configuration for the critical masking ratio experiment. In this experiment, the masker was a continuous white noise generated by a Wavetek Model 132 noise generator. The noise was filtered by a Krohn-Hite 3550 filter with 24

Figure 4.   A schematic description of the hardware

configuration for the critical masking ratio

experiment.
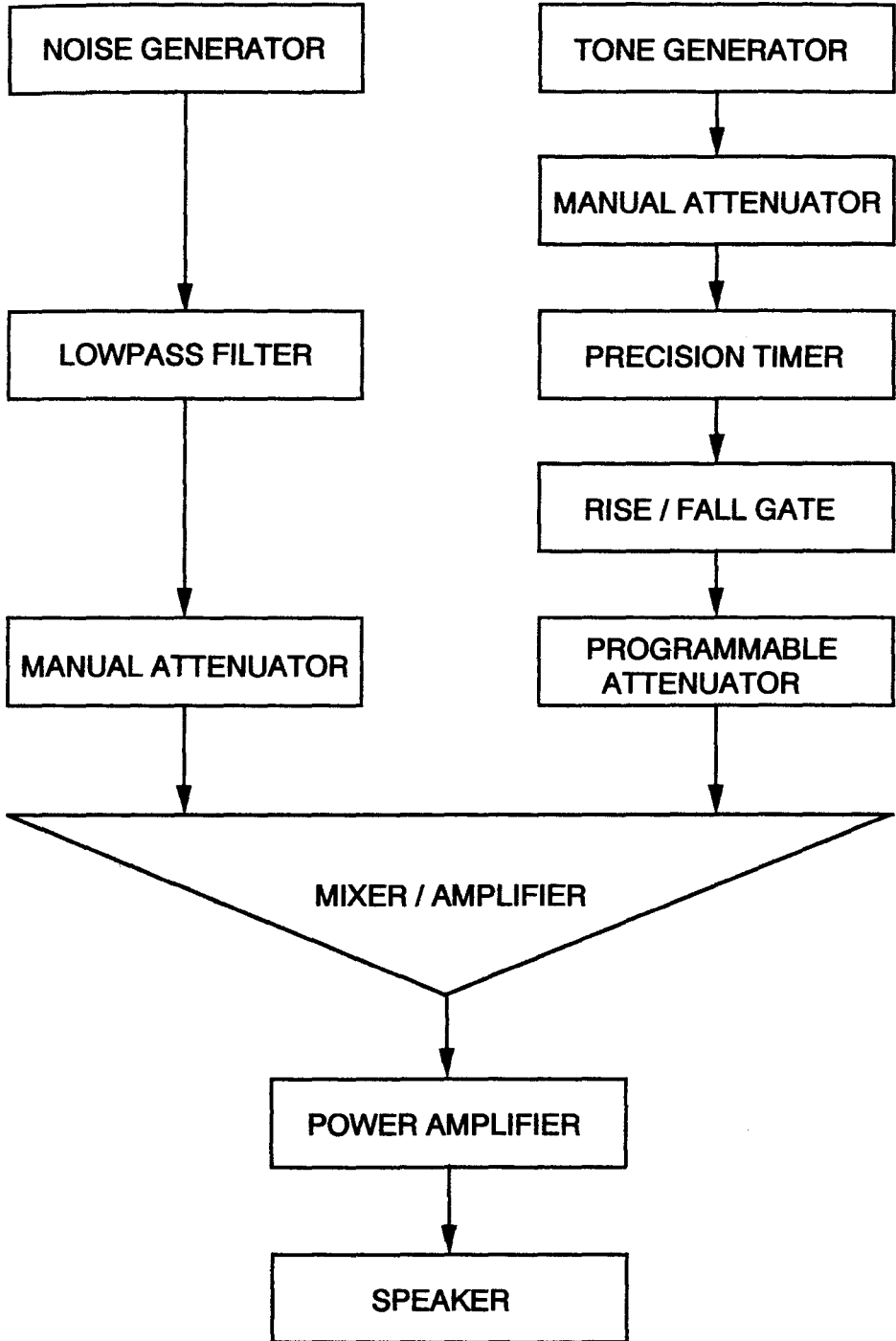
dB/octave rolloff such that it was two octaves wide. The overall level of the noise was adjusted so that its pressure spectrum level (N_0) was 40 dB/Hz. The signal, a one-second pure tone at the center frequency of the noise masker, was generated by a Hewlett-Packard 3312A function generator. The signal was gated on and off with a 20-msec linear ramp by a Coulbourn S84-04 Shaped Rise-Fall Gate. A Coulbourn S85-08 Programmable Attenuator under computer control increased and decreased the level of the tonal signal according to the animal's performance. The signal and masker were mixed using a Coulbourn S82-24 Mixer/Amplifier. The mixed stimuli were amplified by a Bryston 2BLP power amplifier and presented in the sound attenuating chamber via a Realistic Minimus 3.5 speaker.

Masked thresholds for each of the five chinchillas were measured using the behavioral adaptive tracking paradigm described above at signal frequencies of 500, 1000, 2000, 4000, and 8000 Hz. Each chinchilla was run at each signal frequency for at least five days. A typical day's data collection for a chinchilla involved 5 sets of 30 trials, one set at each signal frequency. If the animal responded to more than 20% of the catch trials in a set of 5 blocks, the data from that session were discarded. Typical false alarm rates were below 15%. Critical masking ratios were computed for each chinchilla by subtracting the spectrum

level of the masker (N_0) from the level of the chinchilla's threshold signal.

RESULTS

The critical masking ratios for each of the five chinchillas are shown in Figure 5. Critical masking ratios are plotted as a function of signal frequency at 500, 1000, 2000, 4000, and 8000 Hz. As can be seen from the data, the five chinchillas in this study show very little variability in their critical masking ratios.

Also plotted in this figure are critical masking ratios measured by Miller (1964) and Seaton and Trahiotis (1975). Both Miller (1964) and Seaton and Trahiotis (1975) used shock-avoidance paradigms to measure critical masking ratios. As can be seen in Figure 5, the data from the chinchillas in this study are comparable to those measured using shock-avoidance techniques. On the average, the data measured using the positive-reinforcement behavioral tracking technique were between 2.8 and 8.3 dB higher than those measured using negative reinforcement techniques.

The critical masking ratios shown in Figure 5 were used to compute critical bandwidths. These measures of critical bandwidth are shown in Table 1. The uncorrected measures of critical bandwidth, shown in the top panel of Table 1,

Figure 5.   The critical masking ratios for the five
              chinchillas in this study (C1 CMR - C5 CMR)
              are plotted along with the critical masking
              ratios   measured   using   shock-avoidance
              paradigms (Miller, 1964 and Seaton and
              Trahiotis, 1975).   The   data   from   the
              chinchillas in this experiment are comparable
              to those measured using shock-avoidance
              techniques.

CRITICAL MASKING RATIOS FOR THE CHINCHILLA

Legend:
- MILLER ('64)
- STN&TRAH('75)
- C1 CMR
- C2 CMR
- C3 CMR
- C4 CMR
- C5 CMR

No = 40 dB

CRITICAL MASKING RATIO (dB) vs FREQUENCY (HZ)
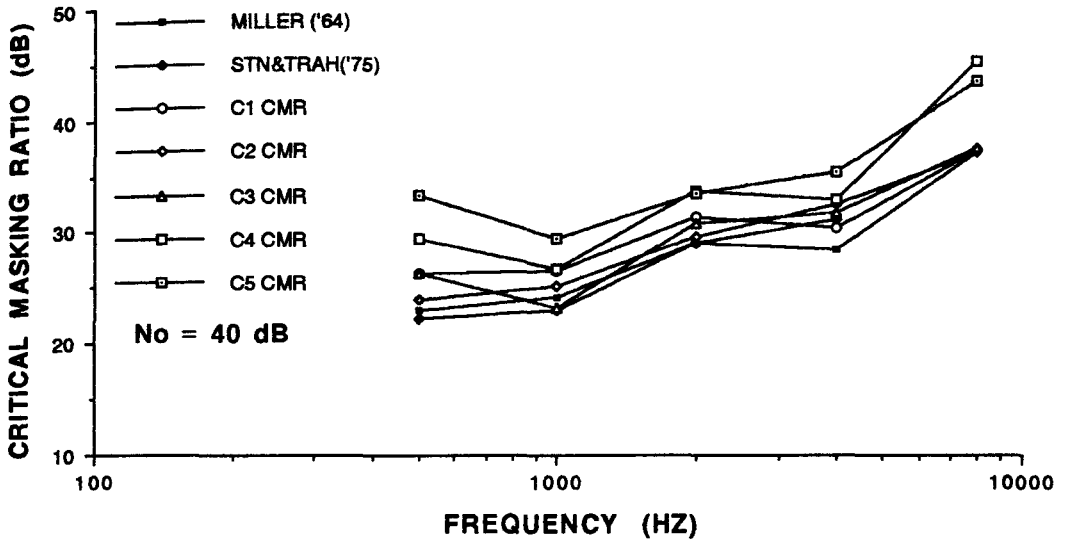
were computed by taking the antilog of the critical masking ratio (CBW (Hz) = $10^{\frac{CMR}{10}}$). These measures were corrected by multiplying the antilog of the critical masking ratio by 2.5 because, in humans, the critical ratio above 200 Hz turns out to be 2.5 times smaller than the critical band (Scharf, 1970). The corrected measures of the critical bandwidth are shown in the bottom panel of Table 1. The critical bandwidths computed in Table 1 indicate that, according to this technique, the chinchilla is very broadly tuned and has quite poor frequency selectivity.

Table 1.   Critical bandwidths (CBWs) derived from the critical masking ratio (CMR) data. The uncorrected critical bandwidths shown in the top panel of the table were computed by taking the antilog of the critical masking ratio $[CBW\ (Hz) = 10^{\frac{CMR}{10}}]$. The corrected critical bandwidths shown in the bottom panel of the table were computed by multiplying the antilog of the critical masking ratio by 2.5.

Critical Bandwidths (Hz) Derived from

Critical Masking Ratios

Uncorrected Critical Bandwidths (Hz)

Signal Frequency (Hz)

Subject	500	1000	2000	4000	8000
C1	417	437	1318	1047	5370
C2	251	316	912	1738	5012
C3	417	209	1148	1265	5495
C4	871	457	2291	1905	33113
C5	2089	871	2188	3467	21878

Corrected Critical Bandwidths (Hz)

Signal Frequency (Hz)

Subject	500	1000	2000	4000	8000
C1	1043	1093	3295	2618	13425
C2	628	790	2280	4345	12530
C3	1043	523	2870	3163	13738
C4	2178	1143	5728	4763	82783
C5	5223	2178	5470	8668	54695

CHAPTER III

DERIVING FILTER SHAPES USING RIPPLED NOISE

Houtgast (1974, 1977) took advantage of linear system analysis and the spectral shape of rippled noise to derive estimates of auditory filter shape in a masking experiment. Rippled noise is a complex, non-periodic stimulus with a cosinusoidal intensity spectrum. For the purpose of estimating auditory filter shapes, there are four types of rippled noise: (1) Cosine Positive (Cos+), (2) Cosine Negative (Cos-), (3) Sine Positive (Sin+), and (4) Sine Negative (Sin-).

Cos+ rippled noise is generated by delaying a source of wideband noise (which has a continuous, flat spectrum) by some amount (τ sec) and adding the output of the delay back to the original noise source. This results in a continuous masking noise with a cosinusoidal intensity spectrum in which spectral peaks occur at integer multiples of $1/\tau$. Cos- rippled noise is generated by subtracting the delayed

Figure 6.   A schematic depicting the circuit used to
              generate the rippled noise masker.   Cos+
              rippled noise is generated by adding the
              delayed noise back to the undelayed noise
              source.   Cos- rippled noise is generated by
              subtracting the delayed noise from the
              undelayed noise source. Sin+ rippled noise
              can be approximated by generating cos+
              rippled noise and adjusting the delay so that

              it is 1.25(τ).   Sin- rippled noise can be

              approximated by generating cos- rippled
              noise, and adjusting the delay so that it is

              also 1.25(τ).

GENERATING RIPPLED NOISE
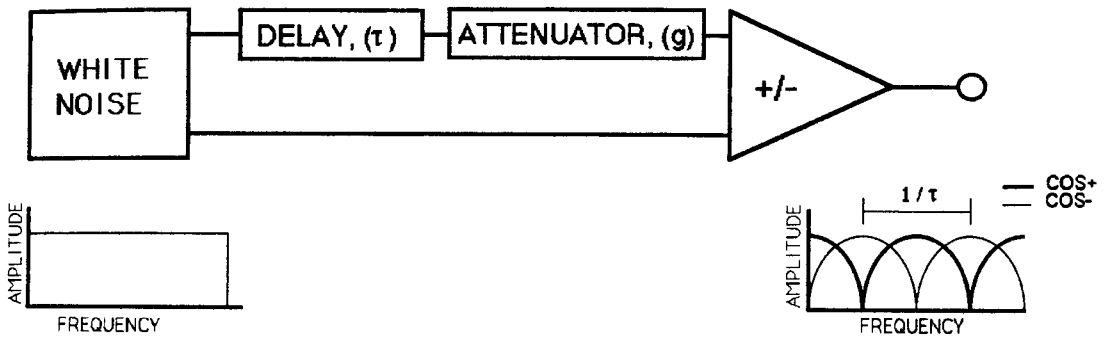
version of the noise from the undelayed noise source. For cos- rippled noise, spectral valleys occur at integer multiples of $1/\tau$. Figure 6 is a diagram depicting the circuit used in the generation of cos+ and cos- rippled noise.

The intensity spectrum, $I(f)$, of rippled noise is:

(1) $I(f) = \overline{I}(1 \pm m \cos(2\pi\tau(f-f_t)))$,

where $\overline{I}$ is the average rippled noise intensity and m is the modulation or ripple depth ($m = 2g/(1+g^2)$, where g is the attenuation of the delayed noise).

There are four parameters of the rippled noise masker which are important when estimating auditory filter shape: (1) $\overline{I}$, the average intensity of the rippled noise, which is the intensity half-way between a peak and a valley; (2) τ, the delay (in seconds), determines the ripple density in terms of frequency (f) (For the purposes of this study, ripple density (n) will be defined as the number of ripples between $f=0$ and f_t, the signal frequency. That is, $n = \tau * f_t$.); (3) the phase ($\pm$), of the ripple at $f=0$, which is determined by the polarity of the delayed noise (addition or subtraction); and (4) the ripple depth, g, which is determined by the attenuation of the delayed noise. The depth of the rippled noise spectrum is a function of the

amplitude of the delayed noise. As the attenuation of the delayed noise increases, the ripple depth decreases.

Houtgast (1974, 1977) measured masked thresholds for a pure tone signal masked by both cos+ and cos- rippled noise as a function of the ripple density. By subtracting the masked thresholds for cos- rippled noise from the masked thresholds for cos+ rippled noise as a function of ripple density, Houtgast measured a cosine masking function, C(d), from which he could derive auditory filter shape. In order to determine whether the auditory filter is symmetric about the signal frequency (f_t), Houtgast also measured two additional conditions. In the first condition, Houtgast shaped the spectrum of the rippled noise masker such that the signal frequency was half-way between the peak and valley on the positive-going slope of the rippled noise spectrum. This is the condition referred to as sin+. In the second condition, Houtgast shaped the spectrum of the rippled noise masker such that the signal frequency was half-way between the peak and valley on the negative-going slope of the rippled noise. This is the condition referred to as sin-. By measuring a sine masking function, S(d), using sin+ and sin- rippled noise as maskers, it is possible to determine the symmetry of the auditory filter.

In order to estimate the shape of the auditory filter function from the rippled noise masking functions, Houtgast

assumed that the power in the signal at masked threshold was proportional to the power in the noise passed by the filter. Since the effective masker can be thought of as the convolution of a filter function, $F(f,f_t)$, and a masking stimulus, $S(f,f_t)$, this assumption can be expressed mathematically as:

(2) amount of masking at $f_t = \int_{-\infty}^{\infty} F(f,f_t) \, S(f,f_t) \, df$.

In this study, rippled noise ($R(f,f_t)$) will be used as the masking stimulus and a weighting or filter function, $W(f,f_t)$, will be derived from the masking functions $C(d)$ and $S(d)$. Given the spectrum in Eq. (1), the intensity of the rippled noise within the filter $W(f,ft)$ can be determined by convolving the rippled noise spectrum with the weighting function:

(3) amount of masking at $f_t = \int_{-\infty}^{\infty} W(f,f_t) \, R(f,f_t) \, df$.

However, because $R(f,f_t)$ and $W(f,f_t)$ can be Fourier transform pairs, $W(f,f_t)$ can be written as:

(4) $W(f,f_t) = 1 + \sum_{1}^{\infty} a_n \cos(2\pi n(f-f_t)/f_t) + \sum_{1}^{\infty} b_n \sin(2\pi n(f-f_t)/f_t)$,

where n is the ripple density and the coefficients a_n and b_n can be derived from the masking functions $C(d)$ and $S(d)$, respectively.

If $E_+(\tau)$ and $E_-(\tau)$ are the noise intensities within a weighting function, $W(f,f_t)$, for the cos+ and cos- rippled noises, respectively, then by convolution of $I(f)$ with $W(f,f_t)$ the level difference (in dB) between the cos+ and the cos- conditions, $C(d)$, can be written as:

(5) $C(d) = 10 \log(E_+(\tau)/E_-(\tau))$.

If it is further assumed that the filter is located within the range $0.5(f_t)$ to $1.5(f_t)$, in that $W(f,f_t) = 0$ for $0.5(f_t) \leq f \geq 1.5(f_t)$, then:

$$E_+(\tau) = \int_{0.5f_t}^{1.5f_t} (1+m\cos 2\pi\tau((f-f_t)/f_t)\ W(f,f_t)\ df \text{ and}$$

$$E_-(\tau) = \int_{0.5f_t}^{1.5f_t} (1-m\cos 2\pi\tau((f-f_t)/f_t)\ W(f,f_t)\ df.$$

By substituting Eq.(4) into Eq.(5), when $\tau = n$, Eq.(5) can be reduced to:

$$(6)\quad C(n) = 10\ \log\frac{1+\frac{m}{2}\ a_n}{1-\frac{m}{2}\ a_n}.$$

Solving for a_n:

$$(7)\quad a_n = \frac{2}{m}\ \frac{10^{\frac{C(n)}{10}} - 1}{10^{\frac{C(n)}{10}} + 1}.$$

solving for b_n:

(8) $\quad b_n = \dfrac{2}{m} \dfrac{10^{\frac{S(n)}{10}} - 1}{10^{\frac{S(n)}{10}} + 1}.$

Eqs.(7) and (8), therefore, allow the derivation of a set of a_n and b_n coefficients from the C(d) and S(d) masking functions. W(f,ft), the auditory filter shape, can then be obtained from Eq.(4). Therefore, by an application of Fourier analysis to the rippled noise masking functions and under the assumption of linearity, it is possible to estimate the shape of the auditory filter.

As mentioned above, the spacing or density of the peaks and valleys in the rippled noise spectrum is a function of the delay (τ). At very short delays, the peaks and valleys are at a low density. That is, they are spaced far apart in frequency. As the delay increases, so does the ripple density. Increasing the ripple density causes the peaks and valleys to move closer together in frequency. The term "ripple density", as it is used in this study, will be defined as the number of ripples between f=0 and f_t, the signal frequency. By measuring masked thresholds for a pure tone signal masked by both cos+ and cos- rippled noise as a function of ripple density and by then subtracting the cos- masked thresholds from the cos+ masked thresholds, it

is possible to obtain the cosine masking function C(d). By measuring masked thresholds for a pure tone signal masked by both sin+ and sin- rippled noise as a function of ripple density and by subtracting the sin- masked thresholds from the sin+ masked thresholds, it is possible to measure the sine masking function S(d).

Figure 7 illustrates how cos+ and cos- rippled noise can be used to derive the cosine masking function, C(d) for a particular signal frequency. The top left figure shows the spectrum of cos+ rippled noise at a low ripple density. Superimposed on this spectrum is a hypothetical auditory filter (the triangle) centered at some signal frequency. The shaded area represents the amount of noise coming through the filter. In this case, the filter contains the maximal amount of noise and, therefore, the threshold for the signal frequency will be high. The bottom left figure shows the spectrum of cos- rippled noise at the same ripple density. Superimposed on this spectrum is the same auditory filter centered at the same signal frequency. The shaded area again represents the amount of noise coming through the filter. In this cos- case there is much less noise coming through the filter than in the cos+ case and, therefore, the threshold for the signal frequency will be low. If the threshold for the cos-, low density condition is subtracted from the threshold for the cos+, low density

Figure 7.   The use of cos+ and cos- rippled noise
              maskers as a function of ripple density to
              derive C(d), the cosine masking function.
              See the text for a detailed explanation of
              the derivation of the cosine masking function.

COSINE POSITIVE, LOW DENSITY
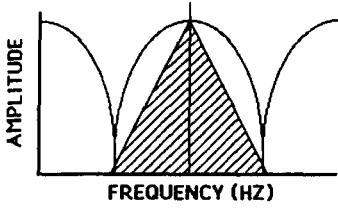
COSINE POSITIVE, HIGH DENSITY
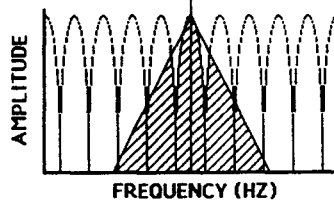
COSINE NEGATIVE, LOW DENSITY
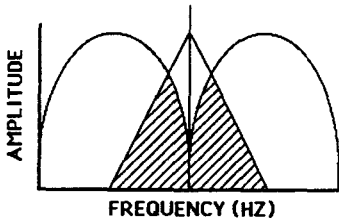
COSINE NEGATIVE, HIGH DENSITY
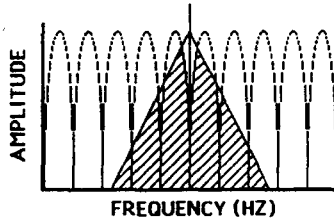
THEREFORE,

COSINE POSITIVE THRESHOLD
- COSINE NEGATIVE THRESHOLD
LARGE THRESHOLD DIFFERENCE

THEREFORE,

COSINE POSITIVE THRESHOLD
- COSINE NEGATIVE THRESHOLD
SMALL THRESHOLD DIFFERENCE

condition, the resulting threshold difference is relatively large. The top right figure shows the amount of noise coming through the filter for a cos+, high density condition. The bottom right figure shows the amount of noise coming through the filter for a cos-, high density condition. Since both of these conditions have about the same amount of noise coming through the filter, the thresholds for the signal frequency should be about the same. If the threshold for the cos-, high density condition is subtracted from the threshold for the cos+, high density condition, the resulting threshold difference is relatively small. Therefore, at low ripple densities, a relatively large threshold difference can be expected. As ripple density increases, the threshold difference should decrease until it finally asymptotes at zero.

Figure 8 shows the general form of the masking functions derived using cos+ and cos- rippled noise. This figure simply plots the expected threshold difference between the cos+ and cos- conditions as a function of ripple density. Two hypothetical masking functions are plotted in this figure. The masking function plotted with the thicker line reaches an asymptote rather quickly and reflects poor frequency resolution as a function of ripple density (a broad filter). The masking function plotted with the thinner line reaches an asymptote more slowly and

Figure 8.   The general form of the cosine masking

function, C(d), which is the threshold

difference between the cos+ and cos-

conditions.   The masking function plotted

with the thick line reflects poor frequency

resolution whereas the masking function

plotted with the thin line reflects better

frequency resolution.

HYPOTHETICAL RIPPLED NOISE MASKING FUNCTIONS
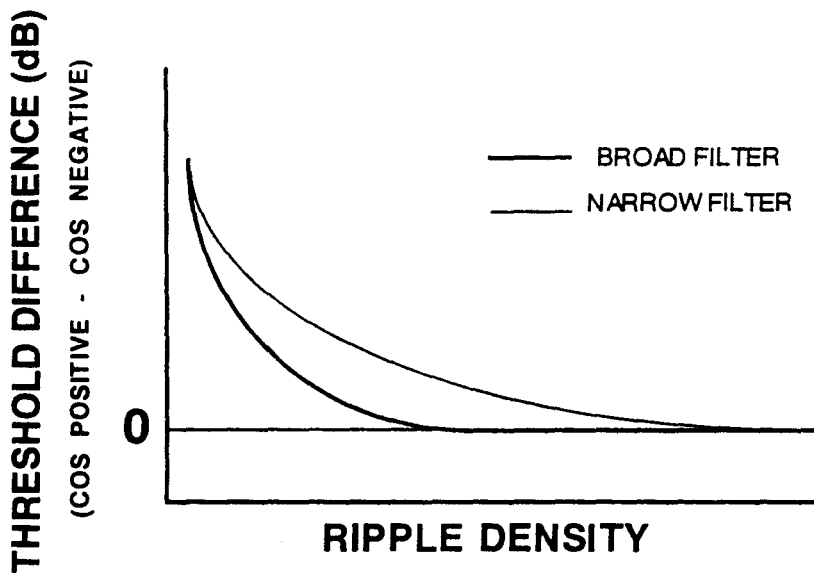
reflects better frequency resolution as a function of ripple density (a narrower assumed internal filter). In essence, the masking function shows the extent to which the auditory system can resolve the sinusoidal modulation of the rippled noise masker.

Theoretically, testing the symmetry of the auditory filter requires sin+ and sin- rippled noise. In practice, these two types of rippled noise are difficult to generate. However, sin+ and sin- rippled noise can be approximated by adjusting the delays of the cos+ and cos- rippled noise. The sin+ condition can be approximated by generating cos+ rippled noise and adjusting the delay such that it is 1.25(τ). The sin- condition can be approximated by generating cos- rippled noise and adjusting the delay such that it is 1.25(τ).

Figure 9 illustrates how the approximated sin+ and sin- rippled noise conditions can be used to derive a sine masking function for a particular signal frequency. The top left figure shows the spectrum of sin+ rippled noise at a low ripple density. Superimposed on this spectrum is the hypothetical auditory filter (the triangle) centered at the signal frequency. The shaded area again represents the amount of noise coming through the filter and the threshold for the signal frequency is again related to the amount of

Figure 9.   The use of approximated sin+ and sin- rippled
             noise maskers as a function of ripple density
             to derive S(d), the sine masking function.
             See the text for a detailed explanation of
             the derivation of the sine masking function.

SINE POSITIVE, LOW DENSITY

SINE NEGATIVE, LOW DENSITY
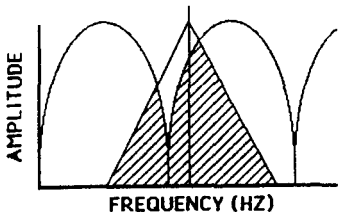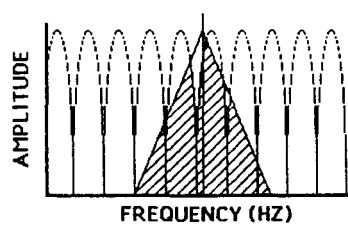
SINE POSITIVE, HIGH DENSITY
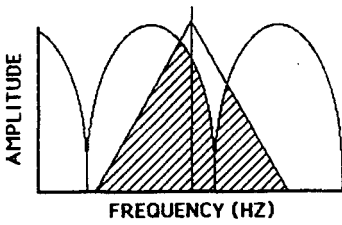
SINE NEGATIVE, HIGH DENSITY
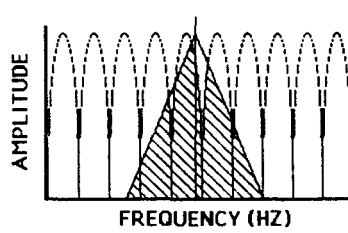
THEREFORE,

SINE POSITIVE THRESHOLD
- SINE NEGATIVE THRESHOLD
NO THRESHOLD DIFFERENCE

THEREFORE,

SINE POSITIVE THRESHOLD
- SINE NEGATIVE THRESHOLD
NO THRESHOLD DIFFERENCE

noise coming through the filter. The bottom left figure shows the spectrum of sin- rippled noise at the same ripple density. Superimposed on this spectrum is the same auditory filter centered at the same signal frequency. Both the sin+ and sin- low density conditions have the same amount of noise coming through the filter. Therefore, the thresholds for these two conditions should be identical. If the threshold for the sin-, low density condition is subtracted from the threshold for the sin+, low density condition, the resulting threshold difference is zero. This can only be true if the filter is symmetrical because only then will the two conditions yield the same thresholds. If the filter is asymmetrical, there will be some threshold difference between the sin+ and sin- conditions. The right half of Figure 9 shows that this relationship remains true as a function of ripple density. That is, if the filter is symmetrical, the threshold difference will be zero despite the increase in ripple density. Therefore, if the auditory filter is symmetrical about the signal frequency, the sin+ thresholds should be identical to the sin- thresholds.

Therefore, by measuring C(d), the cosine masking function and S(d), the sine masking function and by making the assumptions of linearity and constant filter output; a filter characteristic (intensity weighting function),

$W(f, f_t)$, which would give the same masking functions can be specified. If it is further assumed that the weighting function is located within the range $0.5(f_t)$ to $1.5(f_t)$ in that $W(f, f_t) = 0$ for $0.5(f_t) \leq f \geq 1.5(f_t)$, then the filter can be written as stated previously in Eq. (4).

CHAPTER IV

EXPERIMENT 2 - AUDITORY FILTER SHAPES

Houtgast (1974, 1977) derived estimates of auditory filter shape in a masking experiment by taking advantage of linear systems analysis and the spectral shape of rippled noise. This experiment involves measuring auditory filter shapes in five to six chinchillas allowing for a comparison of frequency selectivity between humans and chinchillas and for a comparison between indirect measures of frequency selectivity (critical ratios) and more direct measures of frequency selectivity (rippled noise masking) within the chinchillas.

METHODS

Figure 10 is a schematic description of the hardware configuration for the rippled noise masking experiment. In this experiment, the masker was a continuous rippled noise. As described in Chapter III, the rippled noise masker was generated by delaying a wideband noise and either adding

53

Figure 10.   A schematic description of the hardware
configuration for the rippled noise masking
experiment.
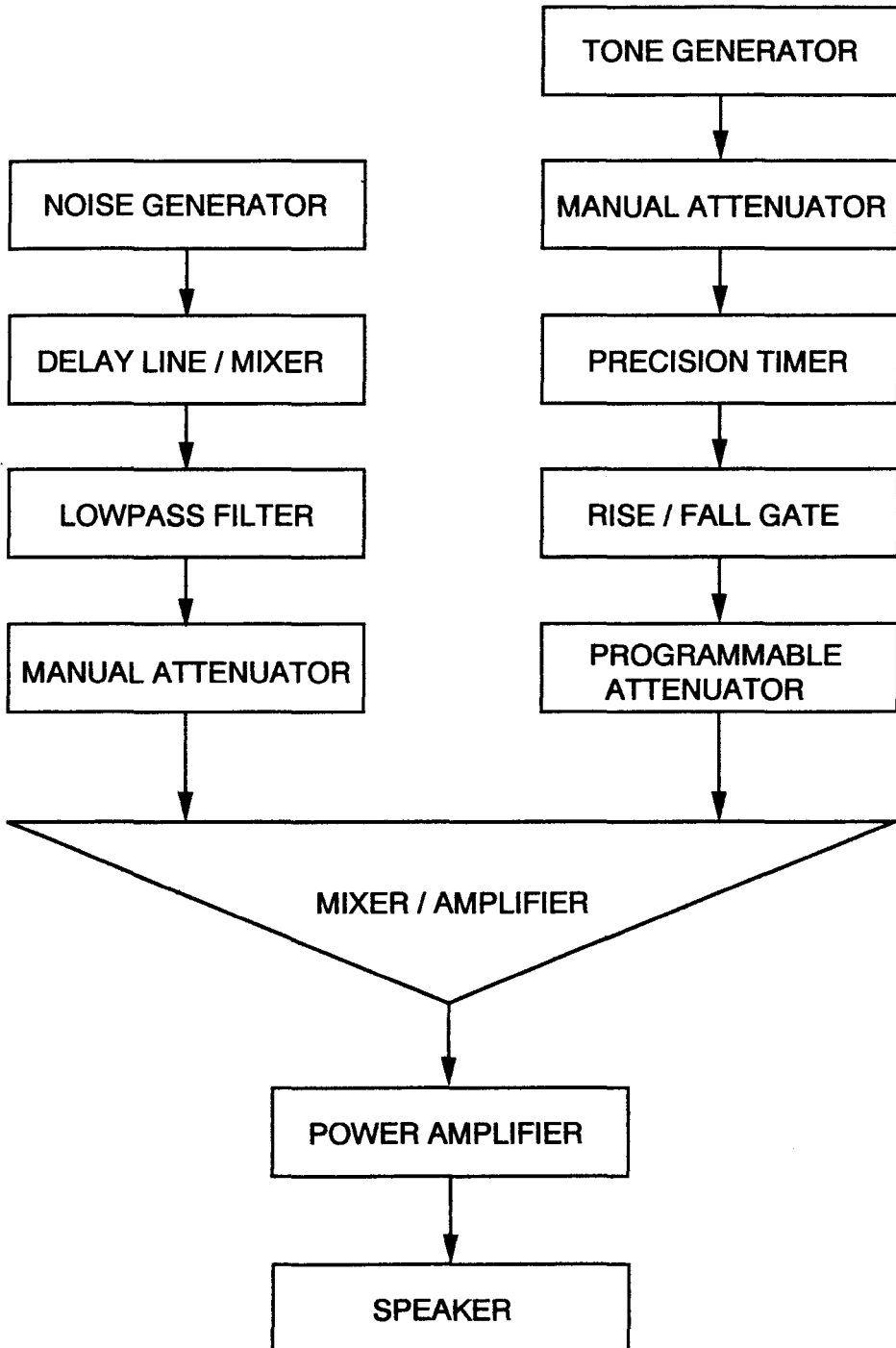
the output of the delay to the original noise source or subtracting the output of the delay from the original noise source. The wideband noise source was a Wavetek Model 132 noise generator. The delay line was a Reticon analog delay with a built-in attenuator and mixer. The rippled noise masker was filtered by a Krohn-Hite 3550 filter with 24 dB/octave rolloff such that it was two octaves wide, centered on the signal frequency. The overall level of the rippled noise was adjusted so that a flat noise at the same overall level would have a pressure spectrum level (N_0) of 43 dB/Hz. The signal, a one-second pure tone at the center frequency of the rippled noise masker, was generated by a Hewlett-Packard 3312A function generator. The signal was gated on and off with a 20-msec linear ramp by a Coulbourn S84-04 Shaped Rise-Fall Gate. A Coulbourn S85-08 Programmable Attenuator under computer control increased and decreased the level of the tonal signal according to the animal's performance. The signal and masker were mixed using a Coulbourn S82-24 Mixer/Amplifier. The mixed stimuli were amplified by a Bryston 2BLP power amplifier and presented in the sound attenuating chamber via a Realistic Minimus 3.5 speaker.

The chinchillas' auditory filter shapes were estimated from masking functions derived from the thresholds measured

in this rippled noise masking experiment. Masking functions were measured for signal frequencies of 500, 1000, and 2000 Hz.

The cosine masking function, C(d), was derived by measuring each animal's masked threshold for a pure tone signal masked by both cos+ and cos- rippled noise as ripple density, n, was varied between 1 and 6. The cosine masking functions were obtained by subtracting the animals' cos-masked thresholds from their cos+ masked thresholds as a function of ripple density. In many cases, data on the cosine limit condition, n = 0, were also collected. The cosine, n = 0 condition is a flat noise masker for which the peak-to-trough difference is equal to the peak-to-trough difference of the cosine rippled noise at the signal frequency. In this experiment the peak-to-trough difference between cos+ and cos- rippled noise maskers at the signal frequency was 23 dB, therefore, the cos+, n = 0 data point corresponds to the threshold for the signal masked by a flat noise at the same level as the cos+ rippled noise masker. The cos-, n = 0 data point corresponds to the threshold for the signal masked by the flat noise after the noise had been attenuated by 23 dB. This n = 0 threshold difference is not used to estimate auditory filter shape, except in the case of the 2000 Hz signal frequency for which the delay line could not

generate the 500 μsec delay needed to collect data for the cos+ and cos-, n = 1 condition. For this signal frequency, the cosine, n = 1 threshold difference was estimated by a second order polynomial regression on the remaining threshold differences in the cosine masking function (n = 0, 2, 3, 4, 5, and 6). A second order polynomial regression was used to estimate the 2000 Hz cosine, n = 1 threshold difference because the cosine masking functions for 500, 1000, and 2000 Hz tended to be shaped like a second order polynomial.

The sine masking functions, S(d), were derived by measuring each animal's masked thresholds for pure tone signals masked by both sin+ and sin- rippled noise as ripple density, n, was varied between 1 and 6. As explained in the previous chapter, the sin+ and sin- rippled noise were approximated by generating cosine rippled noise in the appropriate phase (either + or -) and adjusting the delay such that it is 1.25(τ). Therefore, in this experiment, the sine masking functions were generated using the approximated sin+ and sin- rippled noise. The sine masking functions were obtained by subtracting the animals' sin- masked thresholds from their sin+ masked thresholds as a function of ripple density. The sine, n = 0 condition is a flat noise masking condition for which the peak-to-trough difference is equal to the peak-to-trough

difference of the sine rippled noise at the signal frequency. In this experiment the peak-to-trough difference between sin+ and sin- rippled noise maskers at the signal frequency was 0 dB, therefore, the sin+, $n = 0$ data point corresponds to the threshold for the signal masked by a flat noise at the same level as the sin+ rippled noise masker. The sin-, $n = 0$ data point corresponds to the threshold for the signal masked by the flat noise after an attenuation of 0 dB. Therefore, in theory, the sine, $n = 0$ threshold difference will always be 0 dB. These sine, $n = 0$ threshold differences are not used to estimate auditory filter shape, however, in the case of the 2000 Hz signal frequency the delay line could not generate the 625 μsec delay needed to collect data for the sin+ and sin-, $n = 1$ condition. For this signal frequency, the $n = 1$ threshold difference was estimated by a linear regression on the remaining threshold differences in the sine masking function ($n = 0$, 2, 3, 4, 5, and 6). A linear regression was used to estimate the 2000 Hz sine, $n = 1$ threshold difference because the sine masking functions for 500, 1000, and 2000 Hz tended to be linear.

A typical day's data collection for a chinchilla involved 6-7 sets of 30 trials, one set at each ripple density for either the cos+, cos-, sin+, or sin- conditions. This type of session generally lasted about

one hour. Masked thresholds for each of the five chinchillas were measured using the behavioral adaptive tracking paradigm described in Chapter II. Threshold estimates were measured on at least three different days. Final thresholds were the average of at least three threshold estimates measured on three different days. Typically, a final threshold is the average of five threshold estimates measured on five different days. If the animal responded to more than 20% of the catch trials in the set of 6-7 blocks, the data from that session were discarded. Typical false alarm rates were below 15%. Auditory filter shapes were computed for each chinchilla by using the cosine and sine masking functions to derive the a_n and b_n coefficients needed to solve Eq. (4).

RESULTS

In order to simplify the derivation of the auditory filter shapes, it was initially assumed that the filters were symmetrical about the signal frequency. This assumption simply made the b_n coefficients in Eq. (4) equal to 0 and eliminated the sine term in the equation. Therefore, Eq. (4) became

(9) $W(f,f_t) = 1 + \sum_1^\infty a_n \cos(2\pi n(f-f_t)/f_t).$

By assuming symmetry, the shapes of the auditory filters could be estimated from just the cosine masking functions as explained in Houtgast (1974). Thus, the cosine masking functions were gathered before the sine masking functions for all three signal frequencies.

Figure 11a shows the cosine data from Chinchilla 1 at a signal frequency of 500 Hz. The top panel of the figure shows the raw data from Chinchilla 1. The open symbols are the cos+ thresholds and the closed symbols are the cos- thresholds. The middle panel is the cosine masking function for the same animal. The masking function is simply the cos- threshold subtracted from the cos+ threshold as a function of ripple density. The lower panel shows the relative weighting or auditory filter function derived from this masking function. The fact that the two halves of the weighting function are mirror images is due to the assumption of symmetry. The important part of the auditory filter function is the peak which rises up out of the "noise." The "noise" reflects the fact that the data are noisy, that is, the masking function is not perfectly smooth and may not asymptote exactly at 0. In the upper left hand corner of the lower panel is the equivalent rectangular bandwidth or ERB of the filter. The ERB is

Figure 11a. The rippled noise masking data from Chinchilla 1 at a signal frequency of 500 Hz. The top panel of the figure shows the raw data from Chinchilla 1. The open symbols are the cos+ thresholds and the closed symbols are the cos- thresholds. The middle panel is the cosine masking function for the same animal. The lower panel shows the relative weighting or auditory filter function derived from this masking function as well as the equivalent rectangular bandwidth or ERB of the filter.

CHINCHILLA 1 - 500 HZ COSINE DATA
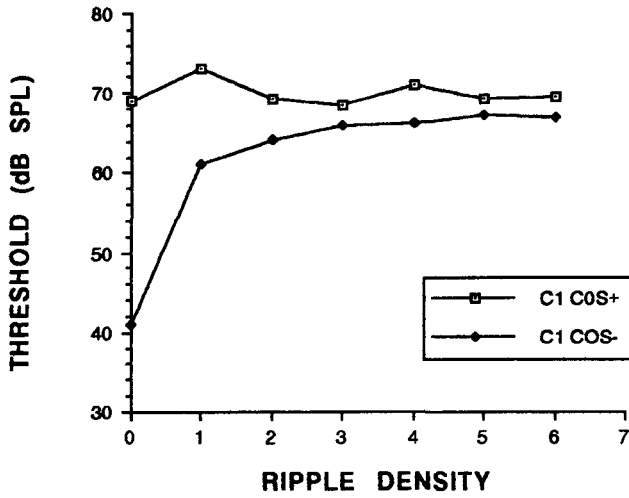
CHINCHILLA 1 - 500 HZ COSINE MASKING FUNCTION
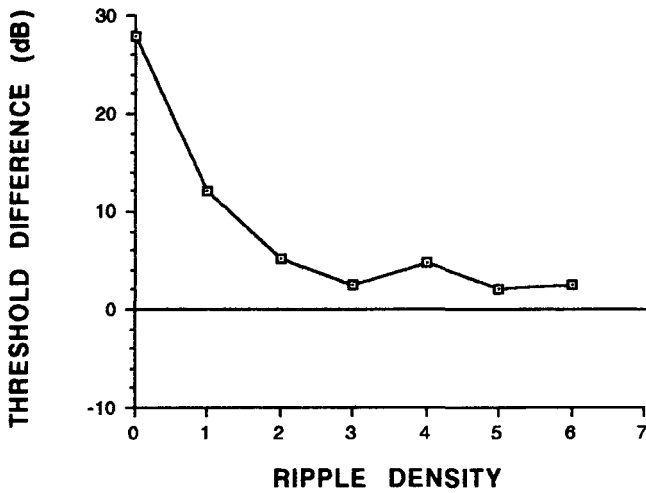
CHINCHILLA 1 - 500 HZ RELATIVE WEIGHTING FUNCTION
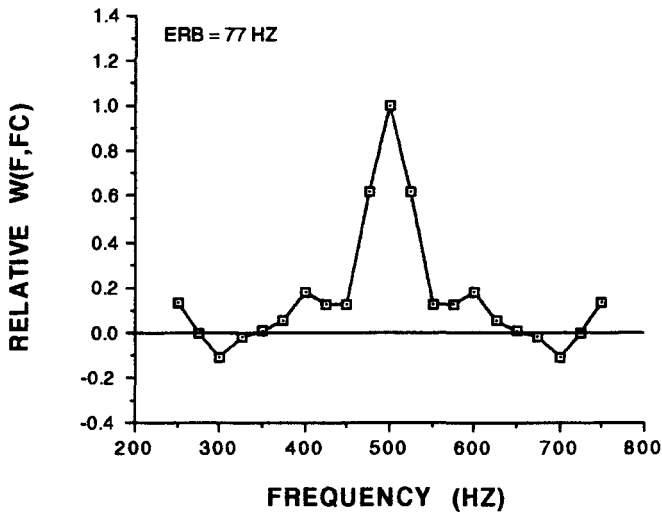
Figure 11b.   The rippled noise masking data from Chinchilla 2 at a signal frequency of 500 Hz. The top panel of the figure shows the raw data from Chinchilla 2. The open symbols are the cos+ thresholds and the closed symbols are the cos- thresholds. The middle panel is the cosine masking function for the same animal. The lower panel shows the relative weighting or auditory filter function derived from this masking function as well as the equivalent rectangular bandwidth or ERB of the filter.

CHINCHILLA 2 - 500 HZ COSINE DATA
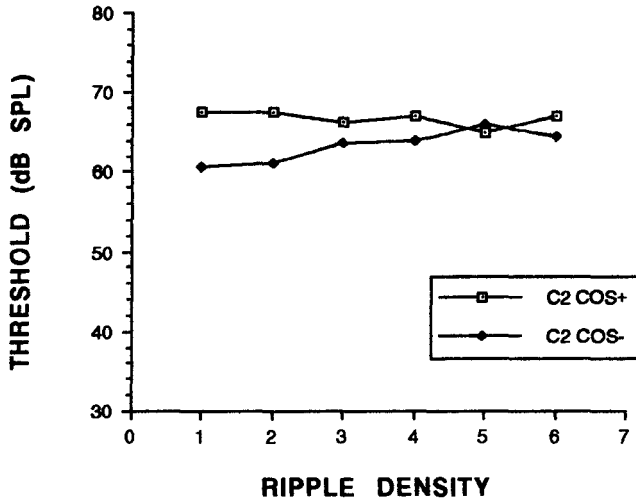
CHINCHILLA 2 - 500 HZ COSINE MASKING FUNCTION
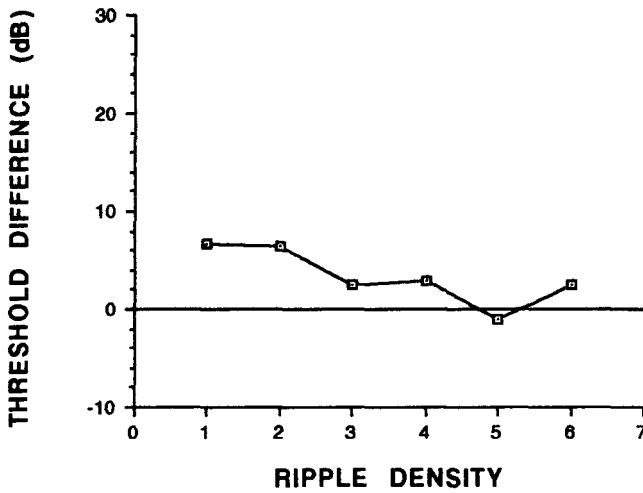
CHINCHILLA 2 - 500 HZ RELATIVE WEIGHTING FUNCTION
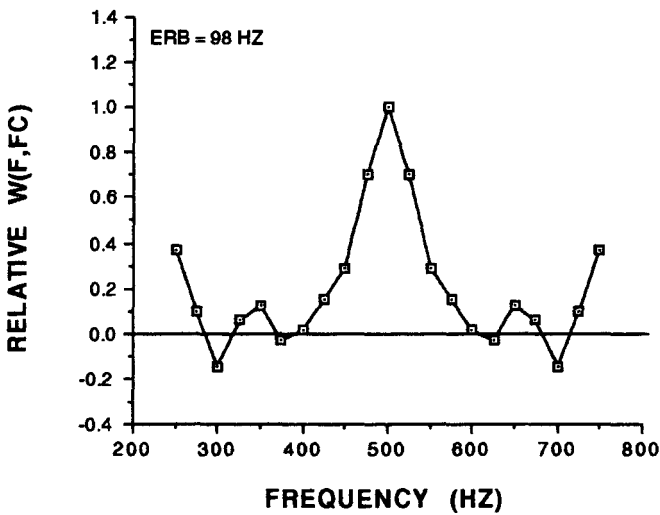
Figure 11c.   The rippled noise masking data from
                Chinchilla 3 at a signal frequency of 500 Hz.
                The top panel of the figure shows the raw
                data from Chinchilla 3. The open symbols are
                the cos+ thresholds and the closed symbols
                are the cos- thresholds. The middle panel is
                the cosine masking function for the same
                animal. The lower panel shows the relative
                weighting or auditory filter function derived
                from this masking function as well as the
                equivalent rectangular bandwidth or ERB of
                the filter.

CHINCHILLA 3 - 500 HZ COSINE DATA
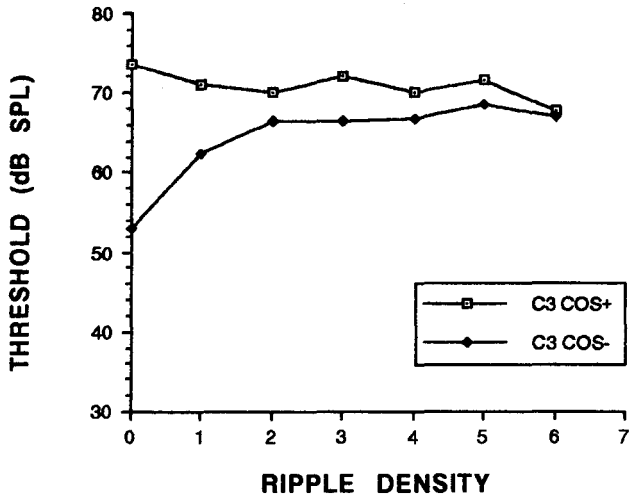
CHINCHILLA 3 - 500 HZ COSINE MASKING FUNCTION
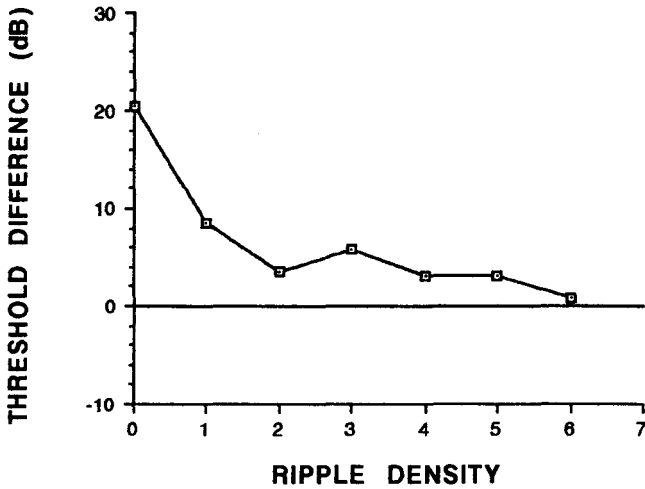
CHINCHILLA 3 - 500 HZ RELATIVE WEIGHTING FUNCTION
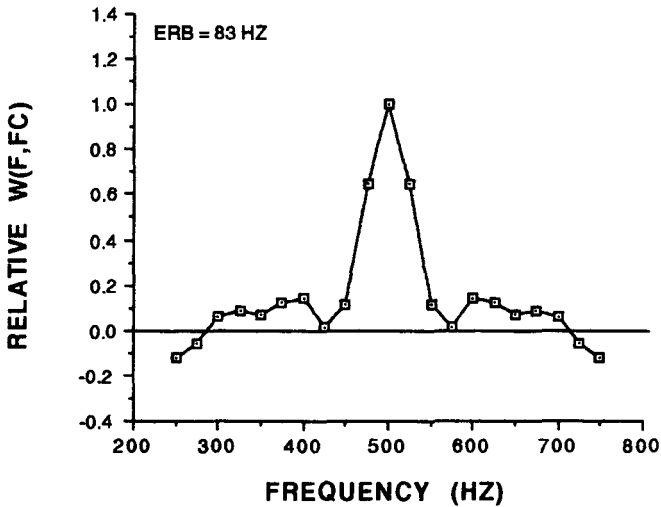
Figure 11d.   The rippled noise masking data from
               Chinchilla 4 at a signal frequency of 500 Hz.
               The top panel of the figure shows the raw
               data from Chinchilla 4. The open symbols are
               the cos+ thresholds and the closed symbols
               are the cos- thresholds. The middle panel is
               the cosine masking function for the same
               animal. The lower panel shows the relative
               weighting or auditory filter function derived
               from this masking function as well as the
               equivalent rectangular bandwidth or ERB of
               the filter.

CHINCHILLA 4 - 500 HZ COSINE DATA
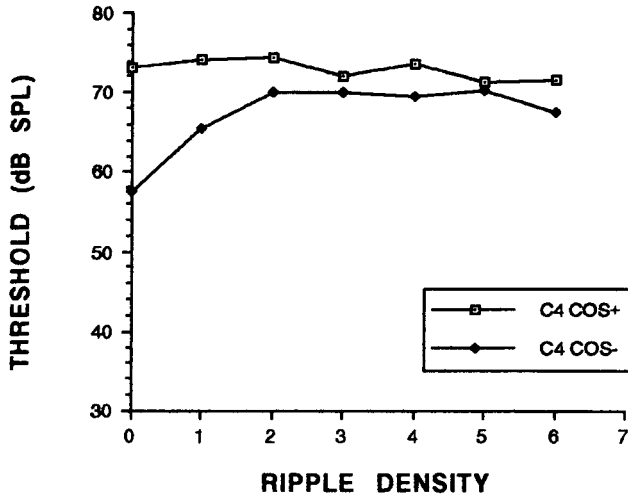
CHINCHILLA 4 - 500 HZ COSINE MASKING FUNCTION
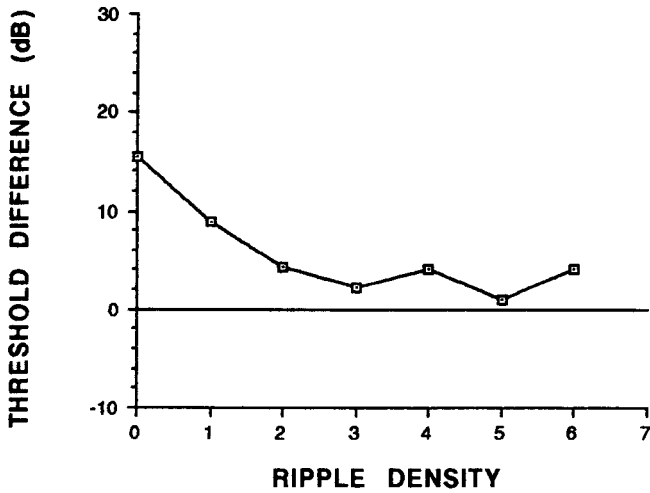
CHINCHILLA 4 - 500 HZ RELATIVE WEIGHTING FUNCTION
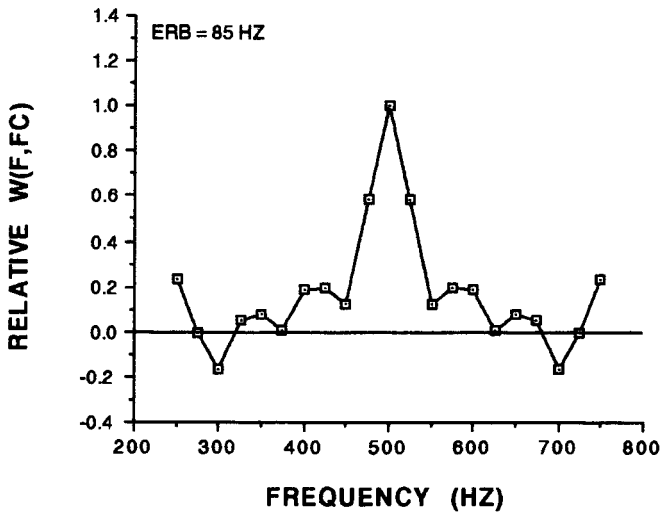
Figure 11e.　The rippled noise masking data from Chinchilla 5 at a signal frequency of 500 Hz. The top panel of the figure shows the raw data from Chinchilla 5. The open symbols are the cos+ thresholds and the closed symbols are the cos- thresholds. The middle panel is the cosine masking function for the same animal. The lower panel shows the relative weighting or auditory filter function derived from this masking function as well as the equivalent rectangular bandwidth or ERB of the filter.

CHINCHILLA 5 - 500 HZ COSINE DATA
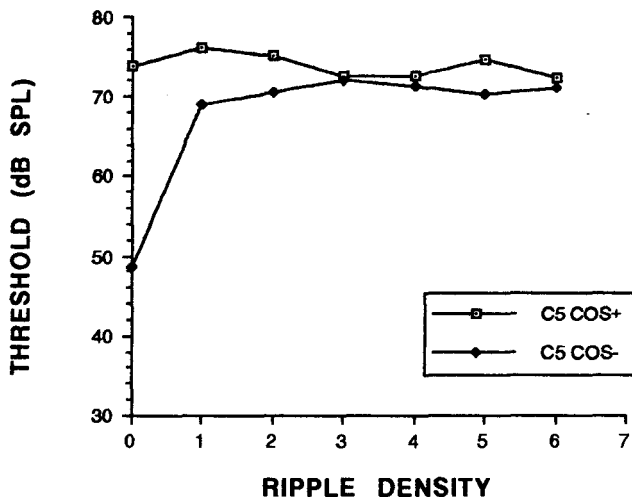
CHINCHILLA 5 - 500 HZ COSINE MASKING FUNCTION
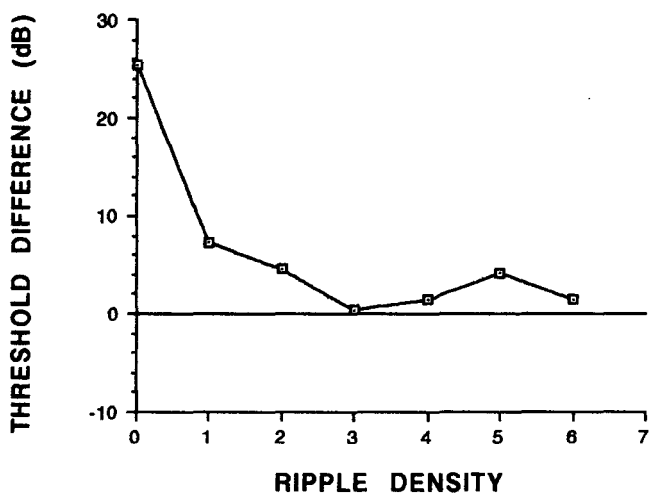
CHINCHILLA 5 - 500 HZ RELATIVE WEIGHTING FUNCTION
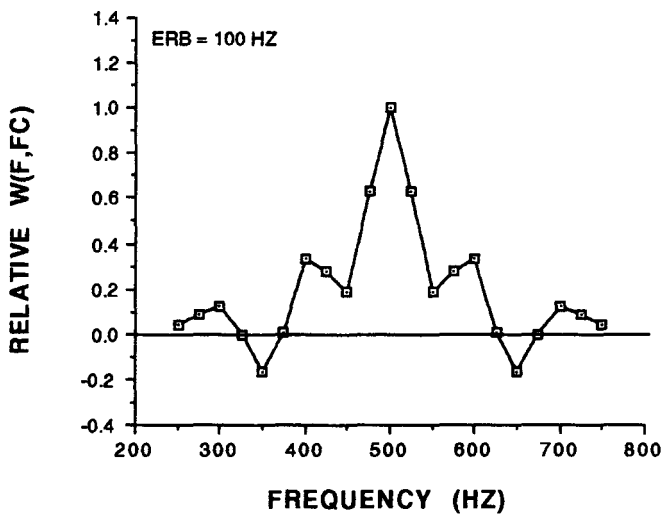
simply the width that a perfectly rectangular filter with a height equal to the measured auditory filter would need to be in order to cover the same area as the measured auditory filter. The ERB is equal to the area under the function $W(f, f_t)$ divided by the value of $W(f, f_t)$ at f_t (See Houtgast, 1977). This can be written as

$$(10) \quad \text{ERB (Hz)} = \frac{f_t}{W(f, f_t) = f_t} = \frac{f_t}{(1 + \sum_{1}^{6} a_n)}.$$

Figures 11b-e show the cosine data for Chinchillas 2-5 at the 500 Hz signal frequency. The data in these figures are shown in the same format as the data from Chinchilla 1. As can be seen from the data, the auditory filter functions of Chinchillas 2-5 are similar to the auditory filter function of Chinchilla 1 both in terms of shape and bandwidth. The ERBs of the chinchillas ranged from 77 to 100 Hz at the 500 Hz signal frequency. The shapes of the chinchillas' derived auditory filters are very similar to the shapes of the auditory filter functions derived for humans run in similar paradigms (Houtgast, 1974 and 1977). That is, the auditory filter shapes of both humans and chinchillas show a simple bandpass characteristic. Figure 12 shows the average 500 Hz cosine masking function along with the corresponding relative weighting function. The average cosine masking function was computed by averaging the 500

Figure 12.   This figure shows the average 500 Hz cosine
masking function along with the corresponding
relative weighting function. The average
cosine masking function was computed by
averaging the 500 Hz cosine threshold
differences of all the chinchillas as a
function of ripple density. This averaged
cosine masking function was then used to
derive the average 500 Hz relative weighting
function of the chinchilla. The average
bandwidth of the chinchilla's 500 Hz auditory
filter function is 86 Hz or about 17% of the
center frequency of the filter.

AVERAGE 500 HZ COSINE MASKING FUNCTION
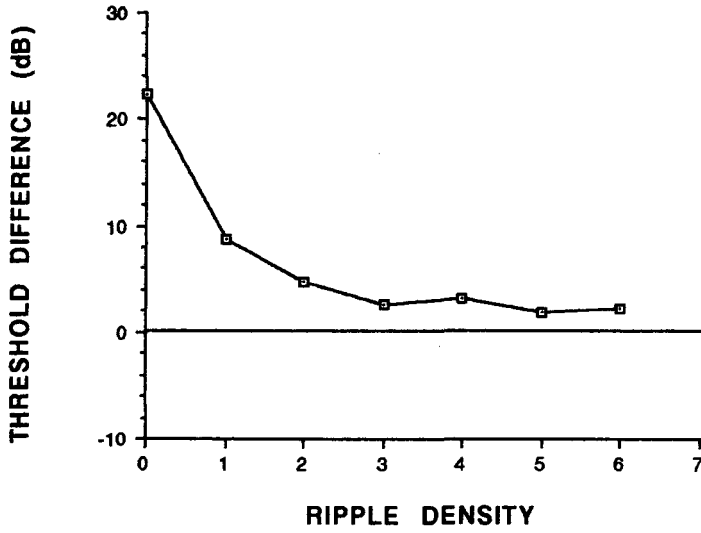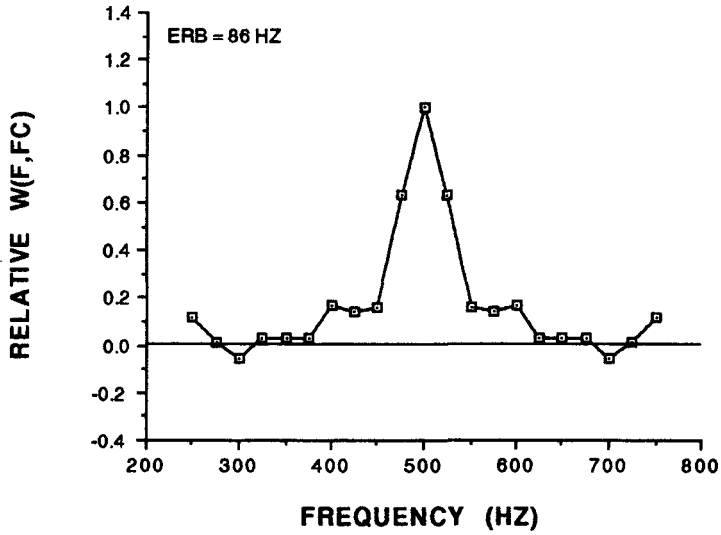
AVERAGE 500 HZ RELATIVE WEIGHTING FUNCTION

Hz cosine threshold differences of all the chinchillas as a function of ripple density. This averaged cosine masking function was then used to derive the average 500 Hz relative weighting function of the chinchilla. Comparison of the average 500 Hz relative weighting function with the individual weighting functions in Figure 11a-e shows that the average is a very good representation of the individual data in terms of both shape and bandwidth. The average bandwidth of the chinchilla's auditory filter function is 86 Hz or about 17% of the center frequency of the filter.

Figures 13a-f show the cosine data from Chinchillas 1-6 at a signal frequency of 1000 Hz. The data in these figures are shown in the same format as the 500 Hz data. As can be seen, the auditory filter functions of Chinchillas 1-6 are similar both in terms of shape and bandwidth. The ERBs of the chinchillas ranged from 209 to 356 Hz at the 1000 Hz signal frequency. Again, the shapes of the chinchillas' derived auditory filters show a simple bandpass characteristic similar to the shapes of the auditory filter functions derived for humans run in similar paradigms. Figure 14 shows the average 1000 Hz cosine masking function along with the corresponding relative weighting function. Again, the average cosine masking function was computed by averaging the individual 1000 Hz cosine masking functions of all the chinchillas. This

Figure 13a. The rippled noise masking data from

Chinchilla 1 at a signal frequency of 1000

Hz. The top panel of the figure shows the

raw data from Chinchilla 1. The open symbols

are the cos+ thresholds and the closed

symbols are the cos- thresholds. The middle

panel is the cosine masking function for the

same animal. The lower panel shows the

relative weighting or auditory filter

function derived from this masking function

as well as the equivalent rectangular

bandwidth or ERB of the filter.

CHINCHILLA 1 - 1kHZ COSINE DATA
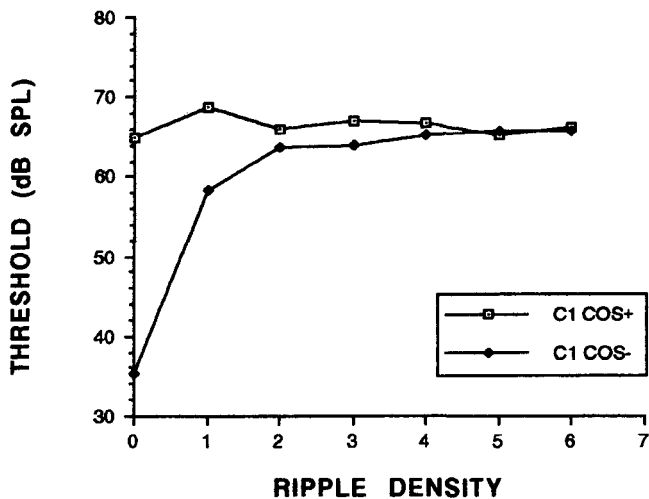
CHINCHILLA 1 - 1kHZ COSINE MASKING FUNCTION
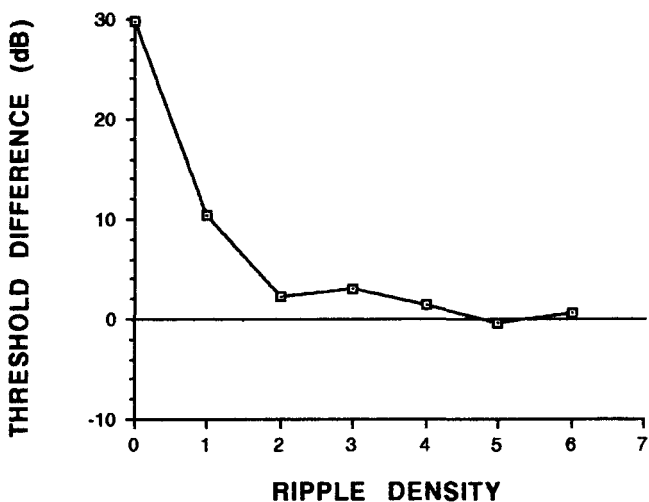
CHINCHILLA 1 - 1kHZ RELATIVE WEIGHTING FUNCTION
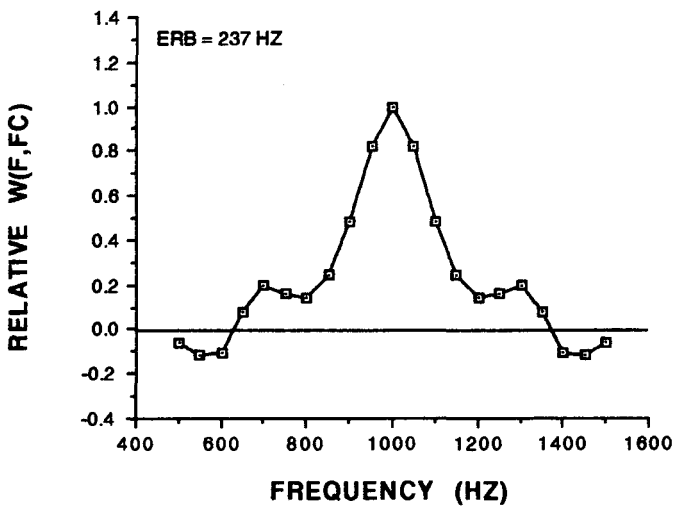
Figure 13b. The rippled noise masking data from Chinchilla 2 at a signal frequency of 1000 Hz. The top panel of the figure shows the raw data from Chinchilla 2. The open symbols are the cos+ thresholds and the closed symbols are the cos- thresholds. The middle panel is the cosine masking function for the same animal. The lower panel shows the relative weighting or auditory filter function derived from this masking function as well as the equivalent rectangular bandwidth or ERB of the filter.

CHINCHILLA 2 - 1kHZ COSINE DATA
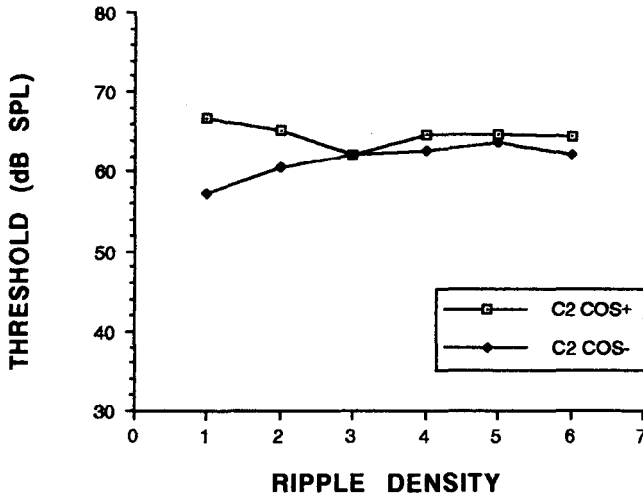
CHINCHILLA 2 - 1kHZ COSINE MASKING FUNCTION
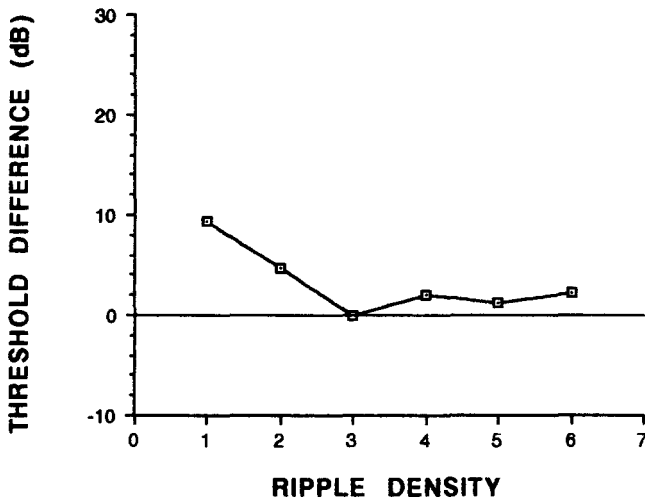
CHINCHILLA 2 - 1kHZ RELATIVE WEIGHTING FUNCTION

79
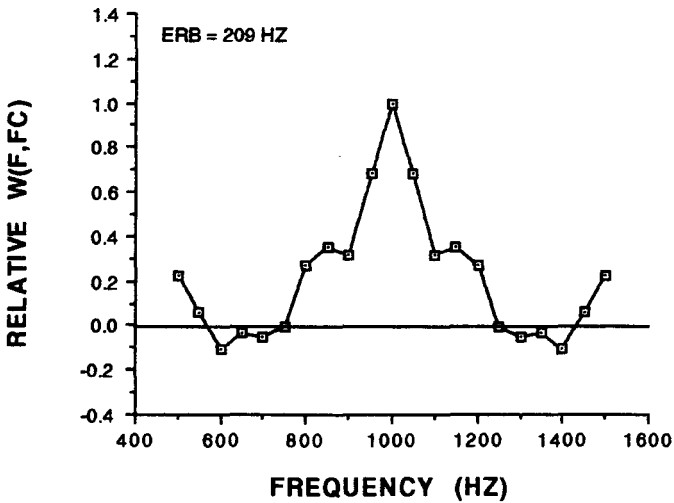
Figure 13c. The rippled noise masking data from Chinchilla 3 at a signal frequency of 1000 Hz. The top panel of the figure shows the raw data from Chinchilla 3. The open symbols are the cos+ thresholds and the closed symbols are the cos- thresholds. The middle panel is the cosine masking function for the same animal. The lower panel shows the relative weighting or auditory filter function derived from this masking function as well as the equivalent rectangular bandwidth or ERB of the filter.

CHINCHILLA 3 - 1kHZ COSINE DATA
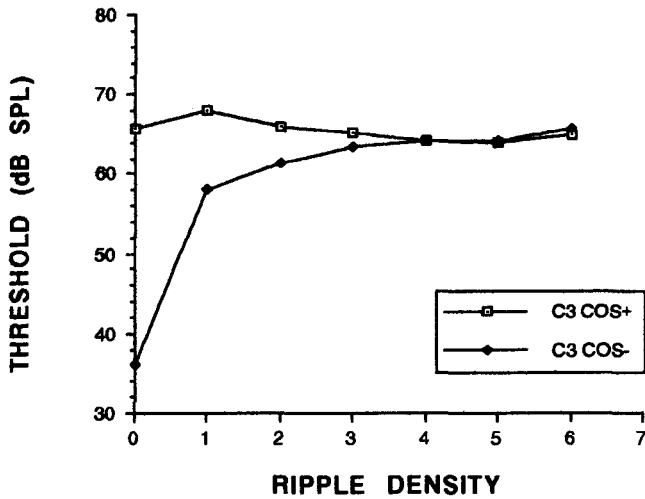
CHINCHILLA 3 - 1kHZ COSINE MASKING FUNCTION
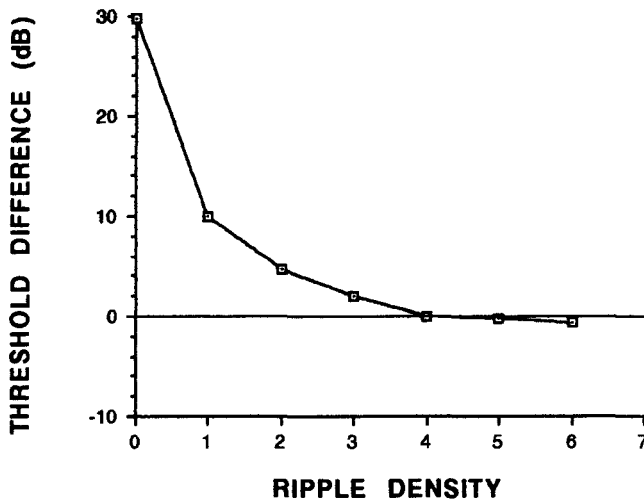
CHINCHILLA 3 - 1kHZ RELATIVE WEIGHTING FUNCTION
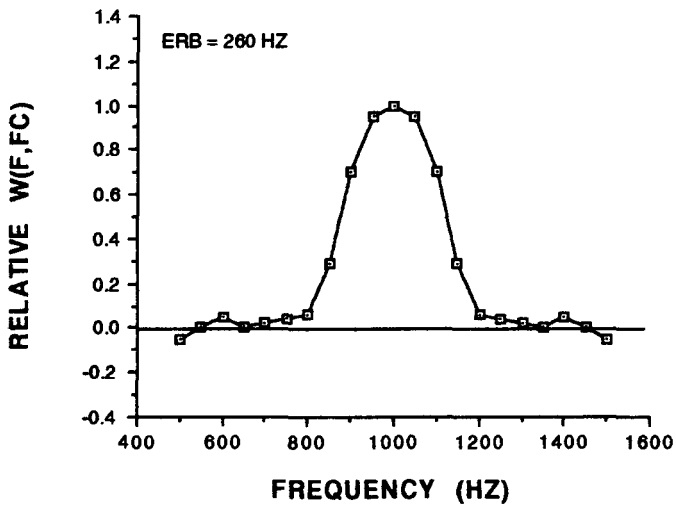
Figure 13d.   The rippled noise masking data from Chinchilla 4 at a signal frequency of 1000 Hz.   The top panel of the figure shows the raw data from Chinchilla 4.   The open symbols are the cos+ thresholds and the closed symbols are the cos- thresholds.   The middle panel is the cosine masking function for the same animal.   The lower panel shows the relative weighting or auditory filter function derived from this masking function as well as the equivalent rectangular bandwidth or ERB of the filter.

CHINCHILLA 4 - 1kHZ COSINE DATA
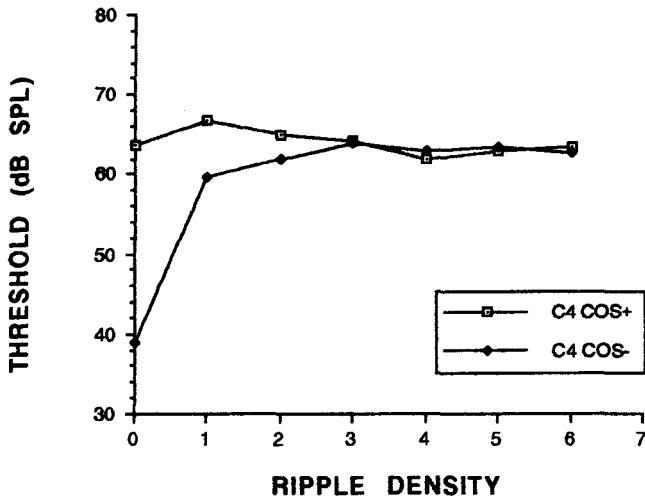
CHINCHILLA 4 - 1kHZ COSINE MASKING FUNCTION
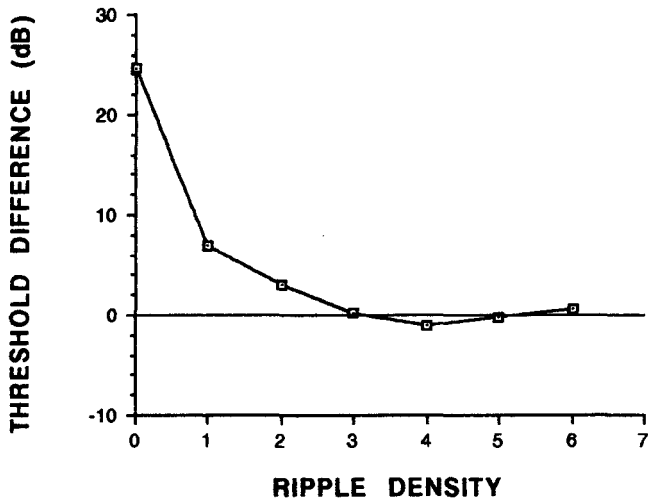
CHINCHILLA 4 - 1kHZ RELATIVE WEIGHTING FUNCTION
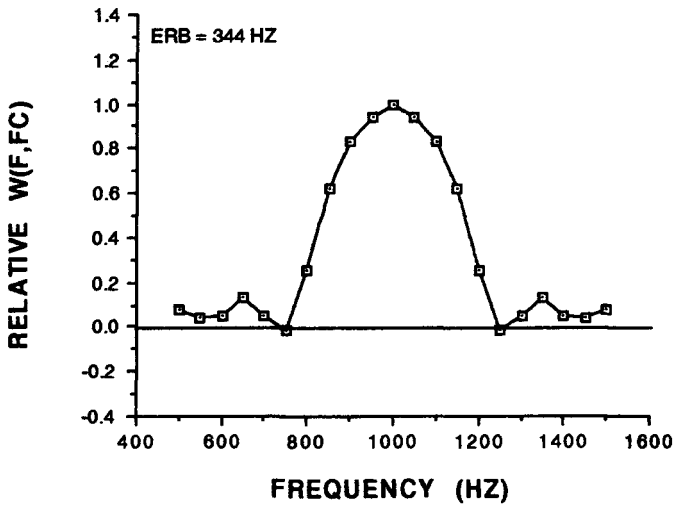
Figure 13e.   The rippled noise masking data from
              Chinchilla 5 at a signal frequency of 1000
              Hz.   The top panel of the figure shows the
              raw data from Chinchilla 5.   The open symbols
              are the cos+ thresholds and the closed
              symbols are the cos- thresholds.   The middle
              panel is the cosine masking function for the
              same animal.   The lower panel shows the
              relative weighting or auditory filter
              function derived from this masking function
              as well as the equivalent rectangular
              bandwidth or ERB of the filter.

CHINCHILLA 5 - 1kHZ COSINE DATA
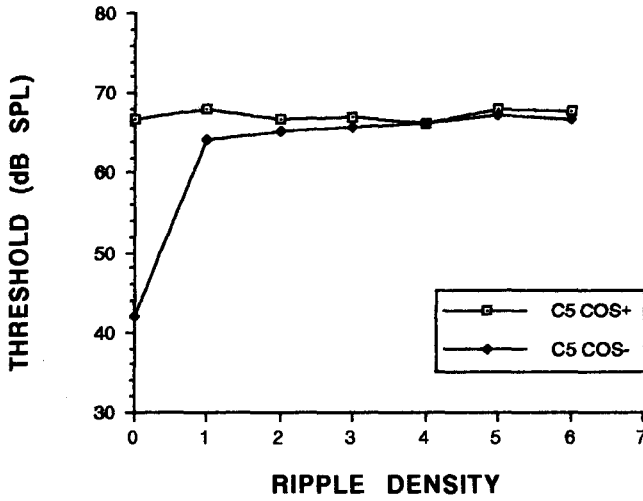
CHINCHILLA 5 - 1kHZ COSINE MASKING FUNCTION
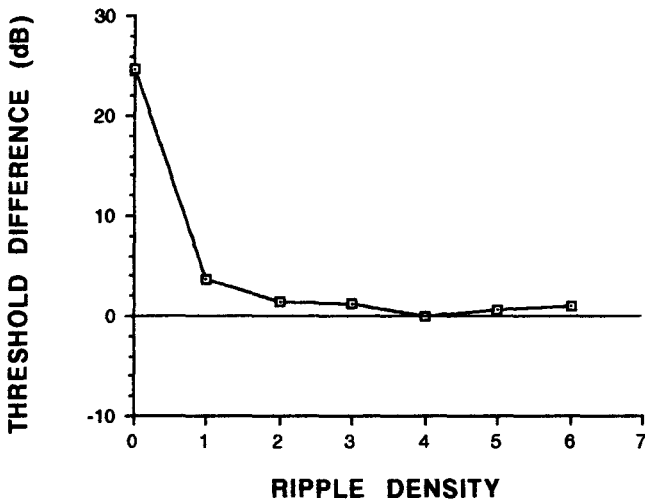
CHINCHILLA 5 - 1kHZ RELATIVE WEIGHTING FUNCTION
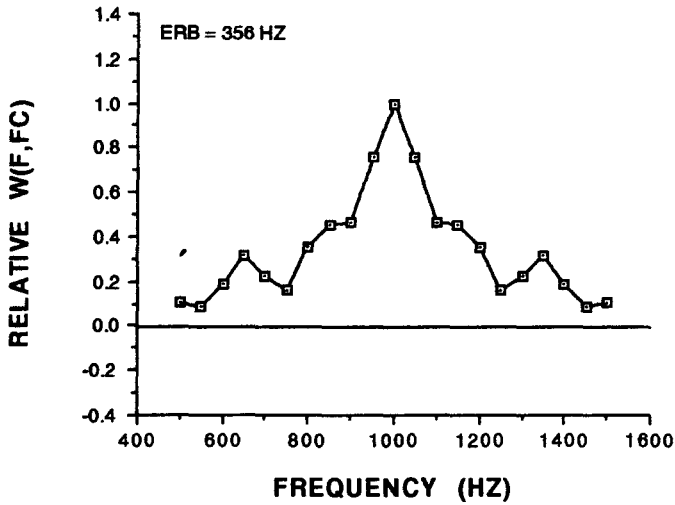
Figure 13f.   The rippled noise masking data from Chinchilla 6 at a signal frequency of 1000 Hz. The top panel of the figure shows the raw data from Chinchilla 6. The open symbols are the cos+ thresholds and the closed symbols are the cos- thresholds. The middle panel is the cosine masking function for the same animal. The lower panel shows the relative weighting or auditory filter function derived from this masking function as well as the equivalent rectangular bandwidth or ERB of the filter.

CHINCHILLA 6 - 1kHZ COSINE DATA
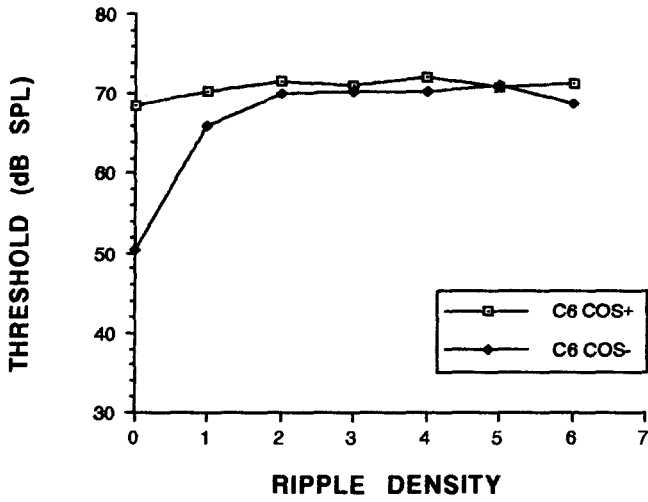
CHINCHILLA 6 - 1kHZ COSINE MASKING FUNCTION
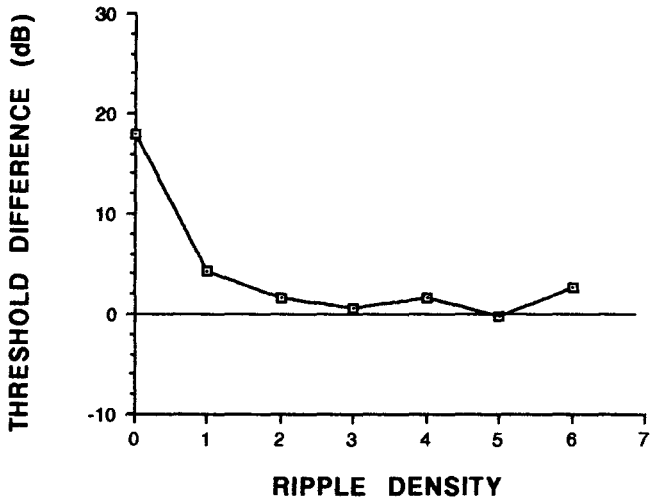
CHINCHILLA 6 - 1kHZ RELATIVE WEIGHTING FUNCTION
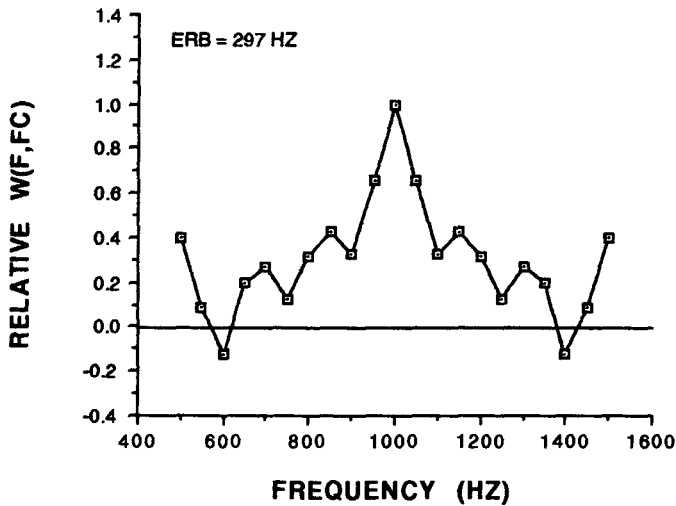
Figure 14.   This figure shows the average 1000 Hz cosine

masking function along with the corresponding

relative weighting function.   The average

cosine masking function was computed by

averaging the 1000 Hz cosine masking

functions of all the chinchillas.   This

averaged cosine masking function was then

used to derive the average 1000 Hz relative

weighting function of the chinchilla.   The

average bandwidth of the chinchilla's 1000 Hz

auditory filter function is 265 Hz or about

27% of the center frequency of the filter.

AVERAGE 1kHZ COSINE MASKING FUNCTION
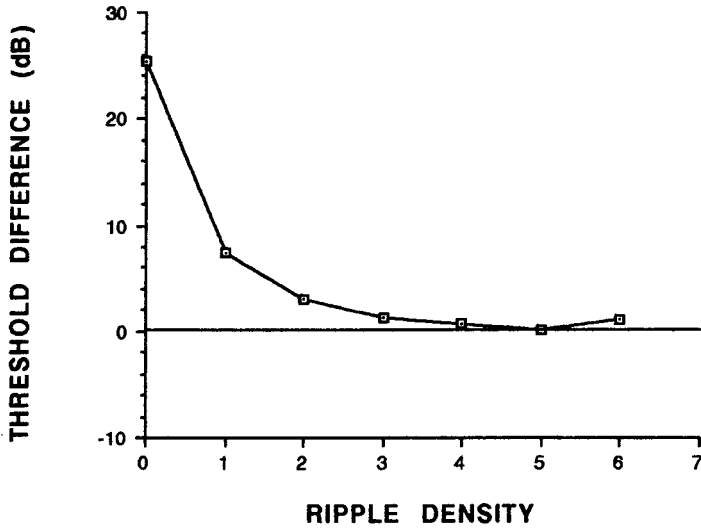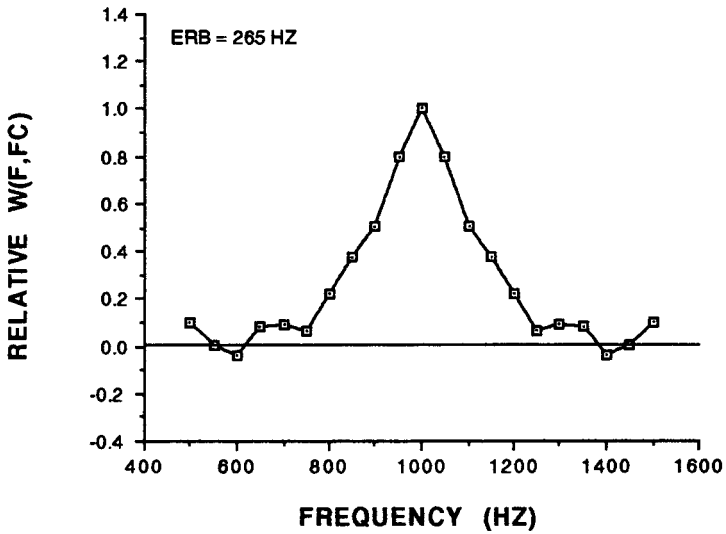
AVERAGE 1kHZ RELATIVE WEIGHTING FUNCTION

averaged cosine masking function was then used to derive
the average 1000 Hz relative weighting function of the
chinchilla. Comparison of the average 1000 Hz relative
weighting function with the individual weighting functions
in Figure 13a-f shows that the average is, again, a good
representation of the individual data in terms of both
shape and bandwidth. The average bandwidth of the
chinchilla's 1000 Hz auditory filter function is 265 Hz or
about 27% of the center frequency of the filter.

Figures 15a-e show the cosine data from Chinchillas 1,
3, 4, 5, and 6 at a signal frequency of 2000 Hz.
Chinchilla 2 died before data collection at this frequency
was completed. The data in these figures are shown in the
same format as the 500 and 1000 Hz data. Again, the data
show that the auditory filter functions of the chinchillas
are similar both in terms of their shape and bandwidth.
The ERBs of the chinchillas ranged from 322 to 527 Hz at
the 2000 Hz signal frequency. The shapes of the
chinchillas' derived auditory filters once again show a
simple bandpass characteristic similar to the shapes of the
auditory filter functions derived for humans run in
analogous paradigms. Figure 16 shows the average 2000 Hz
cosine masking function along with the corresponding
relative weighting function. Again, the average cosine
masking function was computed by averaging the individual

Figure 15a. The rippled noise masking data from Chinchilla 1 at a signal frequency of 2000 Hz. The top panel of the figure shows the raw data from Chinchilla 1. The open symbols are the cos+ thresholds and the closed symbols are the cos- thresholds. The middle panel is the cosine masking function for the same animal. The lower panel shows the relative weighting or auditory filter function derived from this masking function as well as the equivalent rectangular bandwidth or ERB of the filter.

CHINCHILLA 1 - 2kHZ COSINE DATA
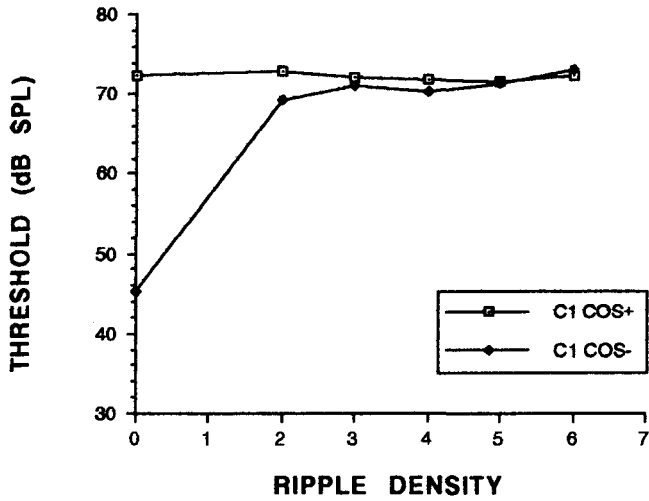
CHINCHILLA 1 - 2kHZ COSINE MASKING FUNCTION

CHINCHILLA 1 - 2kHZ RELATIVE WEIGHTING FUNCTION

ERB = 489 HZ
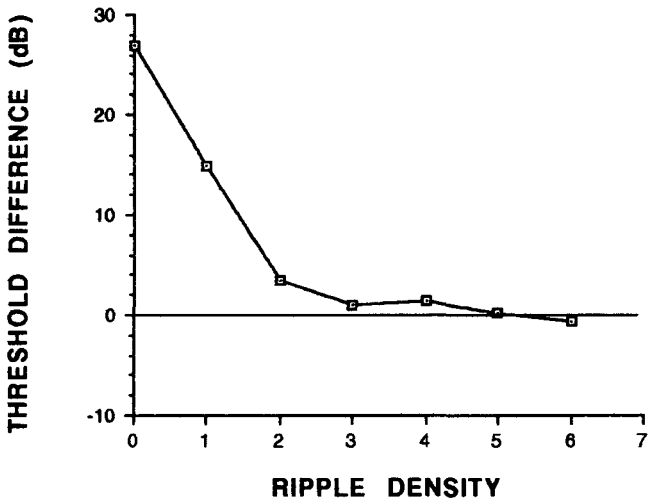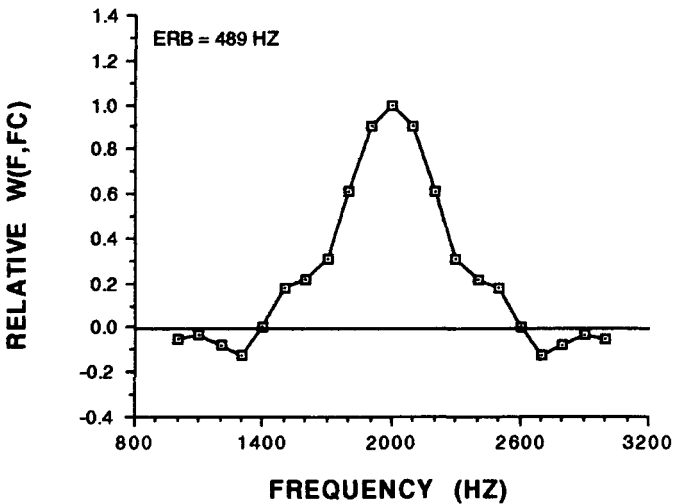
Figure 15b.   The   rippled   noise   masking   data   from
              Chinchilla 3 at a signal frequency of 2000
              Hz.   The top panel of the figure shows the
              raw data from Chinchilla 3.   The open symbols
              are   the   cos+   thresholds   and   the   closed
              symbols are the cos- thresholds.   The middle
              panel is the cosine masking function for the
              same   animal.   The   lower   panel   shows   the
              relative   weighting   or   auditory   filter
              function derived from this masking function
              as   well   as   the   equivalent   rectangular
              bandwidth or ERB of the filter.

CHINCHILLA 3 - 2kHZ COSINE DATA
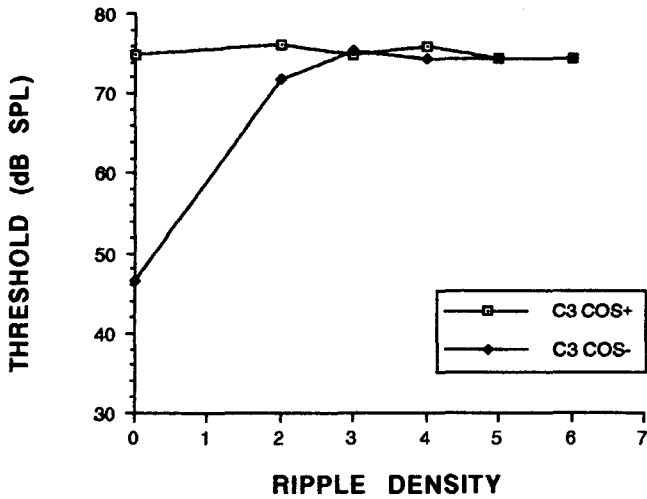
CHINCHILLA 3 - 2kHZ COSINE MASKING FUNCTION
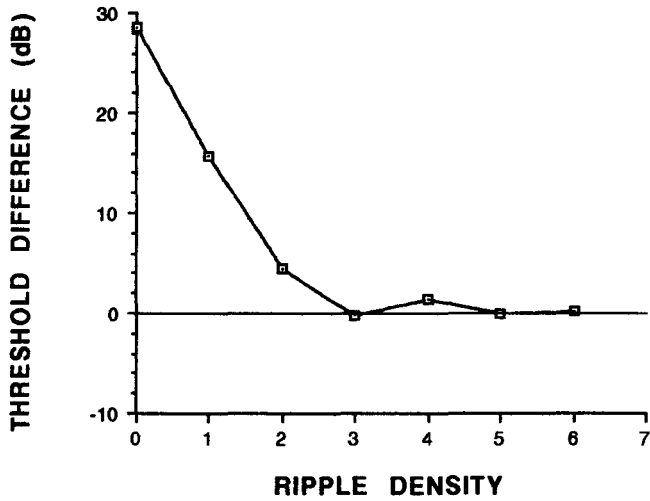
CHINCHILLA 3 - 2kHZ RELATIVE WEIGHTING FUNCTION
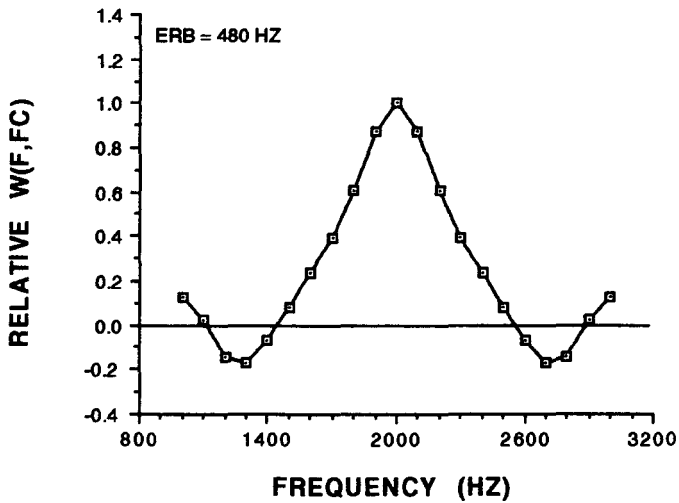
Figure 15c. The rippled noise masking data from
Chinchilla 4 at a signal frequency of 2000
Hz. The top panel of the figure shows the
raw data from Chinchilla 4. The open symbols
are the cos+ thresholds and the closed
symbols are the cos- thresholds. The middle
panel is the cosine masking function for the
same animal. The lower panel shows the
relative weighting or auditory filter
function derived from this masking function
as well as the equivalent rectangular
bandwidth or ERB of the filter.

CHINCHILLA 4 - 2kHZ COSINE DATA
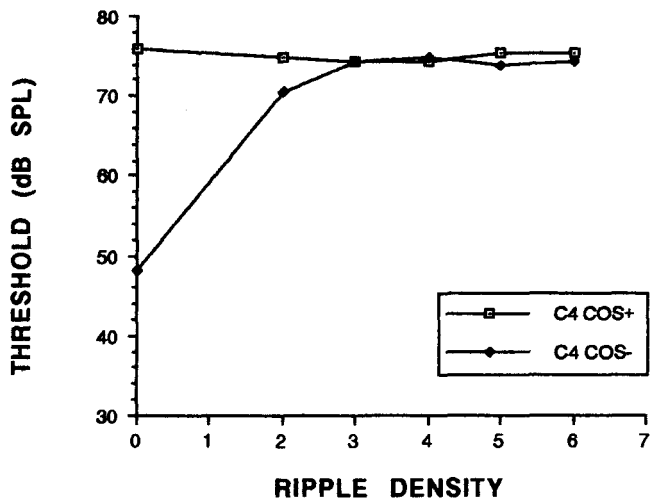
CHINCHILLA 4 - 2kHZ COSINE MASKING FUNCTION
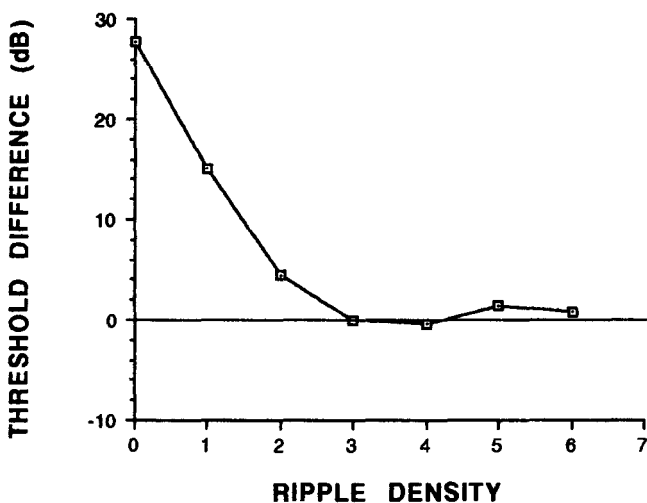
CHINCHILLA 4 - 2kHZ RELATIVE WEIGHTING FUNCTION
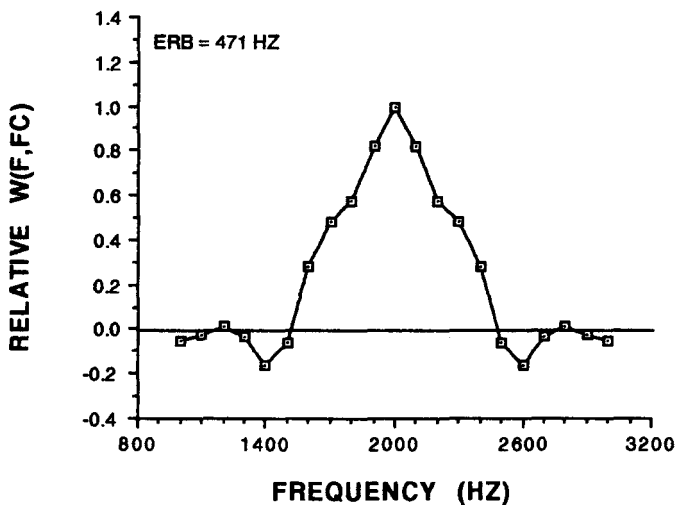
Figure 15d.   The rippled noise masking data from
               Chinchilla 5 at a signal frequency of 2000
               Hz.   The top panel of the figure shows the
               raw data from Chinchilla 5.   The open symbols
               are the cos+ thresholds and the closed
               symbols are the cos- thresholds.   The middle
               panel is the cosine masking function for the
               same animal.   The lower panel shows the
               relative weighting or auditory filter
               function derived from this masking function
               as well as the equivalent rectangular
               bandwidth or ERB of the filter.

CHINCHILLA 5 - 2kHZ COSINE DATA
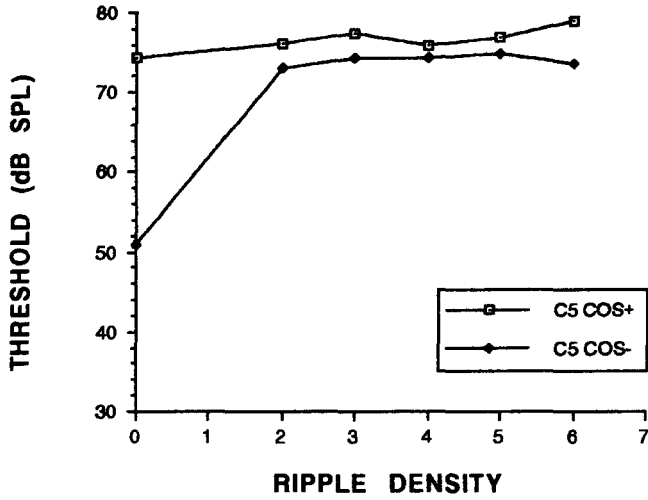
CHINCHILLA 5 - 2kHZ COSINE MASKING FUNCTION
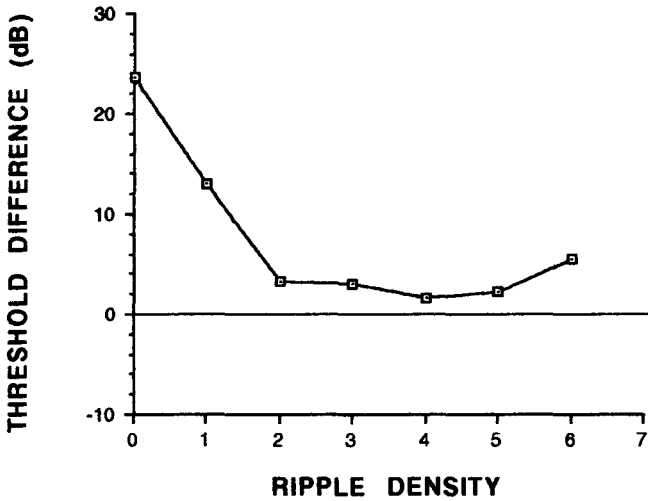
CHINCHILLA 5 - 2kHZ RELATIVE WEIGHTING FUNCTION
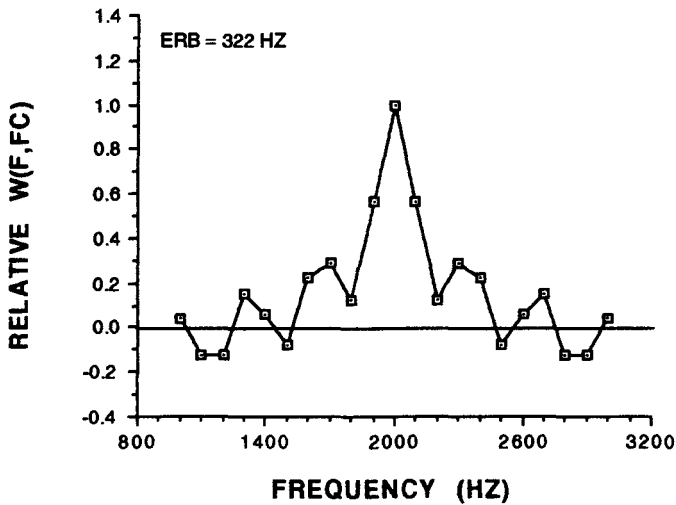
Figure 15e. The rippled noise masking data from Chinchilla 6 at a signal frequency of 2000 Hz. The top panel of the figure shows the raw data from Chinchilla 6. The open symbols are the cos+ thresholds and the closed symbols are the cos- thresholds. The middle panel is the cosine masking function for the same animal. The lower panel shows the relative weighting or auditory filter function derived from this masking function as well as the equivalent rectangular bandwidth or ERB of the filter.

CHINCHILLA 6 - 2kHZ COSINE DATA
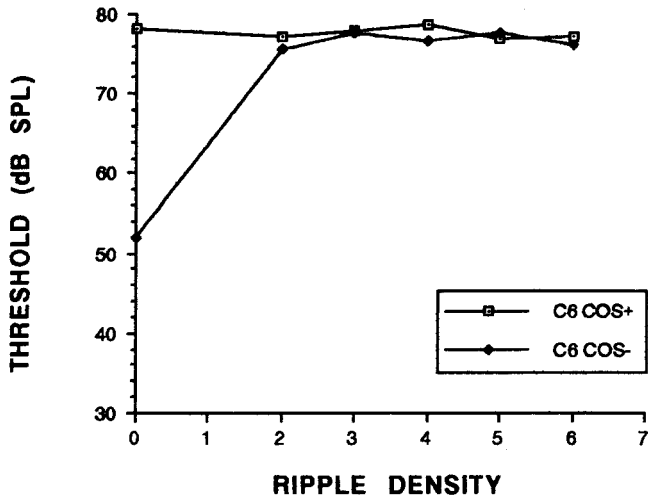
CHINCHILLA 6 - 2kHZ COSINE MASKING FUNCTION
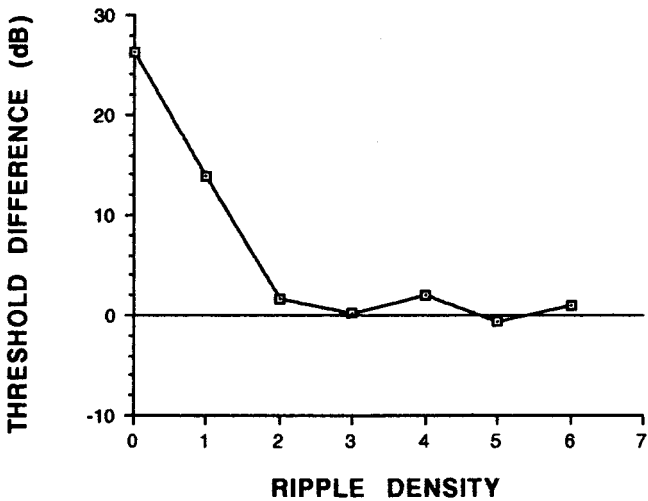
CHINCHILLA 6 - 2kHZ RELATIVE WEIGHTING FUNCTION
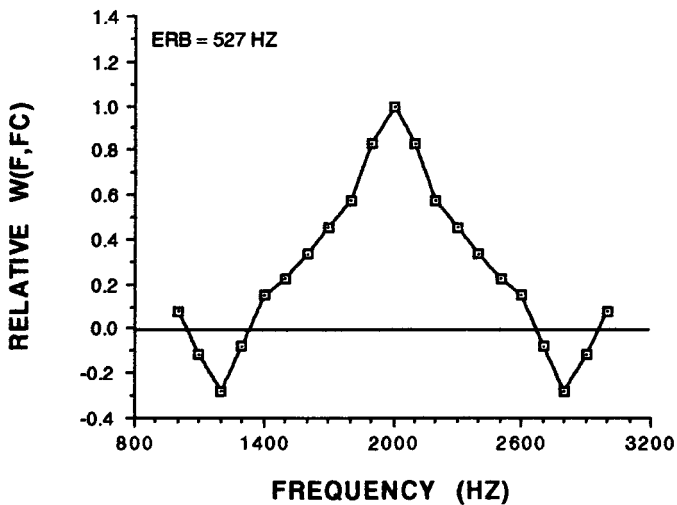
Figure 16.   This figure shows the average 2000 Hz cosine masking function along with the corresponding relative weighting function.   The average cosine masking function was computed by averaging the 2000 Hz cosine threshold differences of all the chinchillas as a function of ripple density.   This averaged cosine masking function was then used to derive the average 2000 Hz relative weighting function of the chinchilla.   The average bandwidth of the chinchilla's 2000 Hz auditory filter function is 440 Hz or about 22% of the center frequency of the filter.

AVERAGE 2kHZ COSINE MASKING FUNCTION
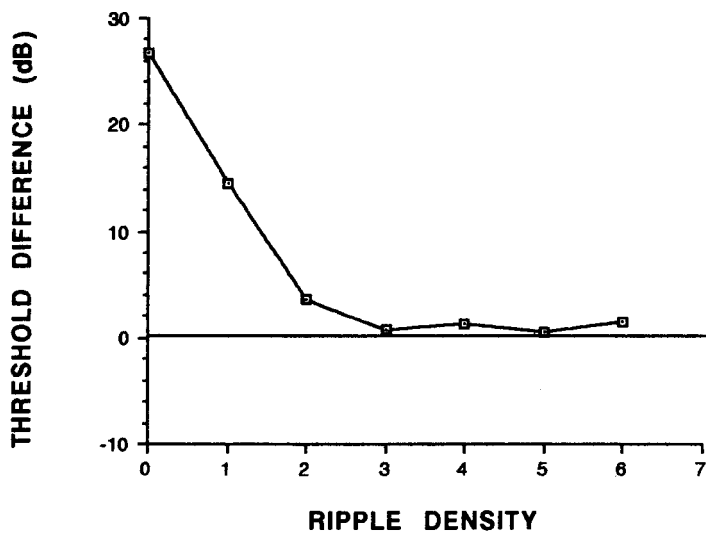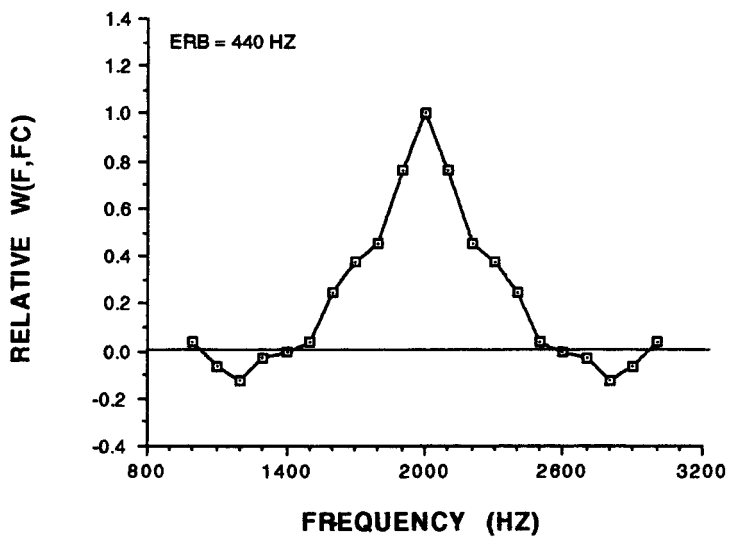
AVERAGE 2kHZ RELATIVE WEIGHTING FUNCTION

2000 Hz cosine masking functions of all the chinchillas. This averaged cosine masking function was then used to derive the average 2000 Hz relative weighting function of the chinchilla. Comparison of the average 2000 Hz relative weighting function with the individual weighting functions in Figure 15a-e shows that the average is, again, a good representation of the individual data in terms of both shape and bandwidth. The average bandwidth of the chinchilla's 2000 Hz auditory filter function is 440 Hz or about 22% of the center frequency of the filter.

Assuming symmetry, the data shown in Figures 11-16 consistently showed that the auditory filter shapes of chinchillas have a simple bandpass characteristic and that the bandwidths of these filters are about 17-27% of the center frequency. The next step in the experiment was to test the symmetry assumption by collecting the data necessary to derive the sine masking functions, $S(d)$, and to derive the relative weighting functions using both the a_n and the b_n coefficients in Eq. (4).

Because sine rippled noise is rather difficult to generate, the symmetry assumption was tested using an approximated sin+ and sin- rippled noise. As mentioned in Chapter III, the sine rippled noise can be approximated by generating the appropriate phase of cosine rippled noise (positive or negative) and adjusting the delay such that it

is 1.25(τ). This method was used to test the symmetry of the chinchillas' auditory filters.

Figures 17a-d show the sine data from chinchillas 1, 3, 4, and 5 at a signal frequency of 500 Hz. The top panels of the figures show the raw sine data. The open symbols are the sin+ thresholds and the closed symbols are the sin-thresholds. In most cases, the sin- thresholds lie on top of the sin+ thresholds, indicating that there are only very small threshold differences as a function of ripple density. The middle panels are the sine masking functions for the animals. The masking functions are simply the animal's sin- thresholds subtracted from their sin+ thresholds as a function of ripple density. The sine masking functions of these animals all lie very close to zero, indicating that there is little, if any, asymmetry in the shapes of the animals' auditory filters. The lower panels show the relative weighting or auditory filter functions derived using both the sine and cosine masking functions. In general, the two halves of the weighting functions are quite similar, however, some asymmetry is evident in the "noise" located at the lower edges of the functions. In the upper left hand corners of the lower panels are the equivalent rectangular bandwidths or ERBs of the filters. The ERBs of the filters do not change with the addition of the sine data.

Figure 17a. The rippled noise masking data from
Chinchilla 1 at a signal frequency of 500 Hz.
The top panel of the figure shows the raw
sine data from Chinchilla 1.   The open
symbols are the sin+ thresholds and the
closed symbols are the sin- thresholds. The
middle panel is the sine masking function for
the same animal. The lower panel shows the
relative weighting or auditory filter
function derived using the sine and cosine
masking functions as well as the equivalent
rectangular bandwidth or ERB of the filter.

CHINCHILLA 1 - 500 HZ SINE DATA
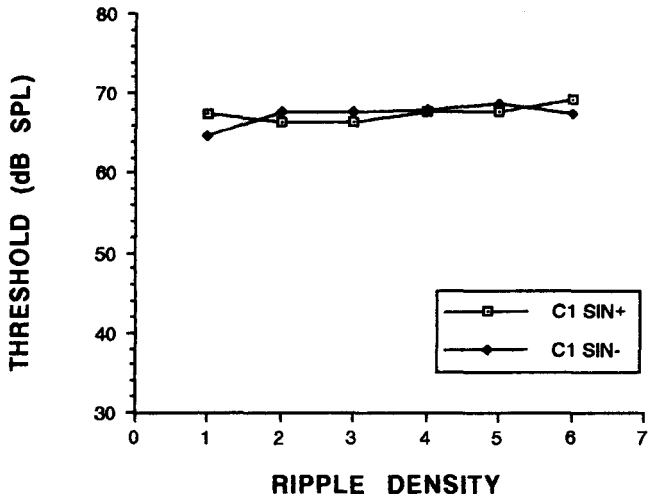
CHINCHILLA 1 - 500 HZ SINE MASKING FUNCTION
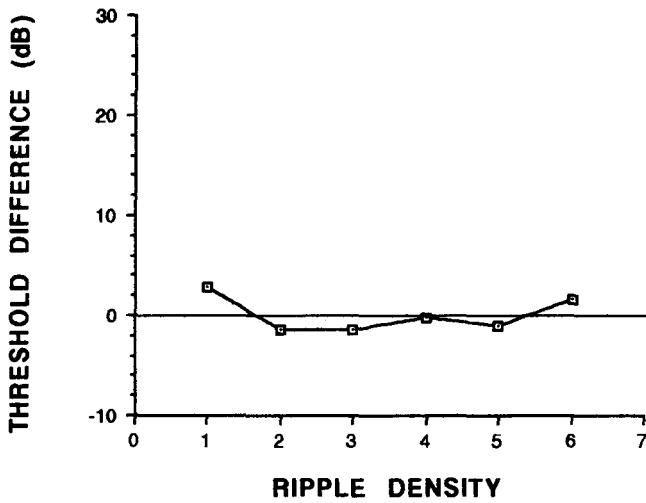
CHINCHILLA 1 - 500 HZ RELATIVE WEIGHTING FUNCTION
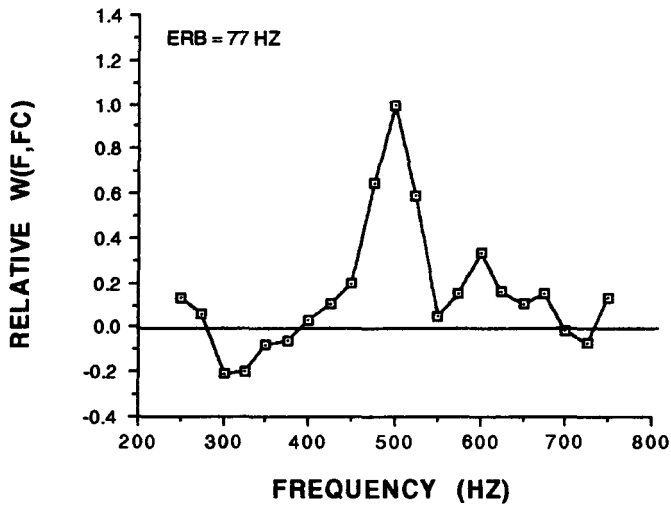
Figure 17b.   The rippled noise masking data from Chinchilla 3 at a signal frequency of 500 Hz. The top panel of the figure shows the raw sine data from Chinchilla 3. The open symbols are the sin+ thresholds and the closed symbols are the sin- thresholds. The middle panel is the sine masking function for the same animal. The lower panel shows the relative weighting or auditory filter function derived using the sine and cosine masking functions as well as the equivalent rectangular bandwidth or ERB of the filter.

CHINCHILLA 3 - 500 HZ SINE DATA
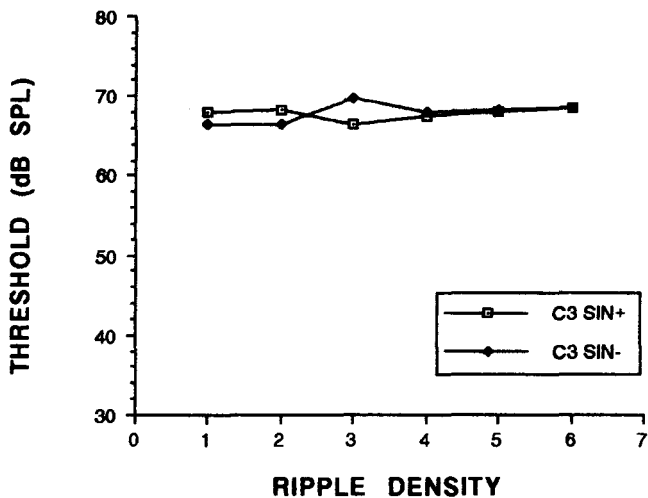
CHINCHILLA 3 - 500 HZ SINE MASKING FUNCTION
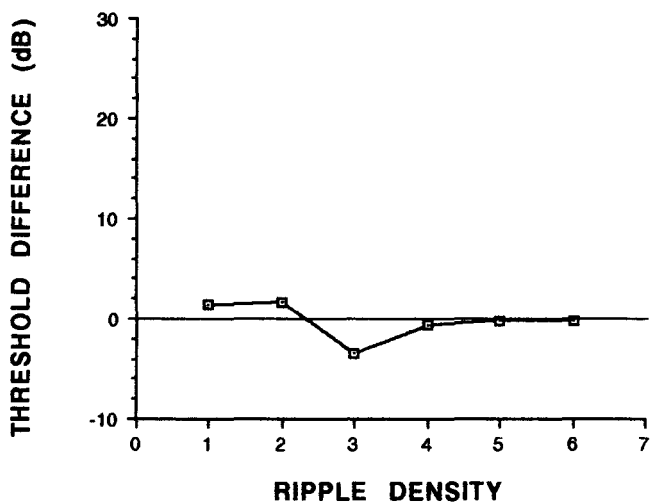
CHINCHILLA 3 - 500 HZ RELATIVE WEIGHTING FUNCTION
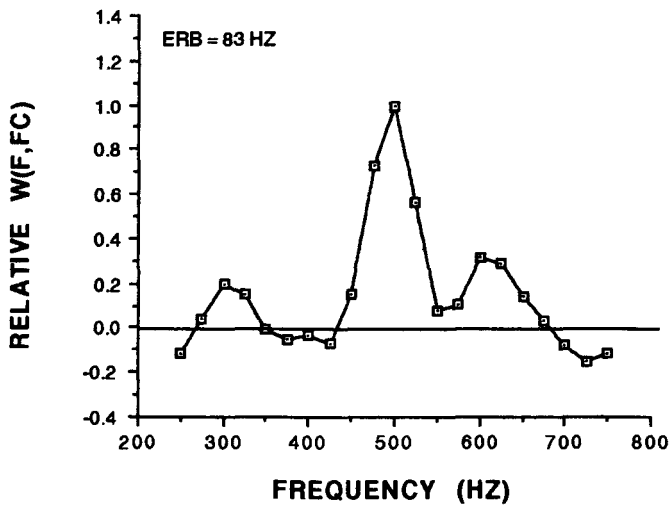
Figure 17c.   The rippled noise masking data from
              Chinchilla 4 at a signal frequency of 500 Hz.
              The top panel of the figure shows the raw
              sine data from Chinchilla 4.   The open
              symbols are the sin+ thresholds and the
              closed symbols are the sin- thresholds.   The
              middle panel is the sine masking function for
              the same animal.   The lower panel shows the
              relative weighting or auditory filter
              function derived using the sine and cosine
              masking functions as well as the equivalent
              rectangular bandwidth or ERB of the filter.

CHINCHILLA 4 - 500 HZ SINE DATA
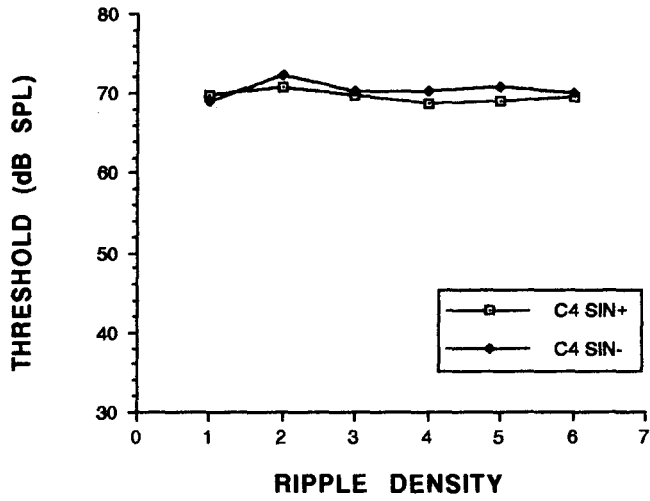
CHINCHILLA 4 - 500 HZ SINE MASKING FUNCTION
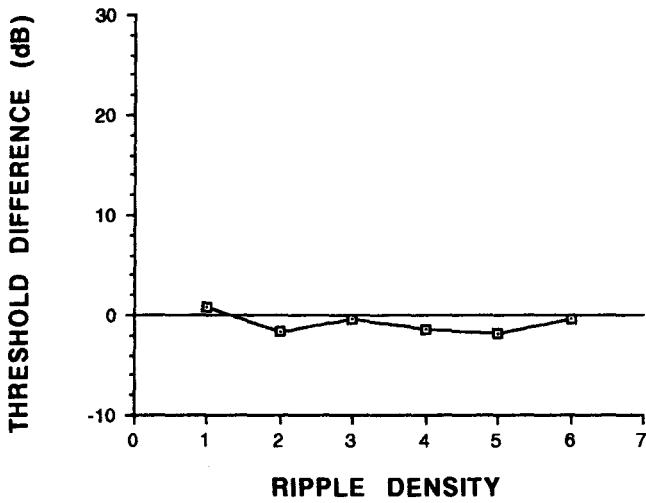
CHINCHILLA 4 - 500 HZ RELATIVE WEIGHTING FUNCTION
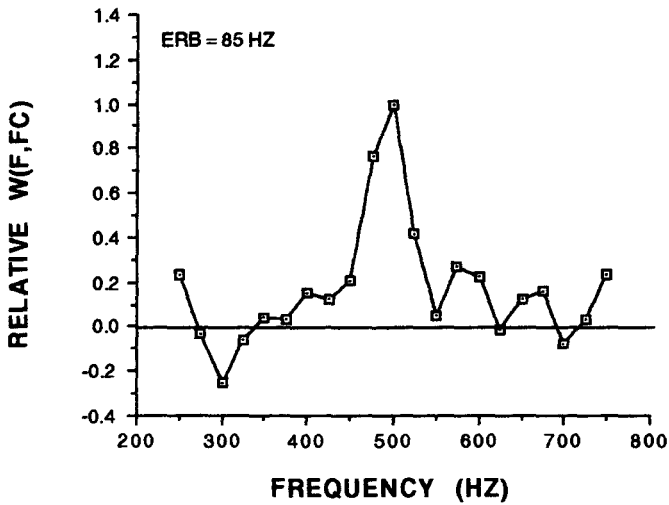
Figure 17d.   The rippled noise masking data from Chinchilla 5 at a signal frequency of 500 Hz. The top panel of the figure shows the raw sine data from Chinchilla 5.   The open symbols are the sin+ thresholds and the closed symbols are the sin- thresholds.   The middle panel is the sine masking function for the same animal.   The lower panel shows the relative weighting or auditory filter function derived using the sine and cosine masking functions as well as the equivalent rectangular bandwidth or ERB of the filter.

CHINCHILLA 5 - 500 HZ SINE DATA
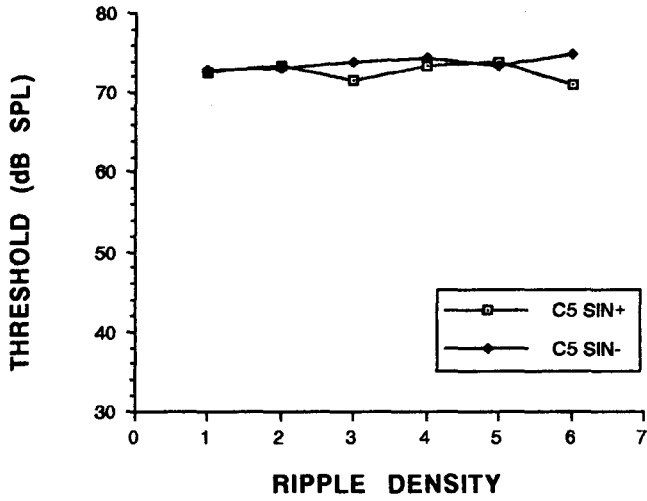
CHINCHILLA 5 - 500 HZ SINE MASKING FUNCTION
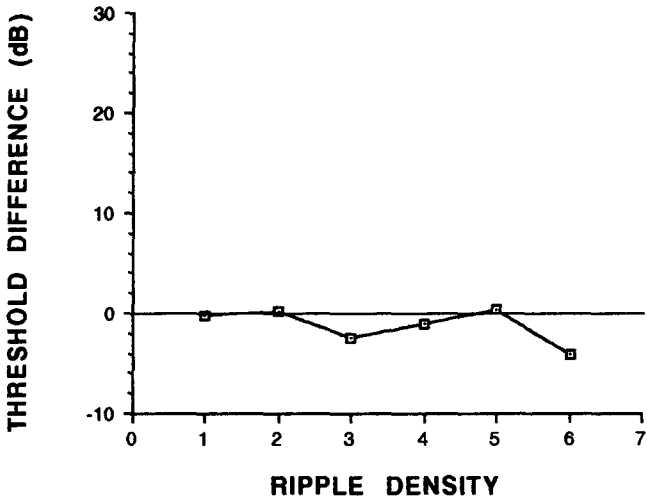
CHINCHILLA 5 - 500 HZ RELATIVE WEIGHTING FUNCTION
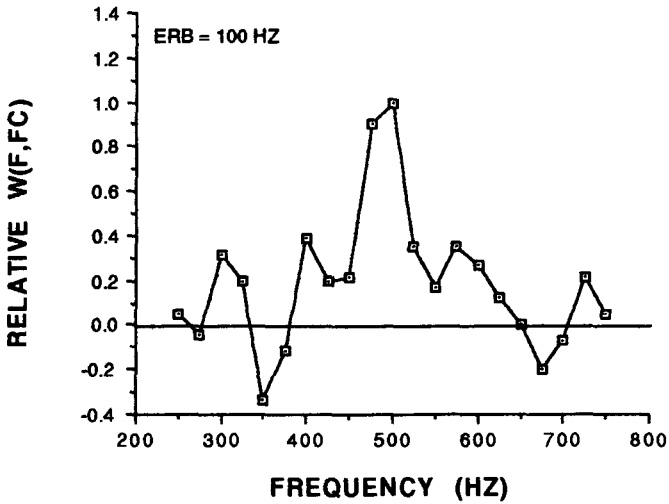
Figure 18 shows the average 500 Hz sine masking function along with the corresponding relative weighting function. The average sine masking function was computed by averaging the 500 Hz sine masking functions of all the chinchillas as a function of ripple density. This averaged sine masking function was then used in conjunction with the average cosine masking function to derive the average 500 Hz relative weighting function of the chinchilla. Comparison of the average 500 Hz relative weighting function with the individual weighting functions in Figure 17a-d shows that the average is representative of the individual data in terms of its shape. That is, the average 500 Hz relative weighting function also remains symmetrical about the center frequency of the filter.

Figures 19a and 19b compare the 500 Hz weighting functions derived using only the cosine masking functions with the weighting functions derived using both sine and cosine masking functions. Although there are some differences in each animal's auditory filter "noise", there are few, if any, differences in the shapes of the animal's auditory filter peaks. In general, these figures show that the chinchillas' 500 Hz auditory filter shapes do not change appreciably with the inclusion of the sine data.

Figures 20a-d show the sine data from Chinchillas 1, 3, 4, and 5 at a signal frequency of 1000 Hz. The top panels

Figure 18.   This figure shows the average 500 Hz sine

masking function along with the corresponding

relative weighting function.   The average

sine masking function was computed by

averaging the 500 Hz sine threshold

differences of all the chinchillas as a

function of ripple density.   This averaged

sine masking function was then used in

conjunction with the average 500 Hz cosine

masking function to derive the average 500 Hz

relative   weighting   function   of   the

chinchilla.

AVERAGE 500 HZ SINE MASKING FUNCTION
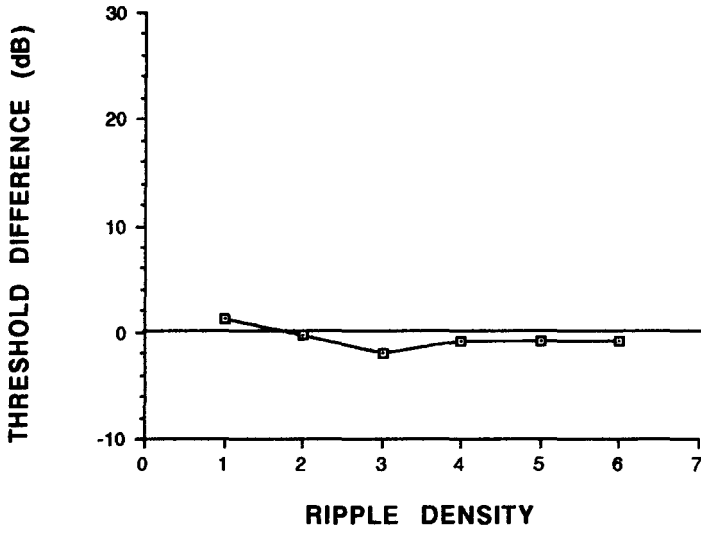
AVERAGE 500 HZ RELATIVE WEIGHTING FUNCTION
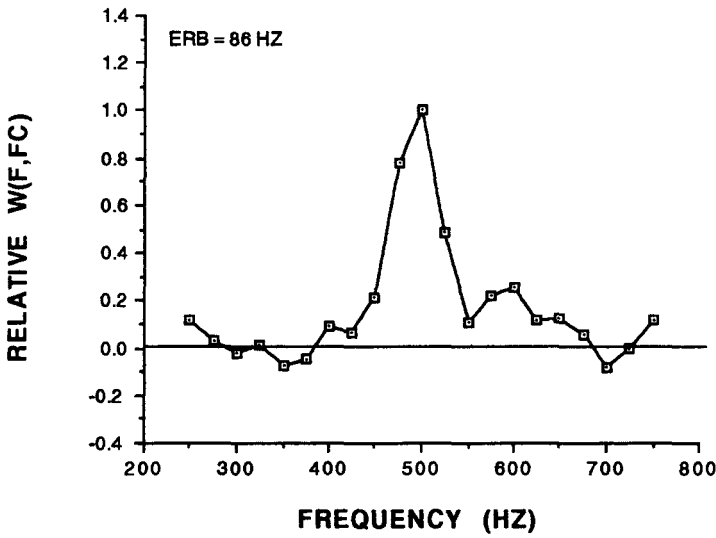
Figure 19a.   This figure compares the 500 Hz weighting

functions derived using only the cosine

masking functions (labelled COS W(F)) with

the weighting functions derived using both

sine and cosine masking functions (labelled

SIN W(F)) for Chinchillas 1 and 3. Although

there are some differences in each animal's

auditory filter "noise", there are few, if

any, differences in the shapes of the

animal's auditory filter peaks. In general,

this figure shows that estimates of the 500

Hz auditory filter shapes are not influenced

much by the sine data.

CHINCHILLA 1 - 500 HZ RELATIVE WEIGHTING FUNCTIONS
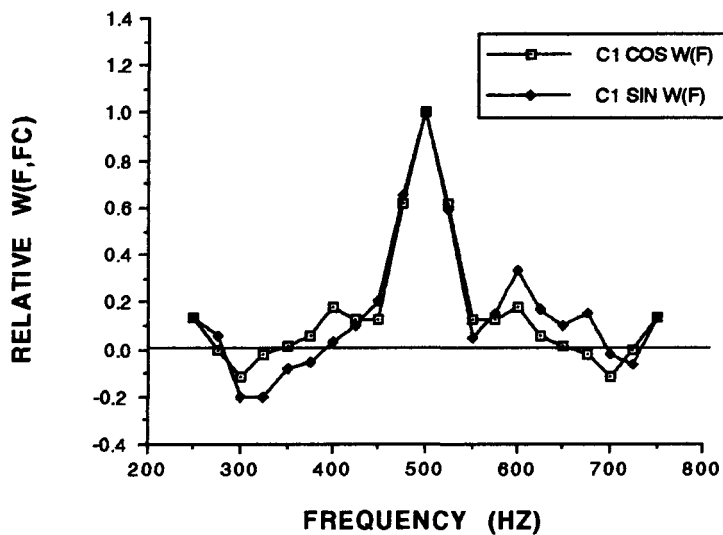
CHINCHILLA 3 - 500 HZ RELATIVE WEIGHTING FUNCTIONS
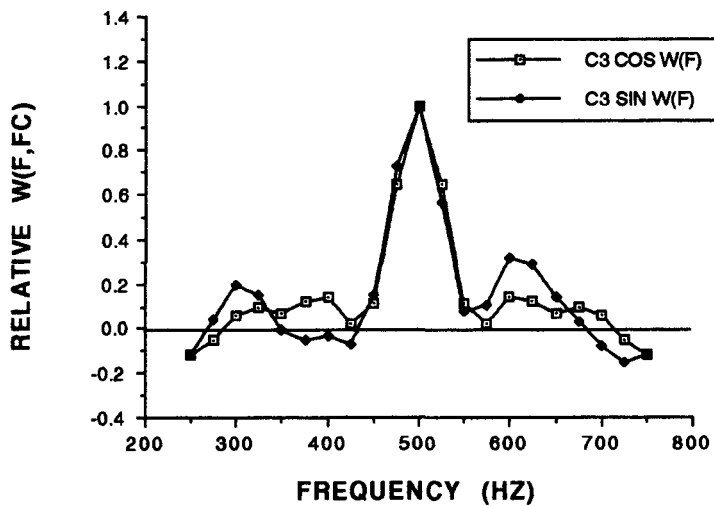
Figure 19b.   This figure compares the 500 Hz weighting
              functions derived using only the cosine
              masking functions (labelled COS W(F)) with
              the weighting functions derived using both
              sine and cosine masking functions (labelled
              SIN W(F)) for Chinchillas 4 and 5. Although
              there are some differences in each animal's
              auditory filter "noise", there are few, if
              any, differences in the shapes of the
              animal's auditory filter peaks. In general,
              this figure shows that estimates of the 500
              Hz auditory filter shapes are not influenced
              much by the sine data.

CHINCHILLA 4 - 500 HZ RELATIVE WEIGHTING FUNCTIONS
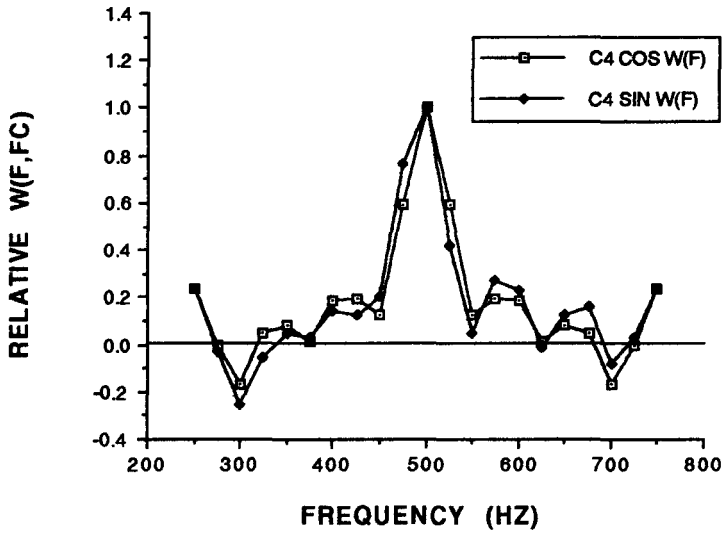
CHINCHILLA 5 - 500 HZ RELATIVE WEIGHTING FUNCTIONS
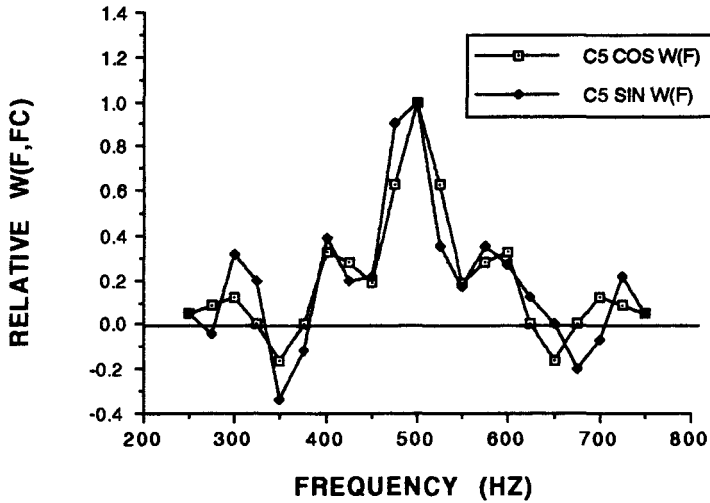
of the figures again show the raw sine data. In most cases, the sin- thresholds lie on top of the sin+ thresholds, indicating again that there are only very small threshold differences as a function of ripple density. The middle panels are the animals' sine masking functions. The sine masking functions of these animals all lie close to zero, indicating that there is little asymmetry in the shapes of the animals' auditory filters. The lower panels show the relative weighting or auditory filter functions derived using both the sine and cosine masking functions. For Chinchillas 1 and 3 the two halves of the weighting functions are quite similar, however, some degree of asymmetry is evident in the weighting functions of Chinchillas 4 and 5. The peak of Chinchilla 4's weighting function shifts slightly towards the low frequency side, whereas Chinchilla 5's weighting function seems to broaden towards the high frequencies.

Figure 21 shows the average 1000 Hz sine masking function along with the corresponding relative weighting function. Again the averaged sine masking function was used in conjunction with the average cosine masking function to derive the average 1000 Hz relative weighting function of the chinchilla. Comparison of the average 1000 Hz relative weighting function with the individual weighting functions in Figures 20a-d shows that the average

Figure 20a. The rippled noise masking data from Chinchilla 1 at a signal frequency of 1000 Hz. The top panel of the figure shows the raw sine data from Chinchilla 1. The open symbols are the sin+ thresholds and the closed symbols are the sin- thresholds. The middle panel is the sine masking function for the same animal. The lower panel shows the relative weighting or auditory filter function derived using the sine and cosine masking functions as well as the equivalent rectangular bandwidth or ERB of the filter.

CHINCHILLA 1 - 1kHZ SINE DATA
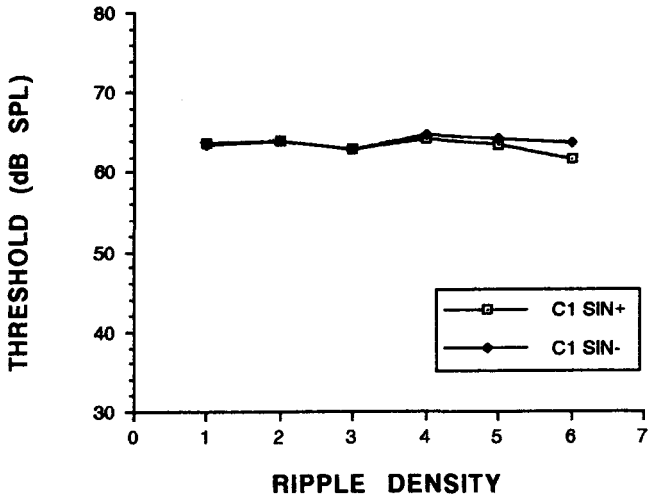
CHINCHILLA 1 - 1kHZ SINE MASKING FUNCTION
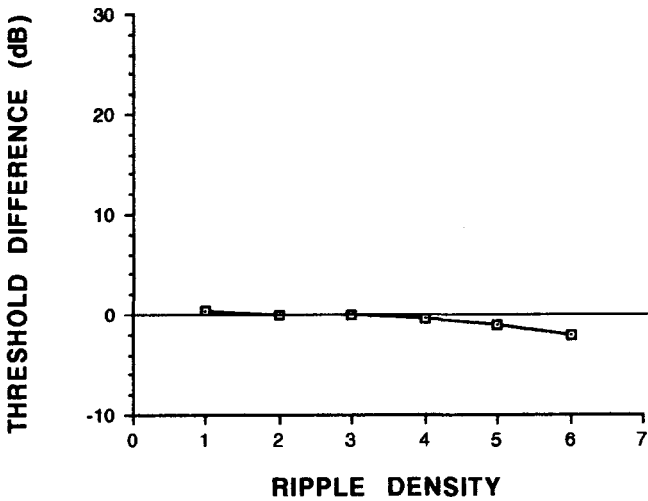
CHINCHILLA 1 - 1kHZ RELATIVE WEIGHTING FUNCTION
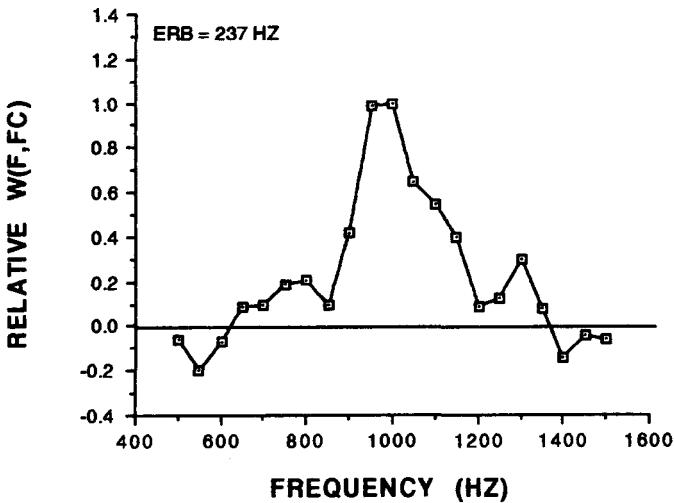
Figure 20b.   The rippled noise masking data from
                Chinchilla 3 at a signal frequency of 1000

                Hz.   The top panel of the figure shows the

                raw sine data from Chinchilla 3.   The open

                symbols are the sin+ thresholds and the

                closed symbols are the sin- thresholds.   The

                middle panel is the sine masking function for

                the same animal.   The lower panel shows the

                relative weighting or auditory filter

                function derived using the sine and cosine

                masking functions as well as the equivalent

                rectangular bandwidth or ERB of the filter.

CHINCHILLA 3 - 1kHZ SINE DATA
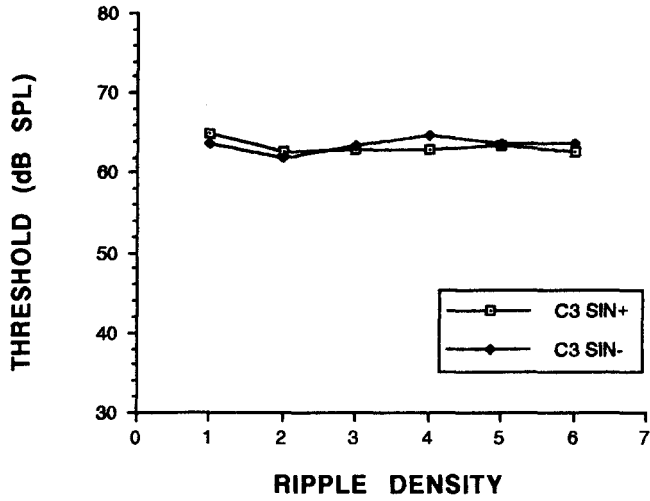
CHINCHILLA 3 - 1kHZ SINE MASKING FUNCTION
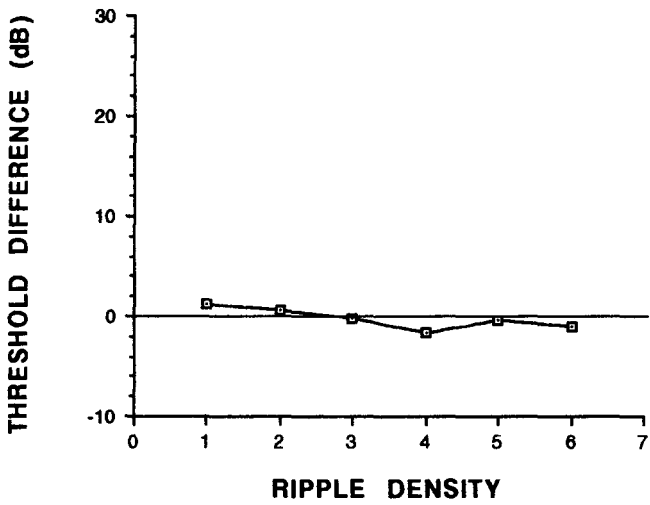
CHINCHILLA 3 - 1kHZ RELATIVE WEIGHTING FUNCTION
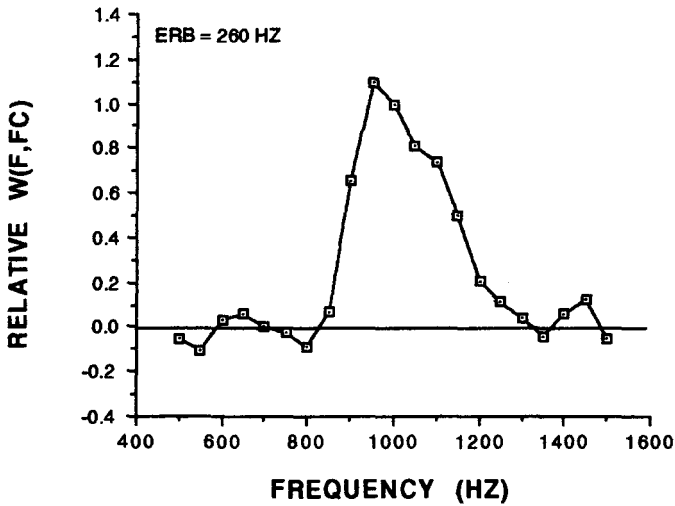
Figure 20c.   The rippled noise masking data from
Chinchilla 4 at a signal frequency of 1000
Hz.   The top panel of the figure shows the
raw sine data from Chinchilla 4.   The open
symbols are the sin+ thresholds and the
closed symbols are the sin- thresholds.   The
middle panel is the sine masking function for
the same animal.   The lower panel shows the
relative weighting or auditory filter
function derived using the sine and cosine
masking functions as well as the equivalent
rectangular bandwidth or ERB of the filter.

CHINCHILLA 4 - 1kHZ SINE DATA
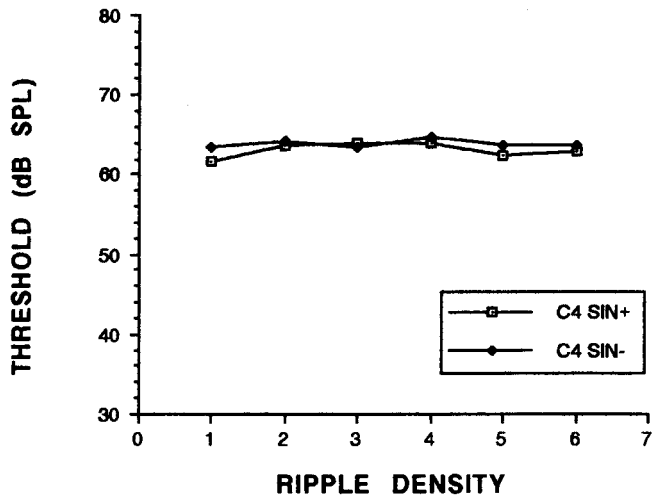
CHINCHILLA 4 - 1kHZ SINE MASKING FUNCTION
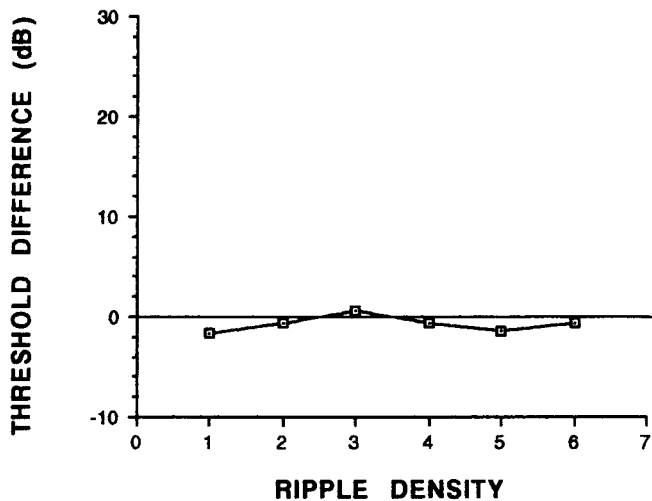
CHINCHILLA 4 - 1kHZ RELATIVE WEIGHTING FUNCTION
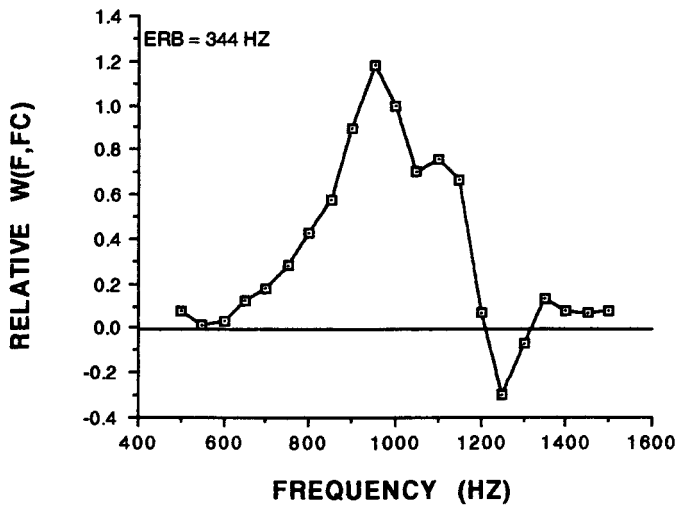
Figure 20d.   The rippled noise masking data from
               Chinchilla 5 at a signal frequency of 1000
               Hz.   The top panel of the figure shows the
               raw sine data from Chinchilla 5.   The open
               symbols are the sin+ thresholds and the
               closed symbols are the sin- thresholds.   The
               middle panel is the sine masking function for
               the same animal.   The lower panel shows the
               relative weighting or auditory filter
               function derived using the sine and cosine
               masking functions as well as the equivalent
               rectangular bandwidth or ERB of the filter.

CHINCHILLA 5 - 1kHZ SINE DATA
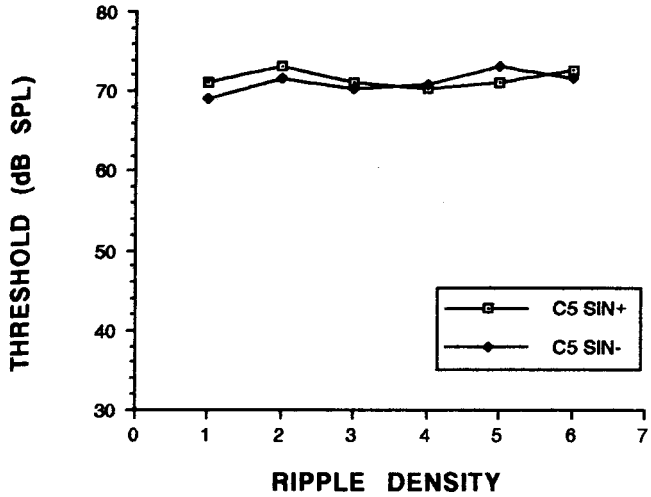
CHINCHILLA 5 - 1kHZ SINE MASKING FUNCTION
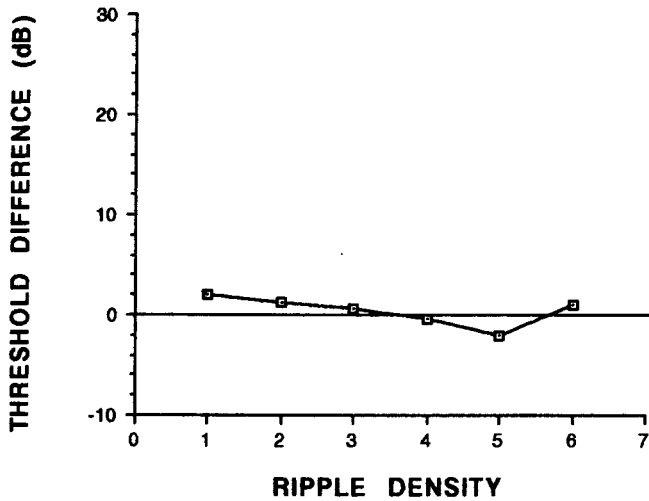
CHINCHILLA 5 - 1kHZ RELATIVE WEIGHTING FUNCTION
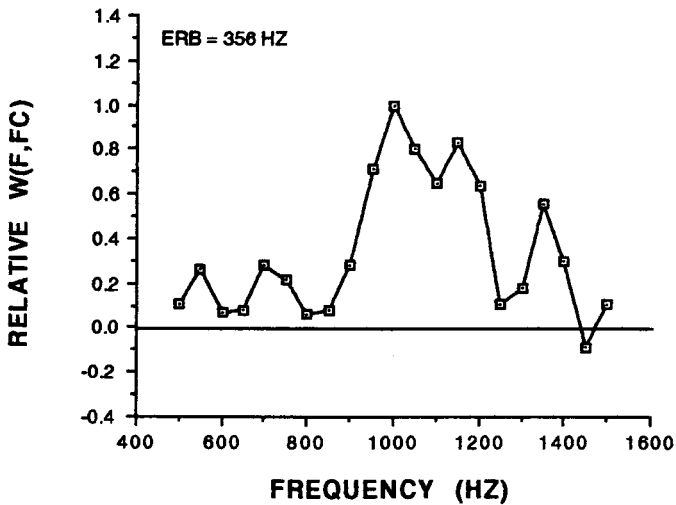
Figure 21.   This figure shows the average 1000 Hz sine
               masking function along with the corresponding
               relative weighting function. The average
               sine masking function was computed by
               averaging the 1000 Hz sine threshold
               differences of all the chinchillas as a
               function of ripple density. This averaged
               sine masking function was then used in
               conjunction with the average 1000 Hz cosine
               masking function to derive the average 1000
               Hz relative weighting function of the
               chinchilla.

AVERAGE 1kHZ SINE MASKING FUNCTION
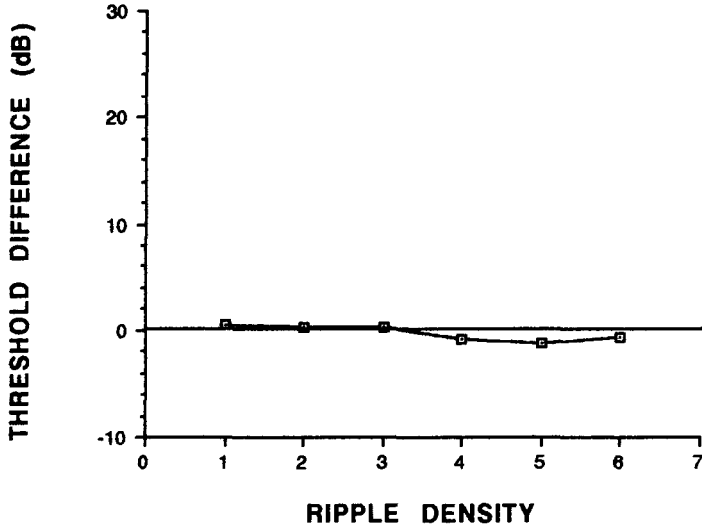
AVERAGE 1kHZ RELATIVE WEIGHTING FUNCTION
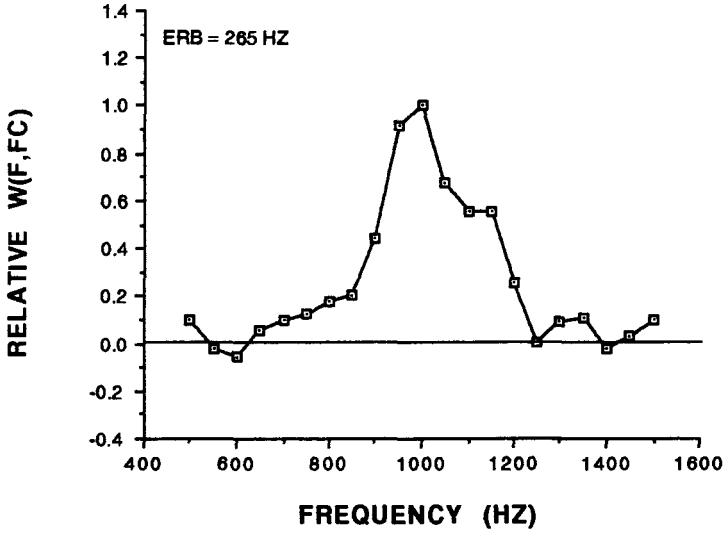
is reasonably representative of the individual data of Chinchillas 1, 3, and 4 in terms of its shape, however, the average 1000 Hz weighting function does not represent Chinchilla 5's weighting function as well as it does the weighting functions of the other chinchillas'. Like the average 500 Hz relative weighting function, the average 1000 Hz relative weighting function also remains fairly symmetrical about the center frequency of the filter.

Figures 22a and 22b compare the 1000 Hz weighting functions derived using only the cosine masking functions with the weighting functions derived using both sine and cosine masking functions. Again, although there are some differences in each animal's auditory filters, there are few differences in the overall shapes of the animal's auditory filters. In general, these figures show that the chinchillas' 1000 Hz auditory filter shapes are, to a first approximation, symmetrical.

Figures 23a-e show the sine data from Chinchillas 1, 3, 4, 5, and 6 at a signal frequency of 2000 Hz in the same format as the 500 and 1000 Hz data. With the exception of Chinchilla 1, whose weighting function shifts slightly towards the low frequency side, the relative weighting functions of the other chinchillas are fairly symmetrical.

Figure 24 shows the average 2000 Hz sine masking function along with the corresponding relative weighting

Figure 22a.   This figure compares the 1000 Hz weighting

functions derived using only the cosine

masking functions (labelled COS W(F)) with

the weighting functions derived using both

sine and cosine masking functions (labelled

SIN W(F)) for Chinchillas 1 and 3. Although

there are some differences in each animal's

auditory filter "noise", there are few, if

any, differences in the shapes of the

animal's auditory filter peaks. In general,

this figure shows that estimates of the 1000

Hz auditory filter shapes are not influenced

much by the sine data.

CHINCHILLA 1 - 1kHZ RELATIVE WEIGHTING FUNCTIONS
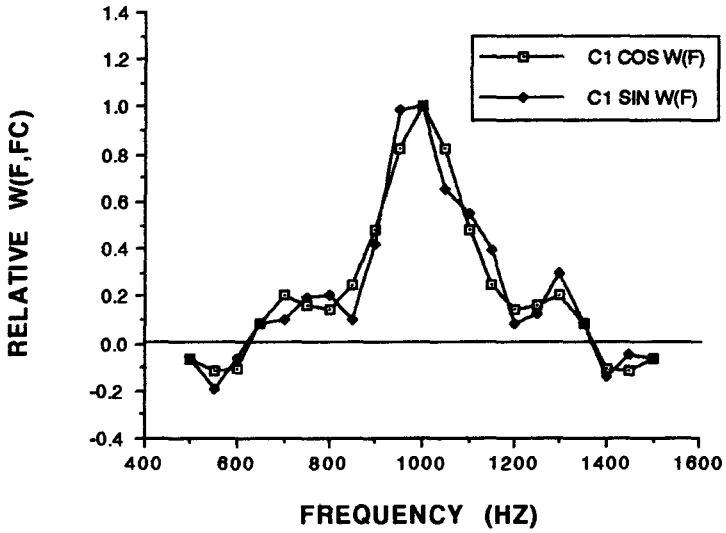
CHINCHILLA 3 - 1kHZ RELATIVE WEIGHTING FUNCTIONS
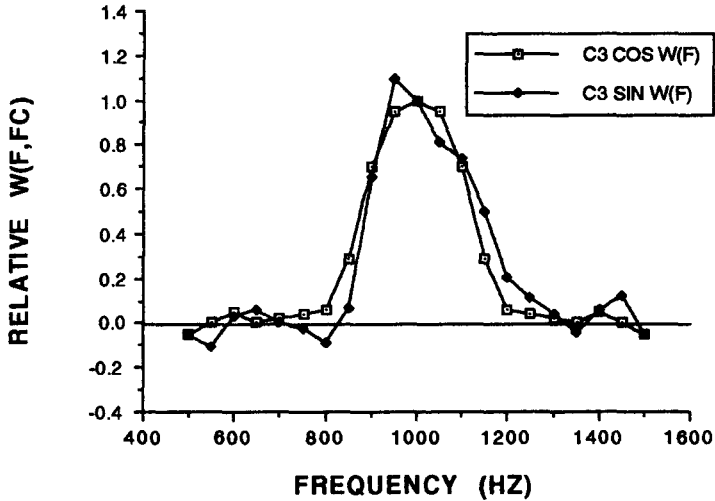
Figure 22b. This figure compares the 1000 Hz weighting
functions derived using only the cosine
masking functions (labelled COS W(F)) with
the weighting functions derived using both
sine and cosine masking functions (labelled
SIN W(F)) for Chinchillas 4 and 5. Both of
these animals show some differences in the
shapes of their auditory filter functions
with the addition of the sine data. In
general, this figure shows that estimates of
the 1000 Hz auditory filter shapes of these
two animals are influenced to some degree by
the sine data.

CHINCHILLA 4 - 1kHZ RELATIVE WEIGHTING FUNCTIONS
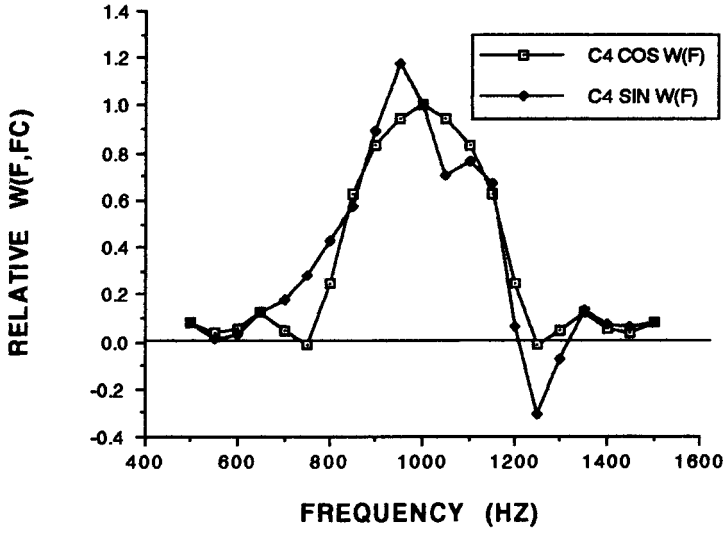
CHINCHILLA 5 - 1kHZ RELATIVE WEIGHTING FUNCTIONS
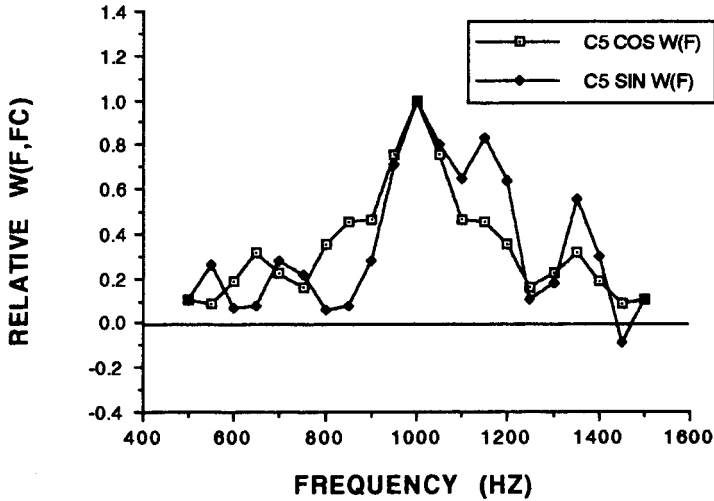
Figure 23a.   The rippled noise masking data from Chinchilla 1 at a signal frequency of 2000 Hz.   The top panel of the figure shows the raw sine data from Chinchilla 1.   The open symbols are the sin+ thresholds and the closed symbols are the sin- thresholds.   The middle panel is the sine masking function for the same animal.   The lower panel shows the relative weighting or auditory filter function derived using the sine and cosine masking functions as well as the equivalent rectangular bandwidth or ERB of the filter.

CHINCHILLA 1 - 2kHZ SINE DATA
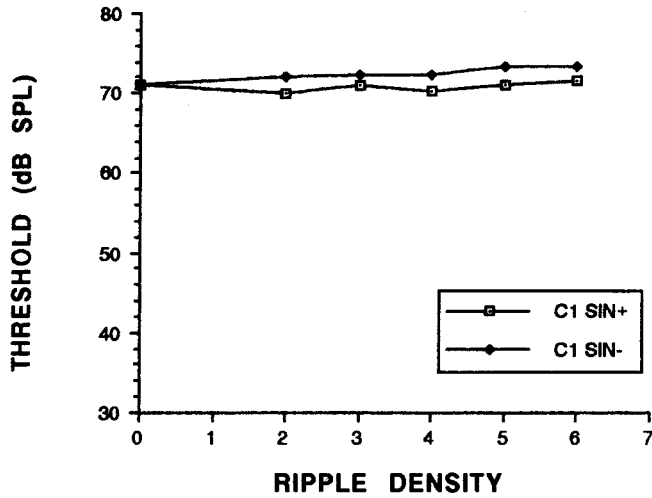
CHINCHILLA 1 - 2kHZ SINE MASKING FUNCTION
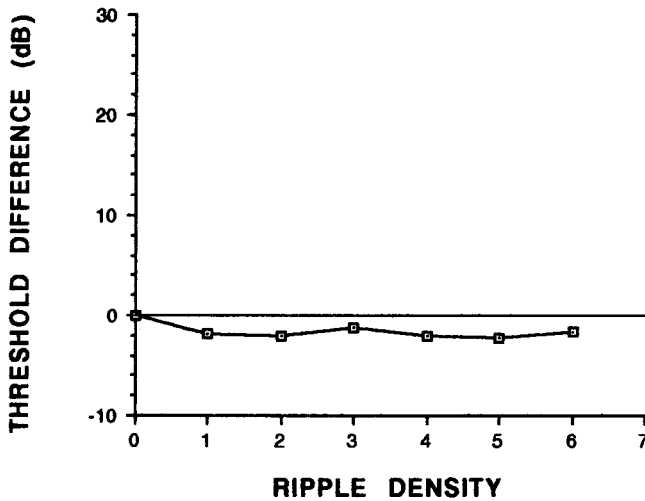
CHINCHILLA 1 - 2kHZ RELATIVE WEIGHTING FUNCTION
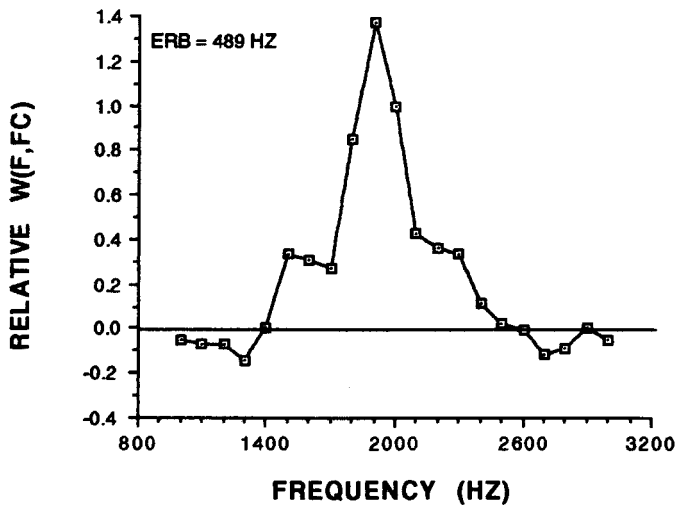
Figure 23b.   The   rippled   noise   masking   data   from
Chinchilla 3 at a signal frequency of 2000
Hz.   The top panel of the figure shows the
raw sine data from Chinchilla 3.   The open
symbols are the sin+ thresholds and the
closed symbols are the sin- thresholds.   The
middle panel is the sine masking function for
the same animal.   The lower panel shows the
relative   weighting   or   auditory   filter
function derived using the sine and cosine
masking functions as well as the equivalent
rectangular bandwidth or ERB of the filter.

CHINCHILLA 3 - 2kHZ SINE DATA
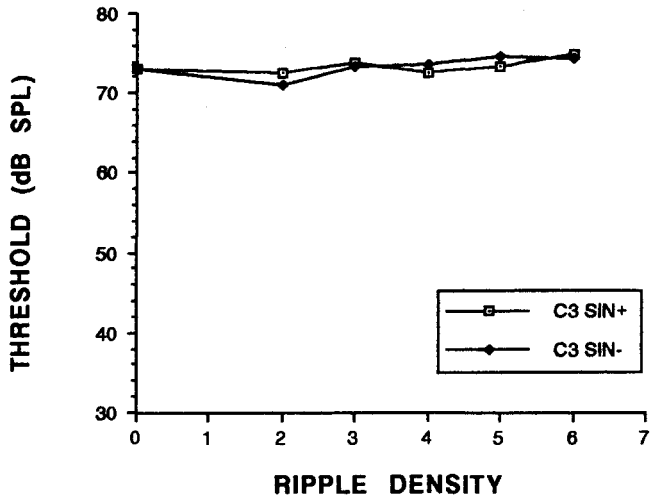
CHINCHILLA 3 - 2kHZ SINE MASKING FUNCTION
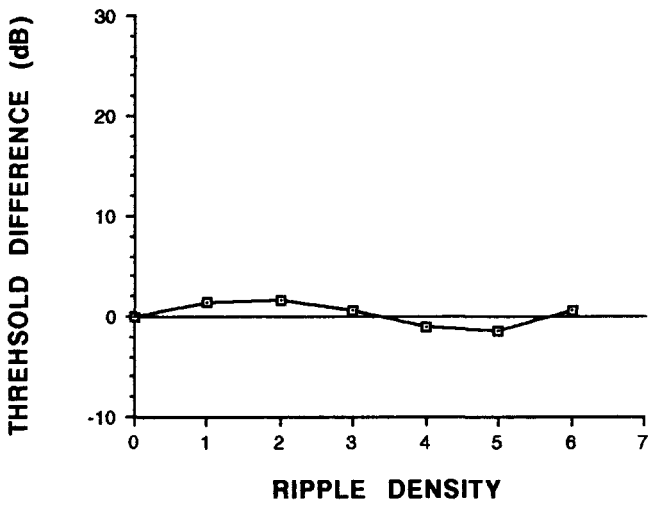
CHINCHILLA 3 - 2kHZ RELATIVE WEIGHTING FUNCTION
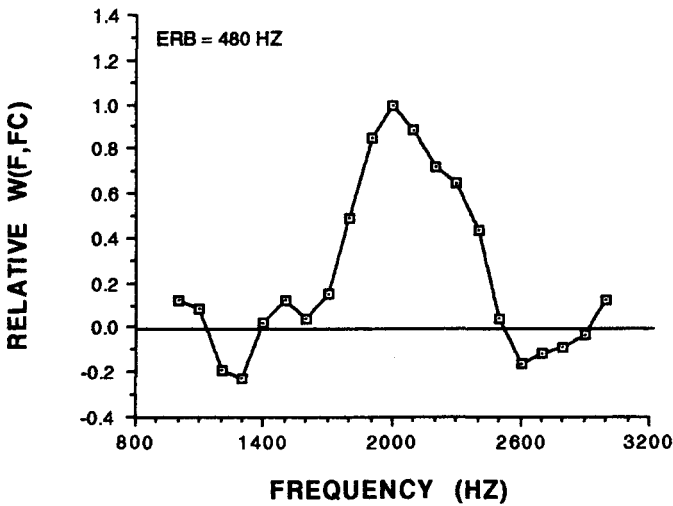
Figure 23c.   The   rippled   noise   masking   data   from
              Chinchilla 4 at a signal frequency of 2000
              Hz.   The top panel of the figure shows the
              raw sine data from Chinchilla 4.   The open
              symbols are the sin+ thresholds and the
              closed symbols are the sin- thresholds.   The
              middle panel is the sine masking function for
              the same animal.   The lower panel shows the
              relative   weighting   or   auditory   filter
              function derived using the sine and cosine
              masking functions as well as the equivalent
              rectangular bandwidth or ERB of the filter.

CHINCHILLA 4 - 2kHZ SINE DATA
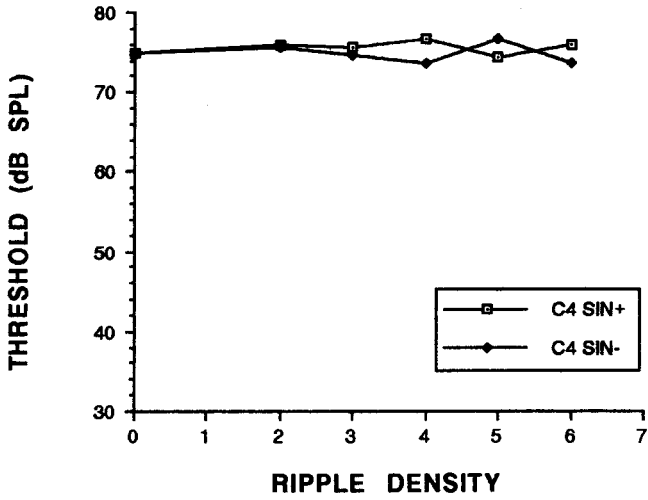
CHINCHILLA 4 - 2kHZ SINE MASKING FUNCTION
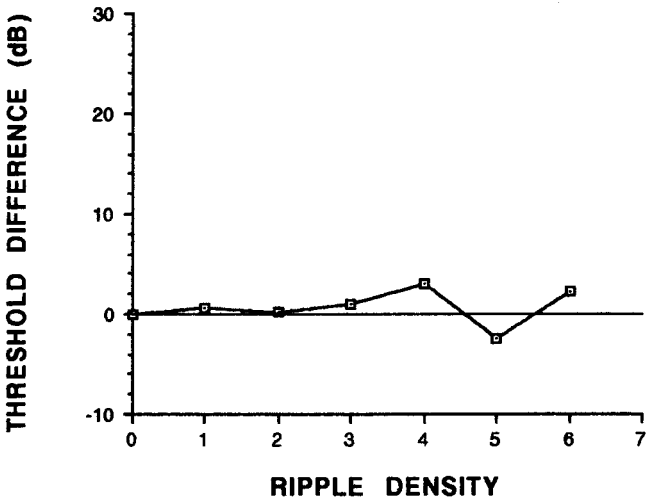
CHINCHILLA 4 - 2kHZ RELATIVE WEIGHTING FUNCTION
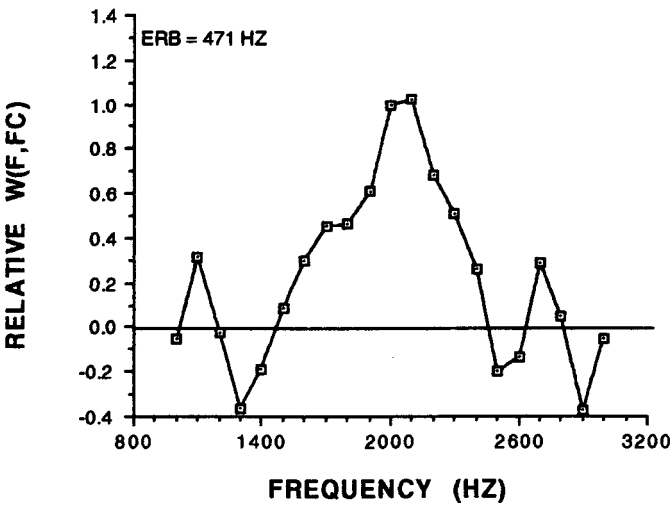
Figure 23d.   The   rippled   noise   masking   data   from
               Chinchilla 5 at a signal frequency of 2000
               Hz.   The top panel of the figure shows the
               raw sine data from Chinchilla 5.   The open
               symbols   are   the   sin+   thresholds   and   the
               closed symbols are the sin- thresholds.   The
               middle panel is the sine masking function for
               the same animal.   The lower panel shows the
               relative   weighting   or   auditory   filter
               function derived using the sine and cosine
               masking functions as well as the equivalent
               rectangular bandwidth or ERB of the filter.

CHINCHILLA 5 - 2kHZ SINE DATA
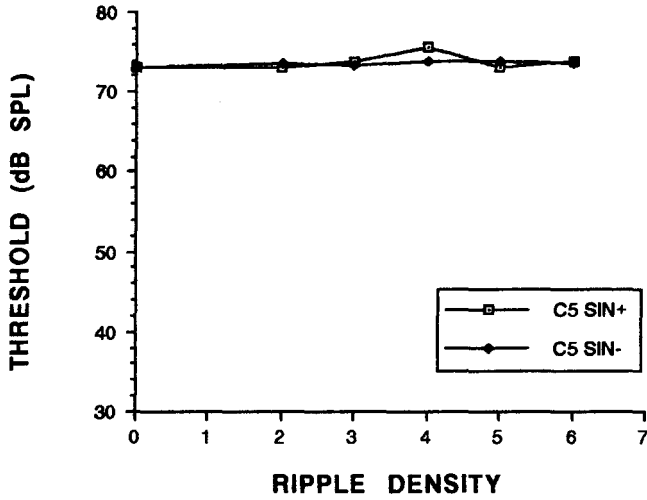
CHINCHILLA 5 - 2kHZ SINE MASKING FUNCTION
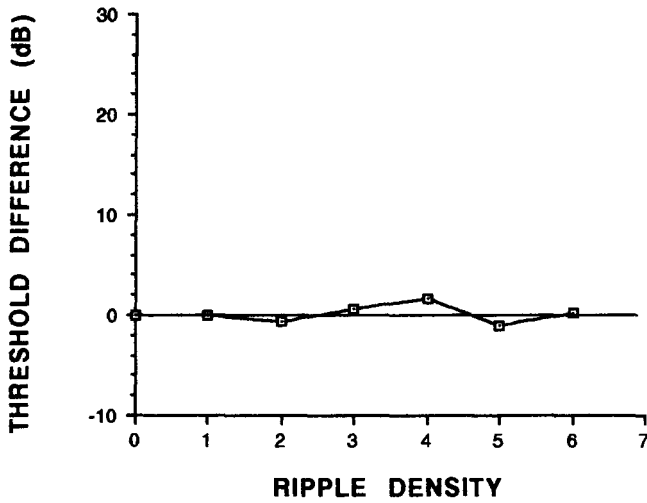
CHINCHILLA 5 - 2kHZ RELATIVE WEIGHTING FUNCTION
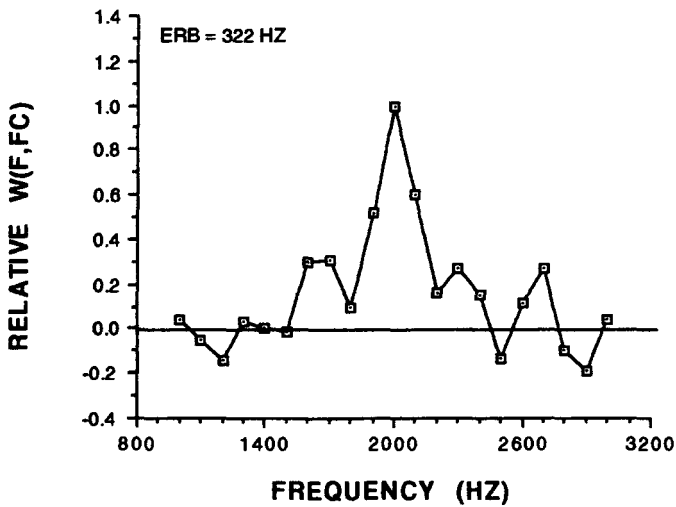
Figure 23e.   The rippled noise masking data from Chinchilla 6 at a signal frequency of 2000 Hz.   The top panel of the figure shows the raw sine data from Chinchilla 6.   The open symbols are the sin+ thresholds and the closed symbols are the sin- thresholds.   The middle panel is the sine masking function for the same animal.   The lower panel shows the relative weighting or auditory filter function derived using the sine and cosine masking functions as well as the equivalent rectangular bandwidth or ERB of the filter.

CHINCHILLA 6 - 2kHZ SINE DATA
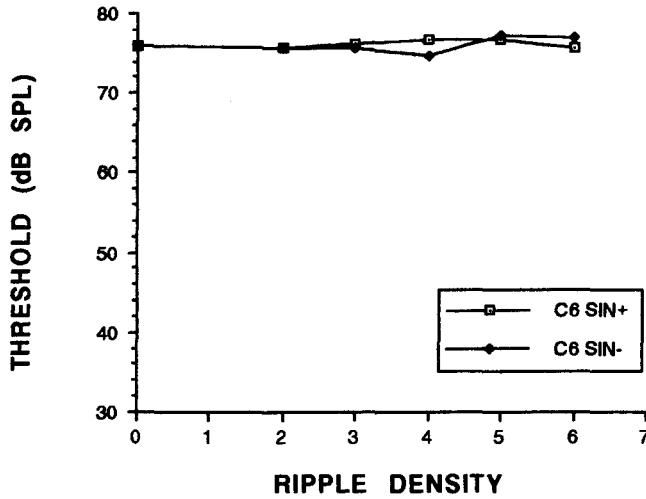
CHINCHILLA 6 - 2kHZ SINE MASKING FUNCTION

CHINCHILLA 6 - 2kHZ RELATIVE WEIGHTING FUNCTION

ERB = 527 HZ
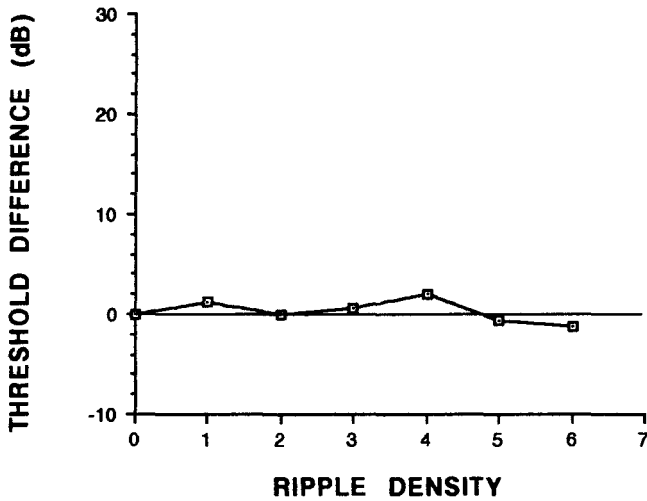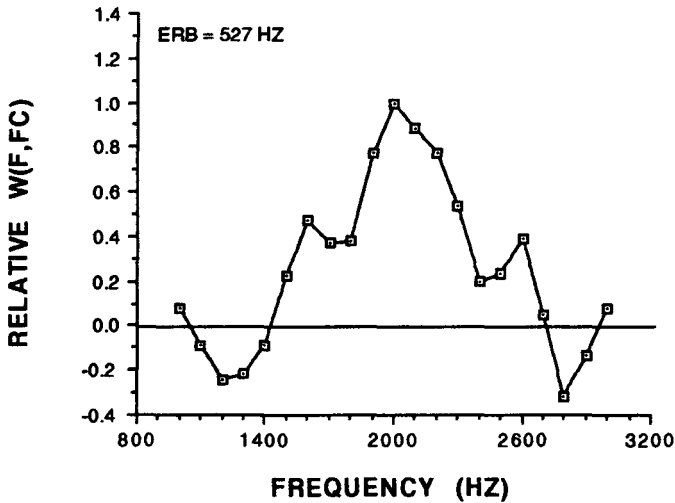
Figure 24.   This figure shows the average 2000 Hz sine
              masking function along with the corresponding
              relative weighting function.   The average
              sine masking function was computed by
              averaging the 2000 Hz sine threshold
              differences of all the chinchillas as a
              function of ripple density.   This averaged
              sine masking function was then used in
              conjunction with the average 2000 Hz cosine
              masking function to derive the average 2000
              Hz relative weighting function of the
              chinchilla.

AVERAGE 2kHZ SINE MASKING FUNCTION
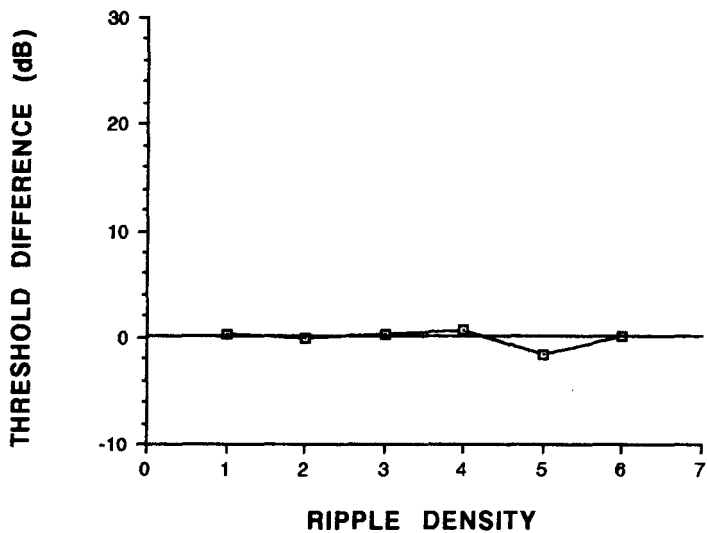
AVERAGE 2kHZ RELATIVE WEIGHTING FUNCTION
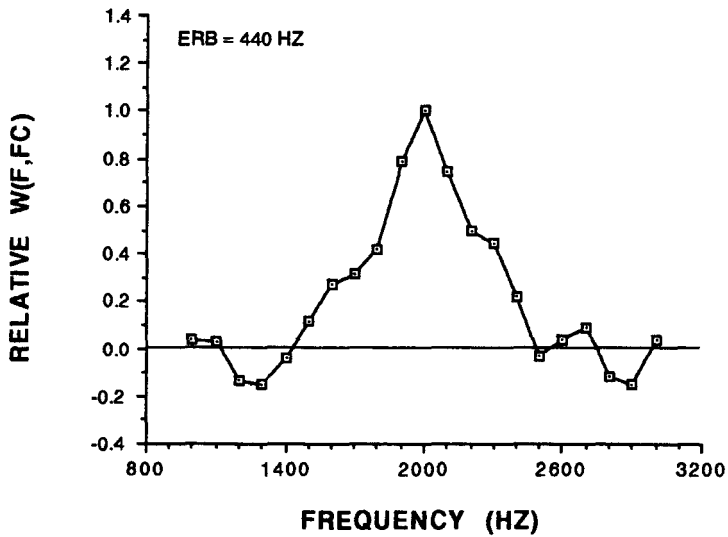
function.   Comparison of the average 2000 Hz relative weighting function with the individual weighting functions in Figures 23a-e shows that the average is reasonably representative of the individual data in terms of its shape.   Like the average 500 and 1000 Hz relative weighting functions, the average 2000 Hz relative weighting function is nearly symmetrical about the center frequency of the filter.

Figures 25a and 25b compare the 2000 Hz weighting functions derived using only the cosine masking functions with the weighting functions derived using both sine and cosine masking functions. With the exception of Chinchilla 1, although there are some differences in each animal's auditory filters, there are few differences in the overall shapes of the animals' auditory filters. In general, these figures show that the chinchillas' 2000 Hz auditory filter shapes are also reasonably symmetrical.

With the exception of a few individual differences, the overall trend of the sine rippled noise data supports the initial assumption that the chinchillas' auditory filters are symmetrical about their center frequencies. This is particularly evident across the averaged weighting functions for each signal frequency. Figure 26 compares the relative weighting functions derived using only the average cosine masking functions with the relative

weighting functions derived using both the average sine and cosine masking functions for all three signal frequencies. When taken together, there are two very strong trends in these data and both of these trends can be seen in the figure. First, the filters at all three signal frequencies are similar in shape. That is, all three filters show a simple bandpass characteristic which is roughly symmetrical about the center frequency. Second, the bandwidths of the filters increase with center frequency. With respect to these two results, it can be concluded that chinchillas respond to rippled noise in a manner which is very similar to humans. It is important to note, however, that the weighting functions are not simply rescaled as a function of center frequency. If this were the case, they would overlay each other exactly when plotted in terms of normalized frequency. Figure 27 shows that the weighting functions do not overlay each other when plotted in terms of normalized frequency.

Figure 25a.   This figure compares the 2000 Hz weighting
               functions derived using only the cosine
               masking functions (labelled COS W(F)) with
               the weighting functions derived using both
               sine and cosine masking functions (labelled
               SIN W(F)) for Chinchillas 1 and 3.   Inclusion
               of Chinchilla 1's sine data causes a shift
               towards low frequencies of his auditory
               filter. Inclusion of Chinchilla 3's sine data
               has little effect on his auditory filter
               function.

CHINCHILLA 1 - 2kHZ RELATIVE WEIGHTING FUNCTIONS
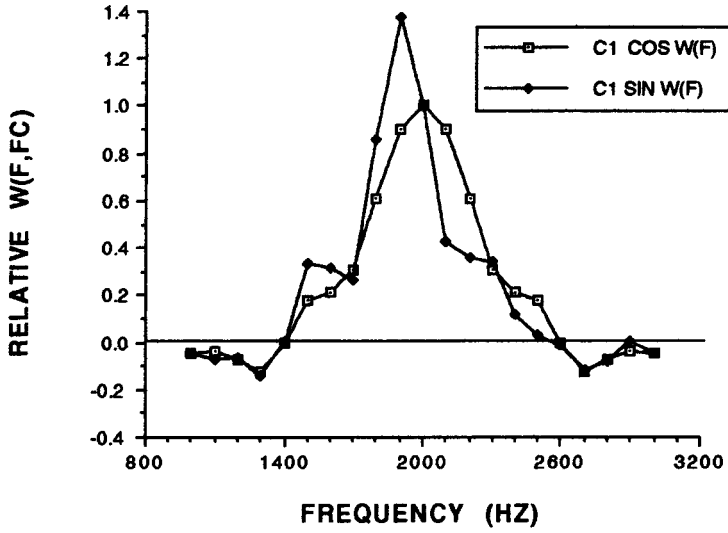
CHINCHILLA 3 - 2kHZ RELATIVE WEIGHTING FUNCTIONS
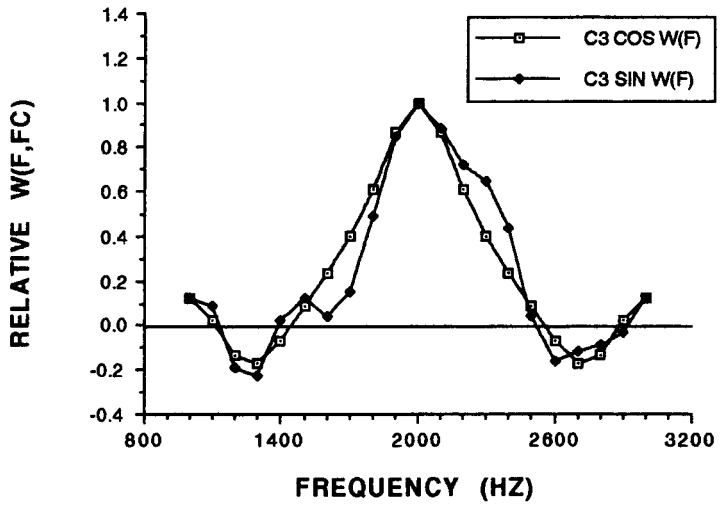
Figure 25b.   This figure compares the 2000 Hz weighting

functions derived using only the cosine

masking functions (labelled COS W(F)) with

the weighting functions derived using both

sine and cosine masking functions (labelled

SIN W(F)) for Chinchillas 4, 5 and 6. All

three of these animals show little difference

in the shapes of their auditory filter

functions with the addition of the sine data.

In general, this figure shows that the

estimated shapes of the 2000 Hz auditory

filters of these three animals are not

influenced much by the sine data.

CHINCHILLA 4 - 2kHZ RELATIVE WEIGHTING FUNCTIONS
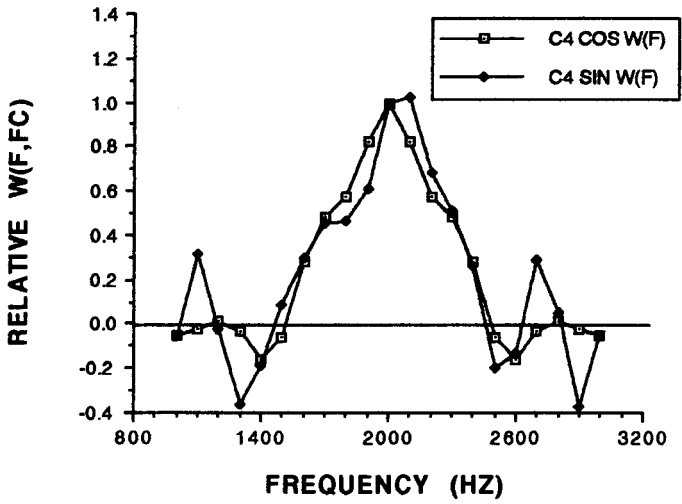
CHINCHILLA 5 - 2kHZ RELATIVE WEIGHTING FUNCTIONS
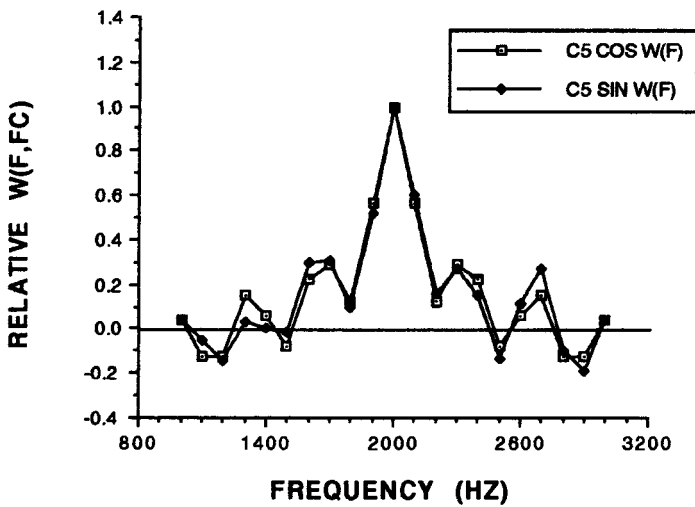
CHINCHILLA 6 - 2kHZ RELATIVE WEIGHTING FUNCTIONS
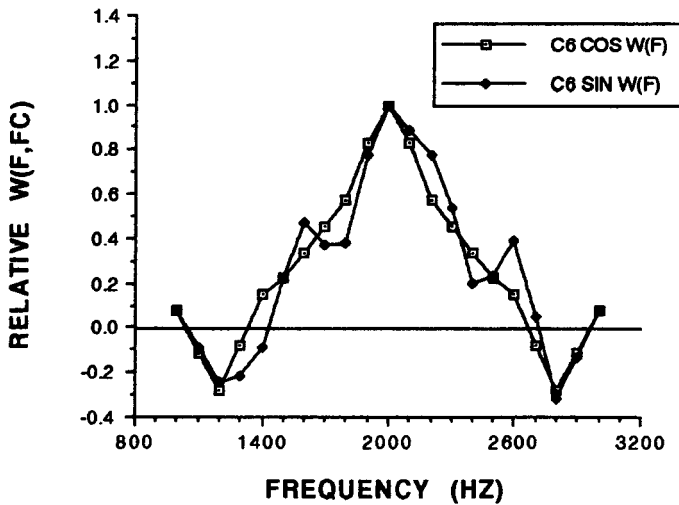
Figure 26.   This figure compares the relative weighting

functions derived using only the average

cosine masking functions (labelled COS W(F))

with the relative weighting functions derived

using both the average sine and cosine

masking functions (labelled SIN W(F)) for all

three signal frequencies.   (Note the scale

change in the abscissa from the top to bottom

panels.) As can be seen from the figure, all

three filters show a simple bandpass

characteristic which is roughly symmetrical

about the center frequency.   In addition to

this, the bandwidths of the filters increase

with center frequency.

AVERAGE 500 HZ RELATIVE WEIGHTING FUNCTIONS
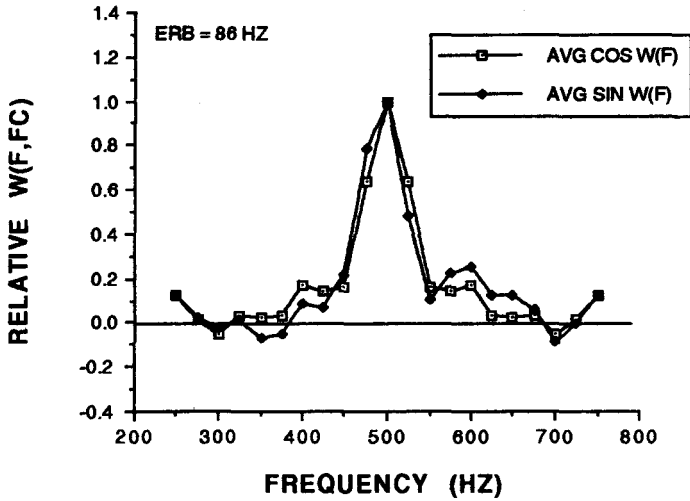
AVERAGE 1kHZ RELATIVE WEIGHTING FUNCTIONS
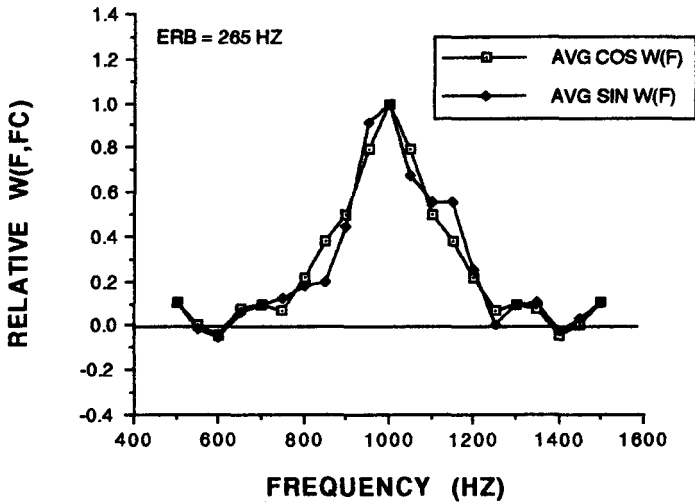
AVERAGE 2kHZ RELATIVE WEIGHTING FUNCTIONS
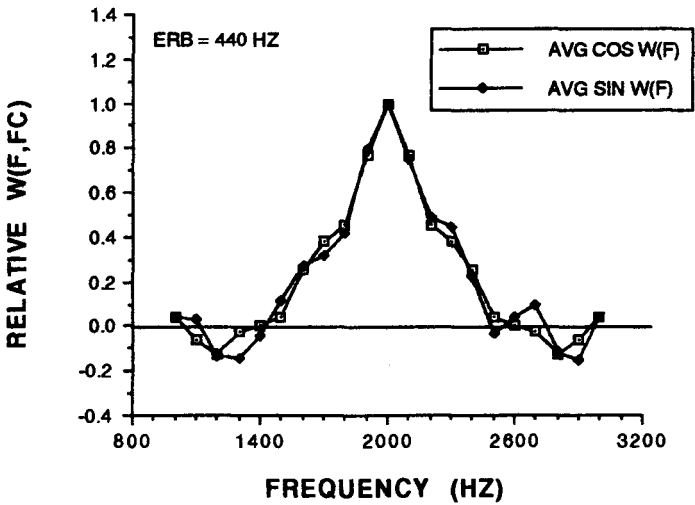
Figure 27.   This figure shows the 500, 1000, and 2000 Hz
              relative weighting functions on a relative
              frequency scale. As can be seen from the
              figure, the weighting functions are not
              simply rescaled as a function of center
              frequency.

AVERAGE WEIGHTING FUNCTIONS
PLOTTED IN TERMS OF RELATIVE FREQUENCY
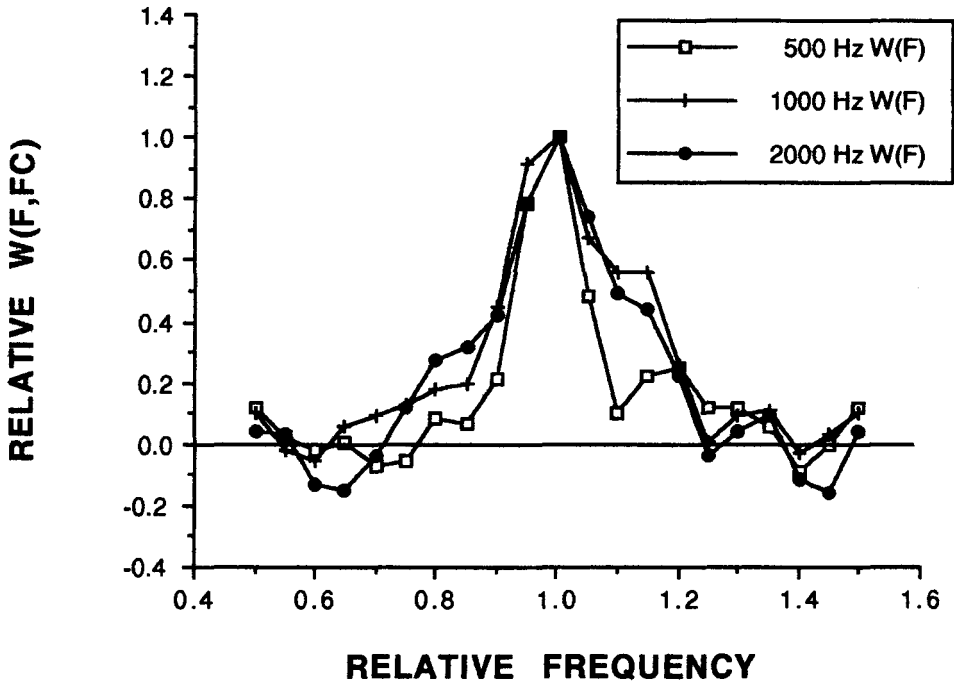
CHAPTER V

MATHEMATICAL APPROXIMATIONS TO THE AUDITORY FILTERS

In order to attempt to provide a simpler mathematical expression for the average auditory filter shapes derived in the previous chapter, the average filter shapes were compared with two common mathematical functions, the Gaussian and the rounded-exponential. This comparison was carried out by assuming a filter shape, either Gaussian or single-parameter rounded-exponential (Roex (p)), and varying the parameter of the assumed function to find the best least squares fit between the actual average cosine masking function and the predicted cosine masking function. Since it has been shown in Experiment 2 that the auditory filters are roughly symmetrical, only the average cosine masking functions will be fitted with the mathematical functions.

The Gaussian filter is of the form:

(11) $W(g) = \exp(-cg^2)$,

where $g = [(f - f_t)/f_t]$ and c is the fitting parameter which determines the steepness of the filter (c > 0). Glasberg,

Moore, and Nimmo-Smith (1984a) showed that the ratio of threshold at the valley to threshold at the peak in the rippled noise spectrum is:

$$(12) \quad \frac{I_V}{I_P} = \frac{[1 + m \, \exp(-\pi^2 n^2/c)]}{[1 - m \, \exp(-\pi^2 n^2/c)]},$$

where m is the modulation depth and n is the ripple density (defined in Chapter III). The predicted intensity ratios were converted to decibels by fitting ten times the logarithm of Eq. (12) to the actual average cosine masking functions. For the 500, 1000, and 2000 Hz average cosine masking functions, the best fitting values of c were 57, 32, and 70, respectively.

Figure 28 shows the results of modeling the average auditory filters as Gaussian functions. This figure plots the average cosine weighting function at each of the three center frequencies with the appropriate Gaussian filter function superimposed on it. The figure also shows the ERBs for both the average cosine weighting functions and the Gaussian weighting functions. It is apparent from this figure that, with the exception of the 2000 Hz filter, the Gaussian filter functions do not provide a particularly good fit to the average cosine weighting functions. With the exception of the 2000 Hz filter, the Gaussian filter functions tend to overestimate the ERBs derived from the average cosine masking functions.

Figure 28.   This figure shows the results of modeling the
               average auditory filters as Gaussians.   The
               figure plots the average cosine weighting
               function at   each   of   the   three   center
               frequencies (500, 1000, and 2000 Hz) with the
               best least-squares fit of a Gaussian filter
               function   superimposed on it.   The figure
               also shows the ERBs for both the average
               cosine weighting functions and the Gaussian
               weighting functions.

AVERAGE 500 HZ GAUSSIAN WEIGHTING FUNCTION

COS ERB = 86 HZ
GAUS ERB = 117 HZ

AVG COS W(F)
AVG GAUS W(F)
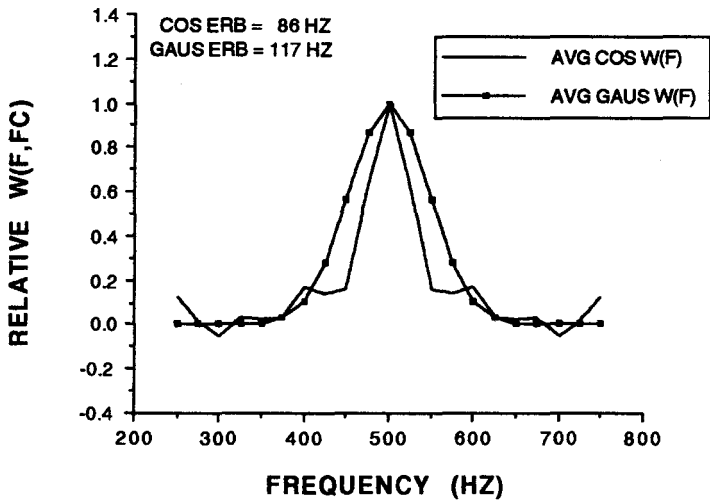
AVERAGE 1kHZ GAUSSIAN WEIGHTING FUNCTION

COS ERB = 265 HZ
GAUS ERB = 313 HZ

AVG COS W(F)
AVG GAUS W(F)
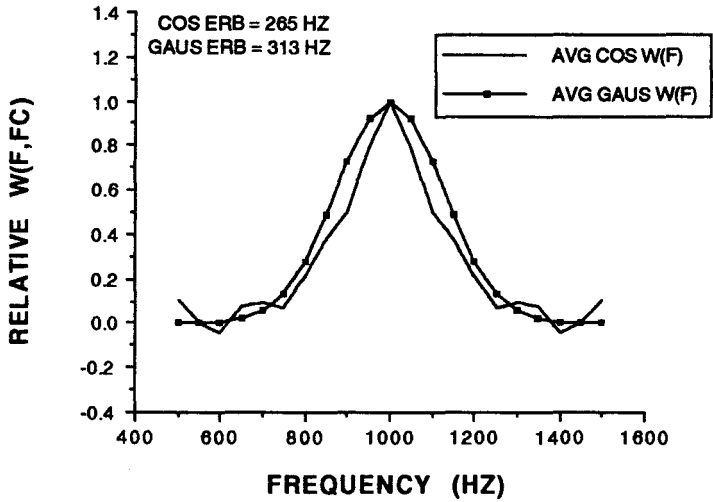
AVERAGE 2kHZ GAUSSIAN WEIGHTING FUNCTION

COS ERB = 440 HZ
GAUS ERB = 424 HZ

AVG COS W(F)
AVG GAUS W(F)
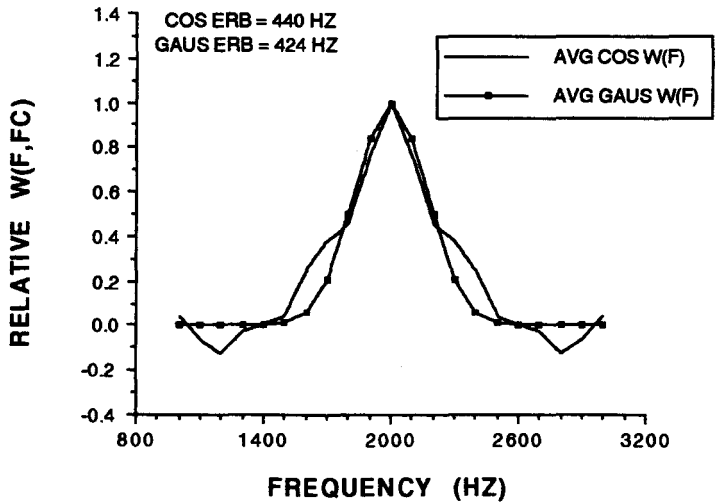
The single-parameter rounded-exponential (Roex(p)) filter has the form:

(13) $W(g) = (1 + pg)\exp(-pg)$,

where p is the fitting parameter which determines the steepness of the filter. Glasberg, et al. (1984a) showed that for this type of filter the ratio of threshold at the valley to threshold at the peak in the rippled noise spectrum is:

(14) $\dfrac{I_v}{I_p} = \dfrac{1 + m\ [p^2/(p^2+4\pi^2 n^2)]^2}{1 - m\ [p^2/(p^2+4\pi^2 n^2)]^2}$,

where m and n are defined as before. The predicted intensity ratios were again converted to decibels by fitting ten times the logarithm of Eq. (14) to the actual average cosine masking functions. For the 500, 1000, and 2000 Hz average cosine masking functions, the best fitting values of p were 20, 14, and 22, respectively.

Figure 29 shows the results of modeling the average auditory filters as Roex(p) filters. This figure plots the average cosine weighting function at each of the three center frequencies with the appropriate Roex(p) filter function superimposed on it. The figure also shows the ERBs for both the average cosine weighting functions and the Roex(p) weighting functions. This figure shows that the Roex(p) filter functions provide a better fit to the

Figure 29.   This figure shows the results of modeling the average auditory filters as single-parameter rounded-exponentials (Roex(p)s). The figure plots the average cosine weighting function at each of the three center frequencies (500, 1000, and 2000 Hz) with the best least-squares fit of the Roex(p) filter function superimposed on it. The figure also shows the ERBs for both the average cosine weighting functions and the Roex(p) weighting functions.

AVERAGE 500 HZ ROEX(p) WEIGHTING FUNCTION
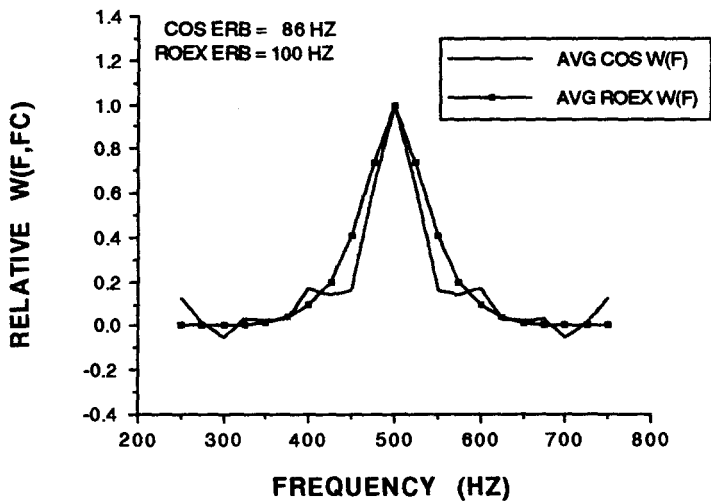
AVERAGE 1kHZ ROEX(p) WEIGHTING FUNCTION
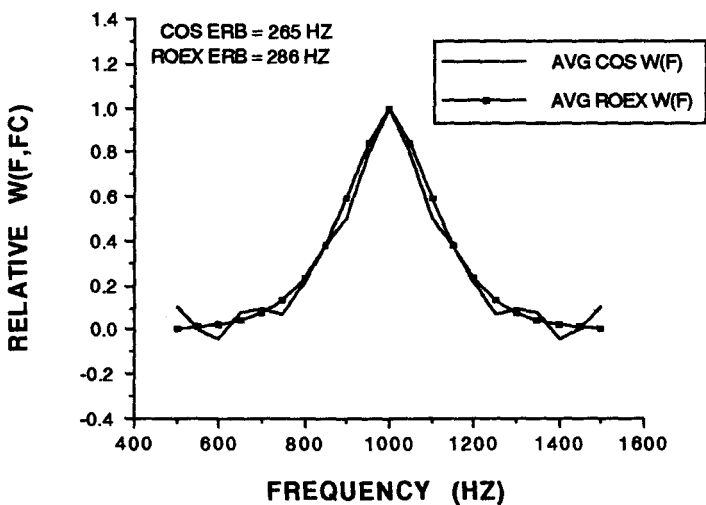
AVERAGE 2kHZ ROEX(p) WEIGHTING FUNCTION
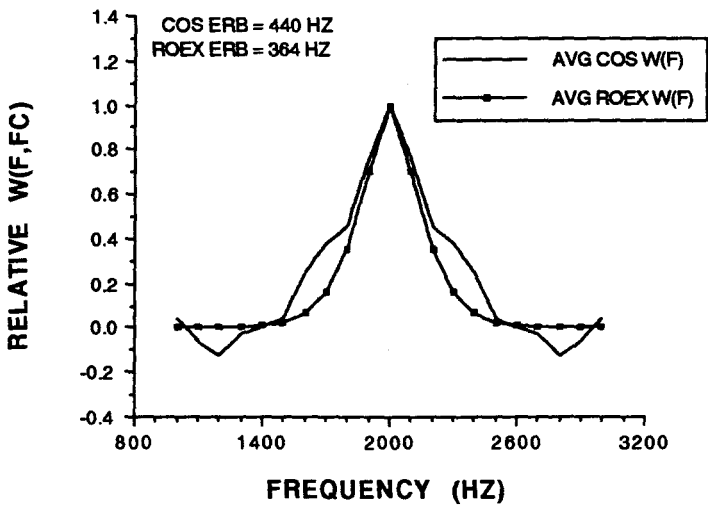
average cosine weighting functions than do the Gaussian filter functions, especially at the tips of the filters. With the exception of the 2000 Hz filter, the Roex(p) filter functions also tend to overestimate the ERBs derived from the cosine masking functions, however, the ERBs derived from the Roex(p) fits to the data are closer to the average cosine weighting function ERBs than are the Gaussian ERBs. Only at 2000 Hz does the Gaussian filter provide a better fit to the average cosine weighting function than the Roex(p) filter.

CHAPTER VI

DISCUSSION AND CONCLUSIONS

This study examined tuning in the chinchilla at several frequencies by using two different measures of frequency selectivity. The first measure, the critical masking ratio, is an indirect measure of frequency selectivity whereas the second measure, rippled noise masking, is more direct. The overall trends in the chinchilla data will be discussed in terms of the average data since, with the exception of a few individual differences, the average data represent the individual.

In general, the results of the critical masking ratio experiment showed that, according to this technique, the chinchilla is very broadly tuned and has very poor frequency selectivity in comparison to humans. Scharf (1970) showed critical masking ratio data for humans which, when corrected by multiplying by 2.5, yielded estimates of critical bandwidth that typically ranged from 15-22% of the center frequency over the frequency range from 500 to 10000 Hz. In this study, which used test tones over

165

approximately the same frequency range, the chinchilla critical masking ratios yielded average uncorrected estimates of critical bandwidth which ranged from 46-177% of the center frequency. The average corrected estimates of critical bandwidth ranged from 115-443% of the center frequency. The critical masking ratios measured in this study are comparable to those measured by Miller (1964) and Seaton and Trahiotis (1975). On the average, the data measured in this study using the positive-reinforcement behavioral tracking technique were between 2.8 and 8.3 dB higher than those measured using negative reinforcement techniques. Therefore, when frequency selectivity is measured by this indirect procedure, the chinchilla does not compare favorably with humans.

The weighting functions derived from the rippled noise masking functions showed that the chinchillas' auditory filter shapes are similar to human auditory filter shapes. Figure 30 compares the 1000 Hz human auditory filter (Houtgast, 1977) with the average 1000 Hz chinchilla auditory filter. The human auditory filter shape is based on the sine and cosine masking functions from Houtgast's direct masking data. Only Houtgast's threshold differences for ripple densities 1-6 were used in this computation of the human auditory filter shape. In this way, both the human and the chinchilla auditory filter shapes are based

Figure 30.   This figure compares the 1000 Hz human
              auditory filter (Houtgast, 1977) with the
              1000 Hz chinchilla auditory filter.   The
              human auditory filter shape is based on the
              sine and cosine masking functions from
              Houtgast's direct masking data.   Only
              Houtgast's threshold differences for ripple
              densities 1-6 were used in this computation
              of the human auditory filter shape.   Both the
              human and the chinchilla auditory filters
              have a simple bandpass characteristic and are
              roughly symmetrical.   In terms of bandwidth,
              the chinchilla weighting function is only
              slightly wider than the human weighting
              function.

HUMAN AND CHINCHILLA
1kHZ RELATIVE WEIGHTING FUNCTIONS
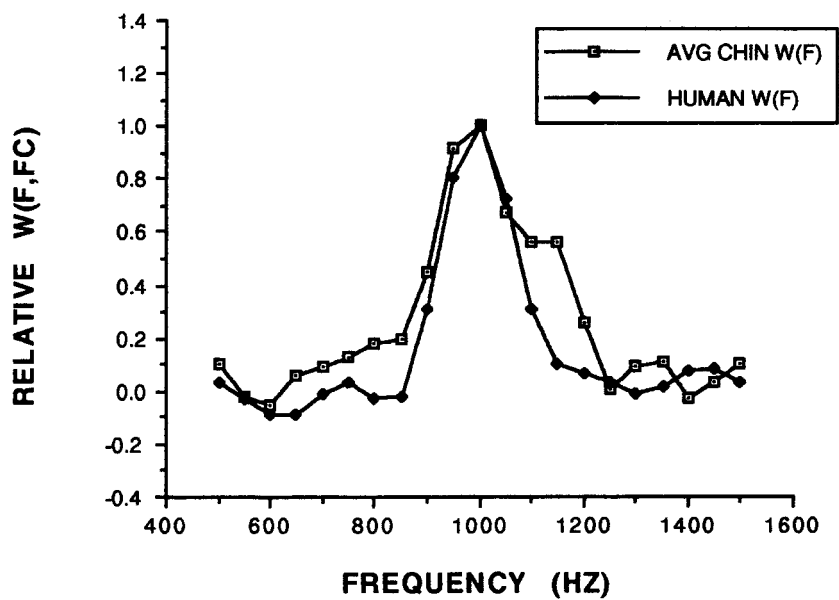
on the same ripple densities. As can be seen from Figure 30, both the human and the chinchilla auditory filters have a simple bandpass characteristic and are roughly symmetrical. In terms of bandwidth, the chinchilla weighting function is only slightly wider than the human weighting function. (Unfortunately, Houtgast did not publish threshold difference data at other signal frequencies, therefore, this is the only direct comparison that can be made between Houtgast's data and the chinchilla data.) Table 2 lists the individual ERBs for each chinchilla as a function of signal frequency. The chinchillas are very consistent in terms of their ERBs at each signal frequency. Houtgast's (1974, 1977) data showed that human ERBs were approximately 15-20% of the center frequency over the frequency range from 500 to 2000 Hz. The data from this study showed that the average chinchilla ERBs were approximately 17-27% of the center frequency over the same frequency range. Based on this comparison between the average human ERBs and the average chinchilla ERBs, it appears that when the chinchilla's frequency selectivity is measured by a more direct means, it compares quite favorably with the human. Therefore, with respect to these results involving the shape and bandwidth of the chinchilla's auditory filter, it can be concluded that

Table 2.   This table lists the individual ERBs for each
                chinchilla as a function of signal frequency
                as well as the average ERB at each signal
                frequency. The ERBs at each signal frequency
                are very consistent across animals.   The
                average ERBs are based on the ERB values
                obtained from the average masking function at
                each signal frequency.

Chinchilla ERBs at 500, 1000, and 2000 Hz

	Signal Frequency (Hz)		
Subject	<u>500</u>	<u>1000</u>	<u>2000</u>
C1	77	237	489
C2	98	209	- - -
C3	83	260	480
C4	85	344	471
C5	100	356	322
C6	- - -	297	527
Average	86	265	440

chinchillas respond to rippled noise in a manner which is similar to humans.

From the previous discussion of the general results of this study, there appears to be a rather large discrepancy between the results of the critical masking ratio experiment and the rippled noise masking experiment. This discrepancy between the results of the two experiments can be seen in Table 3. Table 3 lists the ERBs, uncorrected bandwidths derived from the critical masking ratios (Uncorrected CMR BWs), and the corrected bandwidths derived from the critical masking ratios (Corrected CMR BWs). The most plausible explanation for this discrepancy between the two measures of frequency selectivity is that the rippled noise masking experiment estimates frequency selectivity independent of processing efficiency or absolute signal-to-noise ratio of the subject whereas the critical masking ratio experiment assumes that processing efficiency or signal-to-noise ratio is fixed. Processing efficiency, as used here, refers to the ratio of signal power to noise power required at the output of the auditory filter to achieve threshold. With a broadband noise masker, it is impossible to distinguish between changes in frequency selectivity and changes in processing that are independent of frequency selectivity (Patterson et al.,1982). For example, if one subject has a critical masking ratio which

Table 3.   This table lists the ERBs as well as the
             corrected and uncorrected bandwidths derived
             from the critical masking ratios (CMR BWs)
             for each chinchilla as a function of signal
             frequency. The average ERBs are based on the
             average masking functions whereas the average
             uncorrected and corrected CMR BWs are based
             on the average critical masking ratios.
             Notice the discrepancy between the ERBs and
             the CMR BWs.

Chinchilla ERBs, Uncorrected Critical Masking Ratio
Bandwidths, and Corrected Critical Masking Ratio Bandwidths
at 500, 1000, and 2000 Hz

500 Hz

Subject	ERB(Hz)	Uncorrected CMR BW(Hz)	Corrected CMR BW(Hz)
C1	77	417	1043
C2	98	251	628
C3	83	417	1043
C4	85	871	2178
C5	100	2089	5223
C6	---	----	----
Average	86	631	1578

1000 Hz

Subject	ERB(Hz)	Uncorrected CMR BW(Hz)	Corrected CMR BW(Hz)
C1	237	437	1093
C2	209	316	790
C3	260	209	523
C4	344	457	1143
C5	356	871	2178
C6	297	---	----
Average	265	398	995

2000 Hz

Subject	ERB(Hz)	Uncorrected CMR BW(Hz)	Corrected CMR BW(Hz)
C1	489	1318	3295
C2	---	912	2280
C3	480	1148	2870
C4	471	2291	5728
C5	322	2188	5470
C6	527	----	----
Average	440	1585	3963

is 3 dB higher than another subject, the bandwidth derived from the first subject's critical masking ratio will be twice as wide as the bandwidth derived from the more sensitive subject. This is the case when we compare the chinchillas to humans. In masking experiments, humans typically have signal-to-noise ratios (E/N_o) of 5 to 15 dB over the frequency range from 200 to 10000 Hz (Reed and Bilger, 1973). That is, the signal tone must be 5 to 15 dB higher than the noise spectrum level in order for the tone to be detected. The chinchillas in this study have signal-to-noise ratios (E/N_o) of 25 to 40 dB over the same frequency range. This difference in signal-to-noise ratio between humans and chinchillas explains the chinchillas' inferior frequency selectivity based on the critical masking ratios. The rippled noise masking experiment is not affected by this difference in signal-to-noise ratio because the estimates of frequency selectivity derived from this experiment are based on threshold differences and not on the raw threshold data themselves.

Although this study shows that the shapes of the chinchilla auditory filters are similar to those of humans derived under similar conditions, this study fails to show a similarity to the auditory filter shapes of chinchillas derived by Halpern and Dallos (1986). As mentioned in the introduction, Halpern and Dallos used notched noise in a

forward masking paradigm to study auditory filter shape in the chinchilla. Halpern and Dallos showed that while their notched noise masking technique yielded estimates of tuning that were similar to those obtained using other techniques, there was a major difference in the auditory filter shapes of humans and chinchillas. The auditory filter shapes derived by Halpern and Dallos (1986) showed an unexpected dip in the region of the center frequency whereas the auditory filter shapes in this study show a simple bandpass characteristic. No direct comparison can be made between this study and Halpern and Dallos (1986) due to the differences in paradigms (simultaneous versus forward masking) and masking stimuli (rippled noise versus notched noise). However, this study does shed some additional light on the differences and similarities between humans and chinchillas in terms of their frequency selectivity.

CONCLUSIONS

The major conclusions of this study are:

(1) Chinchilla critical masking ratios measured with a positive-reinforcement behavioral tracking technique were found to be comparable to those measured using shock-avoidance techniques (Miller, 1964 and Seaton and Trahiotis, 1975).

(2) Estimates of frequency selectivity based on critical masking ratios indicate that the chinchilla's auditory system would be very poorly tuned in comparison to humans.

(3) Estimates of auditory filter shape based on Houtgast's (1974, 1977) rippled noise masking technique indicate that the auditory filter shapes of humans and chinchillas are similar. The filters are roughly symmetrical and have a simple bandpass characteristic. In addition to this, both the human and chinchilla auditory filters widen as the center frequency increases.

(4) Estimates of frequency selectivity based on the rippled noise masking technique indicate that the chinchilla auditory filters are only slightly wider than the human

auditory filters, reflecting only slightly poorer frequency selectivity.

(5) The discrepancy between the estimates of frequency selectivity derived from the critical masking ratios and those derived from rippled noise masking can be explained by taking into account the subjects' processing efficiency.

(6) Due to differences in psychophysical procedure we cannot conclude anything about the relationship between our data and those of Halpern and Dallos (1986).

REFERENCES

Clark, W.W. and Bohne, B.A. (1978). Animal model for the 4 kHz tonal dip. _Ann. Otol. Rhinol. Laryngol._ 87, 1-16.

Egan, J.P. and Hake, H.W. (1950). On the masking pattern of a simple auditory stimulus. _J. Acoust. Soc. Am._ 22, 622-630.

Fay, R.R., Yost, W.A., and Coombs, S. (1983). Psychophysics and neurophysiology of repetition noise processing in a vertebrate auditory system. _Hearing Res._ 12, 31-55.

Fletcher, H. (1940). Auditory patterns. _Rev. Mod. Phys._ 12, 47-65.

Glasberg, B.R., Moore, B.C.J., and Nimmo-Smith, I. (1984). Comparison of auditory filter shapes derived with three different maskers. _J. Acoust. Soc. Am._ 75, 536-544.

Greenwood, D.D. (1961). Auditory masking and the critical band. _J. Acoust. Soc. Am._ 33, 484-502.

Halpern, D.L. and Dallos, P. (1986). Auditory filter shapes in the chinchilla. _J. Acoust. Soc. Am._ 80, 765-775.

Hamilton, P.M. (1957). Noise masked thresholds as a function of tonal duration and masking noise band width. _J. Acoust. Soc. Am._ 29, 506-511.

Houtgast, T. (1974). Lateral suppression in hearing: A psychophysical study on the ear's capability to preserve and enhance spectral contrasts. Thesis, Free University of Amsterdam, Academische Pers. BV, Amsterdam.

Houtgast, T. (1977). Auditory-filter characteristics derived from direct-masking and pulsation-threshold data with a rippled-noise masker. J. Acoust. Soc. Am. 62, 409-415.

Levitt, H. (1971). Transformed up-down methods in psychoacoustics. J. Acoust. Soc. Am. 49, 467-477.

Miller, J.D. (1964). Auditory sensitivity of the chinchilla in quiet and in noise. J. Acoust. Soc. Am. 36, 2010 (Abstract).

Miller, J.D. (1970). Audibility curve of the chinchilla. J. Acoust. Soc. Am. 48, 513-523.

Moore, B.C.J. (1978). Psychophysical tuning curves measured in simultaneous and forward masking. J. Acoust. Soc. Am. 63, 524-532.

O'Loughlin, B.J. and Moore, B.C.J. (1981). Off-frequency listening: Effects on psychoacoustical tuning curves obtained in simultaneous and forward masking. J. Acoust. Soc. Am. 69, 1119-1125.

Patterson, R.D. (1976). Auditory filter shapes derived with noise stimuli. J. Acoust. Soc. Am. 59, 640-654.

Patterson, R.D., Nimmo-Smith, I., Weber, D.L. and Milroy, R. (1982). The deterioration of hearing with age: Frequency selectivity, the critical ratio, the audiogram, and speech threshold. J. Acoust. Soc. Am. 72, 1788-1803.

Pick, G.F. (1980). Level dependence of psychophysical frequency resolution and auditory filter shape. J. Acoust. Soc. Am. 68, 1085-1095.

Pickles, J.O. (1979). Psychophysical frequency resolution in the cat as determined by simultaneous masking and its relation to auditory-nerve resolution. J. Acoust. Soc. Am. 66, 1725-1732.

Reed, C.M. and Bilger, R.C. (1973). A comparative study of S/N_o and E/N_o. J. Acoust. Soc. Am. 53, 1039-1044.

Scharf, B. (1970). Critical Bands. In Foundations of Modern Auditory Theory, Vol. 1 (edited by J.V. Tobias), Academic Press, New York.

Seaton, W.H. and Trahiotis, C. (1975). Comparison of critical ratios and critical bands in the monaural chinchilla. _J. Acoust. Soc. Am._ 57, 193-199.

Wegel, R.L. and Lane, C.E. (1924). The auditory masking of one sound by another and its probable relation to the dynamics of the inner ear. _Phys. Rev._ 23, 266-285.

Yost, W.A. (1980). Temporal properties of the pitch and pitch strength of ripple noise. In _Psychophysical, Physiological, and Behavioural Studies in Hearing_ (edited by G. Van Den Brink and F.A. Bilsen), Delft University Press, The Netherlands.

Yost, W.A. (1982). The dominance region and ripple noise pitch: A test of the peripheral weighting model. _J. Acoust. Soc. Am._ 72, 416-425.

Yost, W.A. and Hill, R. (1978). Strength of the pitches associated with ripple noise. _J. Acoust. Soc. Am._ 64, 485-492.

Yost, W.A. and Hill, R. (1979). Models of the pitch and pitch strength of ripple noise. _J. Acoust. Soc. Am._ 66, 400-410.

Yost, W.A., Hill, R., and Perez-Falcon, T. (1978). Pitch and pitch discrimination of broadband signals with rippled power spectra. _J. Acoust. Soc. Am._ 63, 1166-1173.

APPROVAL SHEET

This dissertation submitted by Andrew J. Niemiec has been read and approved by the following committee:

Dr. William A. Yost, Director
Professor of Hearing Sciences
Parmly Hearing Institute
Loyola University Chicago

Dr. Richard R. Fay
Professor of Psychology
Loyola University Chicago

Dr. Raymond H. Dye, Jr.
Associate Professor of Psychology
Loyola University Chicago

The final copies have been examined by the director of the dissertation and the signature which appears below verifies the fact that any necessary changes have been incorporated and that the dissertation is now given final approval by the Committee with reference to content and form.

The dissertation is therefore accepted in partial fulfillment of the requirements for the degree of Doctor of Philosophy.

Jan 18, 1991
Date

Director's Signature